Georgia State University

ScholarWorks @ Georgia State University

Biology Dissertations

Department of Biology

11-30-2008

Characterization of the Structure, Function and Assembly of the DrrAB Antibiotic Efflux Pump in Streptomyces Peucetius

Divya Kishore Rao

Follow this and additional works at: https://scholarworks.gsu.edu/biology_diss

 Part of the Biology Commons

Recommended Citation

Rao, Divya Kishore, "Characterization of the Structure, Function and Assembly of the DrrAB Antibiotic Efflux Pump in Streptomyces Peucetius." Dissertation, Georgia State University, 2008.
doi: https://doi.org/10.57709/1063891

This Dissertation is brought to you for free and open access by the Department of Biology at ScholarWorks @ Georgia State University. It has been accepted for inclusion in Biology Dissertations by an authorized administrator of ScholarWorks @ Georgia State University. For more information, please contact scholarworks@gsu.edu.

CHARACTERIZATION OF THE STRUCTURE, FUNCTION AND ASSEMBLY OF THE DrrAB ANTIBIOTIC EFFLUX PUMP IN *STREPTOMYCES PEUCETIUS*

by

DIVYA KISHORE RAO

Under the Direction of Dr. Parjit Kaur

ABSTRACT

ATP binding cassette (ABC) transporters constitute one of the largest families of transport proteins. The occurrence of multidrug resistance (MDR) in human cancer cells has been correlated with the over expression of human ABC, P-glycoprotein (Pgp). *Streptomyces peucetius* produces two anticancer agents, doxorubicin and daunorubicin, that belong to the anthracycline family of antibiotics. The organism is self-resistant to the potent effects of the antibiotics it produces due to the action of an efflux pump, DrrAB. Both Pgp and DrrAB carry out similar functions, but in two different cell types. An understanding of the bacterial drug transporter DrrAB is thus expected to help in obtaining a better understanding of the function and evolution of the multidrug transporter P-glycoprotein.

In DrrAB, the catalytic and membrane domains are present on separate subunits, DrrA and DrrB respectively. How the catalytic ATP-binding domains and the membrane domains in transporters interact with each other, or how energy is transduced between them, is not well understood. We introduced several single cysteine substitutions in DrrB and then by using a cysteine to amine hetero-bifunctional cross-linker showed that DrrA interacts predominantly with the N-terminal cytoplasmic tail of DrrB. Within this region of DrrB, we also identified a sequence with similarities to the EAA motif found in importers of the ABC family of proteins,

thus leading to the proposal that the EAA or the EAA-like motif may be involved in forming a generalized interface between the ABC and the TMD of both uptake and export systems. By using a combination of approaches, including point mutations and disulfide cross-linking analysis, we show here that the Q-loop region of DrrA plays an important role in dimerization of DrrA as well as in interactions with DrrB. Furthermore, we also show that the interaction of the Q-loop with the N-terminus of DrrB is involved in transmitting conformational changes between DrrA and DrrB. The scope of the present study further extends into identifying the factors involved in the biogenesis of the DrrAB pump. We have identified two accessory proteins namely, FtsH and GroEL that may be involved in proper folding and assembly of the transporter.

INDEX WORDS: ABC transporter, Multidrug resistance, ATPase subunit, Transmembrane subunit, DrrAB, Q-loop, FtsH, GroEL, Disulphide cross-linking.

CHARACTERIZATION OF THE STRUCTURE, FUNCTION AND ASSEMBLY OF THE DrrAB ANTIBIOTIC EFFLUX PUMP IN *STREPTOMYCES PEUCETIUS*

by

DIVYA KISHORE RAO

A Dissertation Submitted in Partial Fulfillment of Requirements for the Degree of

Doctor of Philosophy in the

College of Arts and Sciences

Georgia State University

2007

Copyright by
Divya Kishore Rao
2007

CHARACTERIZATION OF THE STRUCTURE, FUNCTION AND ASSEMBLY OF THE DrrAB ANTIBIOTIC EFFLUX PUMP IN *STREPTOMYCES PEUCETIUS*

by

DIVYA KISHORE RAO

Committee Chair: Parjit Kaur

Committee: P.C.Tai
Zehava Eichenbaum
Chung-Dar Lu

Electronic Version Approved:

Office of Graduate Studies
College of Arts and Sciences
Georgia State University
December 2007

ACKNOWLEDGEMENTS

The last six years have been a wonderful journey of my life. The journey culminated with the fulfillment of my dream of wanting to be an independent scientific researcher. Earning my doctoral degree has been a dream for a very long time. The journey was filled with its good times and some not so good times. There were tears of joy and sometimes of sadness. Some days were challenging while others were smooth sailing. I was able to learn a lot from my experiences, to take the challenges in my stride, to have faith in my work, especially on those days when I was filled with doubts. Today, I feel a great sense of achievement and happiness. All through my six years, my life has been filled with the warmth and support of so many lovely people without whom I would never had made it this far. I would like to acknowledge these people who have come to become my family. It is a very big family, and I may have forgotten to mention a few people for which I truly apologize.

My journey began with the support and inspiring words of my father, Mr. Kishore Rao. He always told me I had potential and that I should strive towards accomplishing my dreams. My mother, Ms. Shanthi Rao, was always there to listen to my concerns and grievances. My sister Ms. Mamta Shamsundar was my pillar of support. My niece, Neha Shamsundar, was always there to cheer me up with her constant chatter and her unconditional love. Thank you my near and dear ones. I will love you forever.

To my advisor, Dr. Parjit Kaur, there are no words to express my gratitude to you. You have moulded me into what I am today, for which I will be grateful to you. There are times when my fears and worries have been lifted after having spoken with you. You have made me a better person. And more than anything, you have inspired me to one day become a researcher and contribute to the scientific community. Thank you for these special years of my life.

My Kaur lab members, Ms. Ling Wei, Dr. Prajakta Pradhan, Ms. Madhu Sharma, Ms. Sonya Iyer, Ms. Gargi Abhyankar and Ms. Han Zhang. Your warmth and friendhip made the lab my second home. We spent such great times together, our signature phrases were “Do you speak whale”, “Did you miss me” and “Silence!! I’ll kill you”. I will always remember our “Kendra” laughs. Prajakta, we share a special bond that will never be broken. Our friendhip has gone through several meandering paths, but has stood the test of time. Thank you all for your support and encouragement.

My committee members, Dr. P.C Tai, Dr. Zehava Eichenbaum and Dr. Chang-Dar Lu, I thank you for your time, guidance and providing direction in my work. I would also like to express my gratitude to members of the core facility, the staff in the biology department, and the computer tech support.

And finally, my husband, Mr. Nitish Pargal. He held my hand all through the journey and never let it go. I hope we will be able to go on many more journeys together. I love you dearly. A special thanks to my extended family, the Pargal family, for their love and encouragement.

TABLE OF CONTENTS

LIST OF TABLES

LIST OF FIGURES

LIST OF ABBREVIATIONS

1. ABC	ATP binding cassette
2. MDR	multidrug resistance
3. Pgp	p-glycoprotein
4. NBD	nucleotide binding domain
5. TMD	transmembrane domain
6. SDS	Sodium dodecyl sulfate
7. p.s.i	Pounds per square inch
8. PAGE	Polyacrylamide gel Electrophoresis
9. PCR	Polymerase Chain Reaction
10. CuPhe	Copper phenanthroline
11. DTME	Dithio-bis-maleimidoethane
12. MTS	3,6,9,12,15-Pentaoxaheptadecane-1methanethiosulfonate
13. GMBS	N-γ-maleimidobutyryloxy]succinimide ester
14. NBD-Cl	7-chloro-4-nitrobenzo-2-oxa-1, 3-diazole
15. MIANS	2-(4'-maleimidylanilino) naphthalene-6-sulfonic acid
16. FRET	fourier resonance energy transfer
17. SELDI	Surface Enhanced Laser Desorption/Ionization

INTRODUCTION

Bacteria of the genus *Streptomyces* are gram positive spore-bearing soil bacteria that belong to the family *Streptomycetece* and resemble filamentous fungi. Members of this family produce various antibiotics and have been well studied and documented in this aspect. *Streptomyces peucetius* produces two clinically important anti-tumor agents, doxorubicin (Dox) and daunorubicin (Dnr) and is itself resistant to the potent action of these drugs (*1*). Resistance to Dox and Dnr in *S. peucetius* is conferred by the resistance genes *drrAB (1)*. This locus was initially cloned into *S. lividans* by Guilfoile and Hutchinson and was found to be sufficient to confer resistance to these drugs in the otherwise sensitive species *S. lividans (1)*. Sequence analysis suggested that this locus consists of two ORFs, *drrA* and *drrB*, both of which were shown to be required for resistance in *S. lividans (1)*. The same study also showed that the resistance genes reside in the dnr gene cluster (Figure 1).

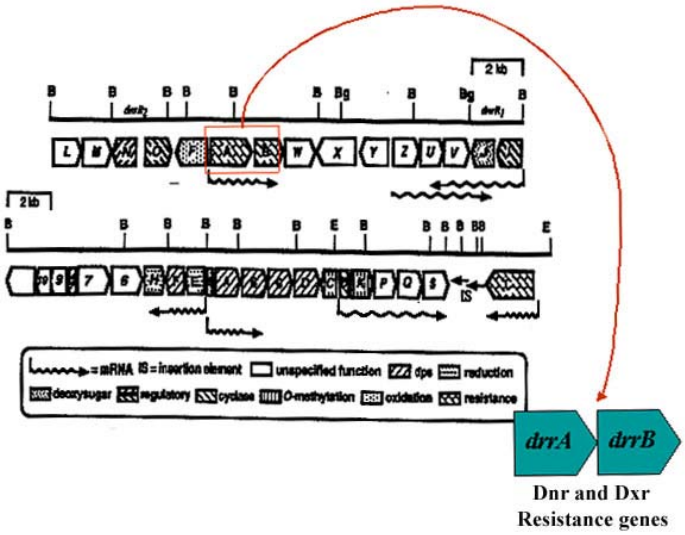

Journal of Industrial Microbiology & Biotechnology (1999) 23, 647–652

FIGURE 1: *Physical map of the dnr gene cluster in Streptomyces peucetius. The cluster contains genes involved in the synthesis, regulation and resistance to the antibiotics Dox and Dnr*

The *dnr* gene cluster contains genes involved in the synthesis, regulation and resistance to the antibiotics Dox and Dnr. The onset of production of the resistance determinants corresponds to the onset of the production of the secondary metabolites in the stationary phase of growth (*1, 2*). A 2 kb DNA fragment consisting of just the *drrAB* genes has been sub-cloned and expressed in *E. coli* in the Kaur laboratory (*3*). Nucleotide sequence of *drrA* and *drrB* suggests that they belong to the ABC (**A**TP *B*inding **C**assette) family of proteins and bear homology to Pgp and other members of the ABC1 family (*1*). Functional analysis of the two proteins in *E. coli* has confirmed that the presence of both the proteins, DrrA and DrrB, is needed to develop resistance to Dox in sensitive *E.coli (3)*. The products of the two open reading frames have been characterized. DrrA has been shown to be a 36-kDa peripheral membrane protein that binds ATP in a UV-catalyzed Dox-dependent manner (*4*). DrrB is a 30-kDa hydrophobic protein that is localized to the inner membrane of *E.coli (4)*. A model for the membrane topology of DrrB is now available (*5*). This model suggests that DrrB contains eight transmembrane domains with both the N-terminal and the C-terminal ends directed in the cytoplasm.

Preliminary studies to determine the function and stability of DrrA and DrrB have shown that the two proteins are dependent on each other for stability and function (*4*). A Western blot analysis of cells containing the *drrB* gene alone shows a dramatic reduction in the level of the DrrB protein (Figure 2, lane 3). However, when DrrA is introduced into the cells in *trans*, the expression level of DrrB is restored (lane 5). This suggests that DrrB depends on DrrA for maintaining its stability. Levels of DrrA are also reduced in cells containing the *drrA* gene alone, but not as dramatically as DrrB alone (lane 1 and 2). However, no ATP binding to DrrA is detected in cells containing DrrA alone, suggesting that DrrA is dependent on DrrB for maintaining its active conformation. The co-dependence of DrrA and DrrB on one another

suggests biochemical coupling between the two proteins. Chemical cross-linking studies have shown that the two proteins interact with each other to form a tetramer with a stoichiometry of $DrrA_2B_2$ (*4*).

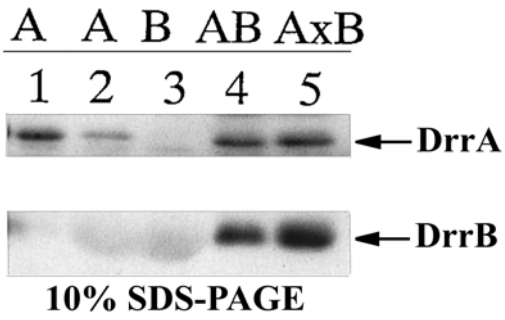

J Biol Chem, (1998) 273, 17933-17939

FIGURE 2: *Effect of co-expression of DrrA and DrrB. E. coli cells, co-transformed with pDX103 and pDX108, were induced with IPTG and lysed as described under "Experimental Procedures". The total lysates were analyzed by SDS-PAGE followed by Western blot analysis using anti-DrrA or anti-DrrB serum. Lane 1, pDX108; lane 2, pDX102; lane 3, pDX103; lane 4, pDX101; lane 5, pDX103 and pDX108.*

Our laboratory is interested in understanding the mechanism by which the DrrAB drug transporter carries out efflux of Dnr and Dox antibiotics. This is important for a variety of reasons - the most important being that drug resistance is an emerging clinical problem and an understanding of the mechanism of resistance can help in designing effective strategies to combat drug resistance. Furthermore, the DrrAB system exhibits similarities with P-glycoprotein (Pgp), an MDR protein overexpressed in cancer cells (*6*). Eventhough the domain architecture of Pgp and DrrAB is different in that Pgp is one large protein containing 2 NBD and 2TMD domains, while DrrAB consists of NBD and TMD present on two separate subunits (Figure 3), the two systems have sequence and functional similarity (*7*). Both belong to the ABC family of proteins and both carry out ATP-dependent efflux of doxorubicin. Thus, a better

understanding the mechanism of function of DrrAB proteins and interaction between them would no doubt throw light on the mechanism and origin of multidrug resistance

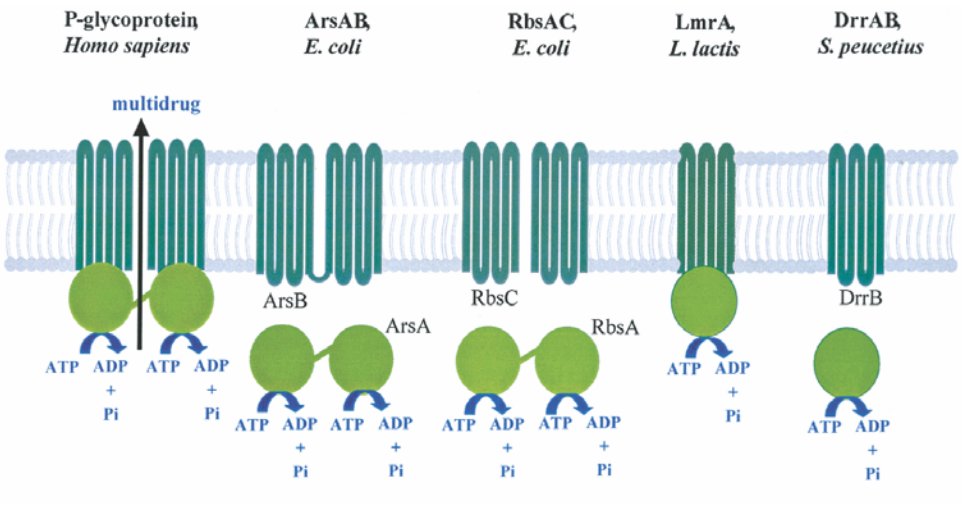

Biochemical Journal (2003) Volume **376**, 313-338

FIGURE 3: *Domain architecture of ABC transporters from microorganism to man.*

How the catalytic ATP-binding domains and the membrane domains in transporters interact with each other, or how energy is transduced between them, is not well understood. Since the domains in the DrrAB system are present on separate subunits, it makes it an ideal model system for the study of interaction between the ATP-binding domains and the membrane domains. Previous cross-linking studies in this laboratory employed membrane-permeable and impermeable amine to amine cross-linkers, DSP and DTSSP, and identified a complex of DrrA and DrrB (*4*). However, using DSP and DTSSP, it was not possible to easily determine the regions involved in cross-linking. The goal of the present study was to directly identify the regions of DrrA and DrrB that are involved in interaction and in transmitting conformational changes between one another. To further our understanding of interactions between DrrA and

DrrB, and the mechanism of the DrrAB complex, the study extends into the characterization of accessory proteins involved in biogenesis of the DrrAB efflux pump. This dissertation comprises of three chapters and an in-depth introduction to each research study has been presented at the beginning of each chapter.

REFERENCES

1. Guilfoile, P. G. & Hutchinson, C. R. (1991) A bacterial analog of the mdr gene of mammalian tumor cells is present in Streptomyces peucetius, the producer of daunorubicin and doxorubicin, *Proc Natl Acad Sci U S A. 88*, 8553-7.

2. Hutchinson, C. R. & Colombo, A. L. (1999) Genetic engineering of doxorubicin production in Streptomyces peucetius: a review, *J Ind Microbiol Biotechnol. 23*, 647-52.

3. Kaur, P. (1997) Expression and characterization of DrrA and DrrB proteins of Streptomyces peucetius in Escherichia coli: DrrA is an ATP binding protein, *J Bacteriol. 179*, 569-75.

4. Kaur, P. & Russell, J. (1998) Biochemical coupling between the DrrA and DrrB proteins of the doxorubicin efflux pump of Streptomyces peucetius, *J Biol Chem. 273*, 17933-9.

5. Gandlur, S. M., Wei, L., Levine, J., Russell, J. & Kaur, P. (2004) Membrane topology of the DrrB protein of the doxorubicin transporter of Streptomyces peucetius, *J Biol Chem. 279*, 27799-806.

6. Gottesman, M. M. & Pastan, I. (1993) Biochemistry of multidrug resistance mediated by the multidrug transporter, *Annu Rev Biochem. 62*, 385-427.

7. McKeegan, K. S., Borges-Walmsley, M. I. & Walmsley, A. R. (2003) The structure and function of drug pumps: an update, *Trends Microbiol. 11*, 21-9.

CHAPTER I

Biochemical Characterization of Domains in the Membrane Subunit DrrB That Interact with the ABC Subunit DrrA: Identification of a Conserved Motif

ABSTRACT

DrrA and DrrB proteins confer resistance to the commonly used anticancer agents daunorubicin and doxorubicin in the producer organism Streptomyces peucetius. The drrAB locus has previously been cloned in Escherichia coli, and the proteins have been found to be functional in this host. DrrA, a soluble protein, belongs to the ABC family of proteins. It forms a complex with the integral membrane protein DrrB. Previous studies suggest that the function and stability of DrrA and DrrB are biochemically coupled. Thus, DrrA binds ATP only when it is in a complex with DrrB in the membrane. Further, DrrB is completely degraded if DrrA is absent. In the present study, we have characterized domains in DrrB that may be directly involved in interaction with DrrA. Several single-cysteine substitutions in DrrB were made. Interaction between DrrA and DrrB was studied by using a cysteine to amine chemical cross-linker that specifically cross-links a free sulfhydryl group in one protein (DrrB) to an amine in another (DrrA). We show here that DrrA cross-links with both the N- and the C-terminal ends of the DrrB protein, implying that they may be involved in interaction. Furthermore, this study identifies a motif within the N-terminal cytoplasmic tail of DrrB, which is similar to a motif recently shown by crystal structure analysis in BtuC and previously shown by sequence analysis to be also present in exporters, including MDR1. We propose that the motif present in DrrB and other exporters is actually a modified version of the EAA motif, which was originally believed to be present only in the importers of the ABC family. The present work is the first report where domains of interaction in the membrane component of an ABC drug exporter have been biochemically characterized.

INTRODUCTION

Daunorubicin and doxorubicin, two commonly used anti-cancer drugs, are produced by the soil organism Streptomyces peucetius. Self-resistance to these antibiotics in S. peucetius is mediated by the action of two proteins, DrrA and DrrB, which are coded by the drrAB operon (1). Subcloning of the drrAB locus has been shown to confer doxorubicin resistance in Escherichia coli (2). DrrA, a peripheral membrane protein, contains one ABC-type (ATP Binding Cassette) (3) consensus nucleotide binding domain (NBD)[1] (1, 2). It forms a complex with DrrB, which is localized to the inner membrane of the E. coli cells (2). Together, DrrA and DrrB are expected to form an ATP-dependent pump for the efflux of daunorubicin and doxorubicin, resulting in resistance to these antibiotics (1, 2). Interestingly, the DrrAB system bears sequence, structural, and functional similarities to P-glycoprotein (Pgp) found in mammalian tumor cells (1, 2, 4). Overexpression of Pgp in cancer cells has been implicated in the development of multidrug resistance to a variety of structurally unrelated drugs, including daunorubicin and doxorubicin (4, 5). Thus, both Pgp and DrrAB carry out similar functions, but in two different cell types. An understanding of the bacterial drug transporter DrrAB is thus expected to help in obtaining a better understanding of the function and evolution of the multidrug transporter P-glycoprotein. Most ABC transporters are made up of four domains-two nucleotide binding domains and two transmembrane (TM) domains. These four domains can be present on the same molecule (Pgp (6), CFTR (7)), on two half-molecules (LmrA (8), Tap1 (9), Tap2 (10), HlyB (11), MsbA (12)), or on completely separate polypeptides (DrrAB (13), BtuCD (14)). In DrrAB, the catalytic and membrane domains are present on separate subunits, which are expected to form a tetramer consisting of two identical subunits of DrrA and two of DrrB (13). Although present on separate subunits, the two domains of DrrAB show a strong dependence on each other for stability and

function (13). Thus, DrrA, the nucleotide binding subunit, binds ATP or GTP in a doxorubicin-dependent manner only if it is in a complex with DrrB (13). Further, DrrB is completely degraded if DrrA is not simultaneously expressed (13). These characteristics of DrrAB make it an ideal model system to study interactions between the ABC domain and the TM domain of ABC transporters and to identify specific regions of interaction.

How the catalytic ATP-binding domains and the membrane domains in transporters interact with each other, or how energy is transduced between them, is not well understood. An effort is currently underway to better understand these interactions in different ABC transporters, including medically relevant transporters Pgp (6) and CFTR (Cystic Fibrosis Transmembrane Regulator) (7, 15, 16). As of now, however, not much is known about the mechanism of interaction between membrane domains and ABC domains in these proteins. Both Pgp and CFTR contain all four domains in the same molecule; thus, analysis of interactions between them involves subcloning of the domains (6, 7), which may not be conducive to retaining proper structure and function. Since the domains in the DrrAB system are present on separate subunits, we have taken advantage of this characteristic, in the present study, to study interaction by a heterobifunctional cysteine to amine cross-linking approach. Previous cross-linking studies in this laboratory employed membrane-permeable and -impermeable amine to amine cross-linkers, DSP and DTSSP, and identified a complex of DrrA and DrrB (13). However, using DSP and DTSSP, it was not possible to easily determine the regions involved in cross-linking. In the present study, we have used a more direct and specific approach to identify regions in DrrB that are physically close to DrrA and thus may be involved in an interaction with DrrA.

DrrB protein contains a single cysteine at position 260, whereas DrrA protein contains none. A cysteine-less DrrB was first created by substituting a serine at position C260 by site-directed

mutagenesis. Twenty single-cysteine substitutions were thus introduced at various positions in the cysteine-less DrrB. The location of the cysteine substitutions in DrrB was based on a recently developed topological model for DrrB (17), which suggests that DrrB consists of eight transmembrane domains with both the N-terminal and the C-terminal ends of the protein directed in the cytoplasm. To directly identify the regions of DrrB that interact with DrrA, a heterobifunctional cysteine to amine chemical cross-linking agent, GMBS (N-[γ-maleimidobutyryloxy]succinimide ester), was employed. Studies reported here show that DrrA cross-links with both the N-terminal and the C-terminal ends of DrrB, suggesting that these two regions may participate in interaction with DrrA. Furthermore, this study identifies a sequence within the N-terminal cytoplasmic tail of DrrB, which is similar to the "L-loop" motif recently identified in the BtuC protein involved in VitB12 uptake in E. coli (18). By crystal structure analysis, the L-loop motif has been shown to lie at the interface of BtuC, the membrane component, and BtuD, the ABC component, where it is involved in forming extensive contacts between the two domains. BtuCD is a binding protein-dependent import system. It has previously been shown that permeases belonging to this group contain an EAA motif within their interaction interfaces (19). A closer look at the sequence of the L-loop suggested to us that it is actually similar, though not identical, to the "EAA-loop" previously identified in this group of proteins. While the L-loop of BtuC retains several features of the EAA loop, it also shares certain features with the motif present in DrrB (shown in this study) and other exporters (described earlier (18)). The sequence analysis and the alignments presented in this article thus allow us to conclude that the exporters, including DrrB, LmrA, MDR1, CFTR, and MsbA, as well as the importer BtuC contain a conserved motif bearing the amino acid sequence $GE_{-1}..A_3R/K..G_7$. We further conclude that this conserved sequence is a modified version of the EAA motif

$E_1AA_3RALG_7$-although a significantly modified version with its own distinct features.

The present study is the first report where interacting domains in the membrane component of a drug efflux system have been biochemically analyzed by using a cross-linking approach. The domain identified by cross-linking was found to contain an EAA-like motif previously identified in the interaction interfaces of importers of the ABC family. We propose that the EAA motif or a modified version of the EAA motif may be involved in forming a generalized interface between the membrane component and the ABC component of both uptake and efflux systems. The evolutionary implications of this finding are discussed.

MATERIALS AND METHODS

Bacterial Strains and Plasmids: E. coli TG1 (20) and XL1 Blue (Clonetech, BD Biosciences) were used in this study.

Media and Growth Conditions: Cells were grown in Luria Broth. Chloramphenicol was added to a final concentration of 20 μg/mL.

DNA Manipulation: The conditions for plasmid isolation, DNA endonuclease restriction analysis, ligation, and sequencing have been described elsewhere (20).

Site-Directed Mutagenesis: The cysteine residue at position 260 in DrrB in the plasmid pDx101 was altered to a serine using a Strategene QuikChange multisite-directed mutagenesis kit (La Jolla, CA). The strategy involved the use of complementary primers that incorporated the change at the required position. The sequence of the primers used is

C260S up:
5'-GGCCTGGTCCTGTCCGTGTCGGCAGGG-3'
C260S dn:
5'-CCCTGCCGACACGGACAGGACCAGGCC-3'

These primers were used for polymerase chain reaction amplification using pDx101 as a template (2). The amplified product bearing the mutation was then transformed into XL1 blue competent cells (provided by the manufacturer) and plated on medium containing chloramphenicol. Plasmid DNA was isolated from the colonies grown on the selection plates and the desired mutation in the drrAB genes was verified by sequencing of DNA. Sequencing was carried out using ABI 377 or 3100 sequencers (Applied Biosystems) in the Core Facilities in the Department of Biology at the Georgia State University. The cysteine-less serine substitution mutant was named C260S in this study. Subsequent single cysteine substitution mutants were then created in the cysteine-less DrrB, C260S. Complementary primers bearing the mutation at

the desired location were used for each of these mutations. Primers used for making S23C mutation are shown here as an example:

S23C up:
5′-CGGACGGTGCTGTCGCGGGTGAACGG-3′
S23C dn:
5′-CCGTTCACCCGCGACAGCACCGTCCG-3′

Single cysteine substitution mutants were created at amino acid positions 4, 15, 23, 35, 44, 53, 70, 80, 92, 107, 116, 129, 149, 160, 173, 213, 236, 249, 270, and 282 in DrrB. The mutants were named S4C, S15C, S23C, S35C, A44C, V53C, T70C, S80C, V92C, S107C, V116C, A129C, T149C, A160C, V173C, S213C, S236C, T249C, A270C, and A282C, respectively. *Doxorubicin Resistance Assay:* Doxorubicin resistance assays were carried out on M9 (Sambrook 1989) plates supplemented with 0.25% casamino acids. The plates were layered with 4 mL of top agar (0.8% agar in M9 medium) containing the desired concentration of doxorubicin. Briefly 4 mL of top agar containing 0, 4, 6, 8, or 10 μg/mL of doxorubicin and 1 mM Thiamine-HCl was poured on top of M9 plates. The plates were covered with foil to prevent exposure to light. Doxorubicin hydrochloride was purchased from Sigma Chemicals and used with the necessary precautions needed for a light-sensitive chemical. A doxorubicin-sensitive strain of E. coli, N43 (21), was transformed with the indicated plasmids. N43 cells freshly transformed with the desired plasmid were grown for 8 h in 3 mL of LB with the appropriate antibiotics. Ten microliters of the 8 h old N43 culture from above was inoculated on the plates containing doxorubicin. N43 containing the plasmid pSU2718 was used as a negative control. The plates were then incubated at 37 °C overnight, and growth was recorded after 24 h of incubation.

Fractionation of Cells into Cytosolic and Membrane Fractions: Competent *E. coli* TG1 cells

were transformed with the plasmid bearing the mutated gene. A 50 mL portion of cells containing the indicated plasmids was grown to mid-log phase and induced with 0.25 mM IPTG. Growth was continued for an additional 3 h at 37 °C. The cells were spun down and resuspended in 1.5 mL of PBS buffer (20 mM sodium phosphate, pH 7.0) and lysed by a single passage through a French pressure cell at 20 000 psi. The cell lysates were then centrifuged at 10 000g for 15 min to remove the unbroken cells. The supernatants were subsequently used to prepare membrane fractions by ultracentrifugation at 100 000g for 1 h. The membrane pellets were suspended in cross-linking buffer (20 mM sodium phosphate, 150 mM sodium chloride, 0.5 mM EDTA, pH 7.4) and used for cross-linking of proteins.

Heterobifunctional Cross-Linking Reaction and Western Blot Analysis: A 100 μL reaction volume containing 250 μg of cell membrane protein in the cross-linking buffer was used. GMBS (N-[γ-maleimidobutyryloxy]sulfosuccinimide ester; 6.4 Å length), prepared in dimethyl sulfoxide (DMSO), was added to a final concentration of 1 mM. DMSO alone was used in the control samples. Where indicated, 5 mM ATP and/or 35 μM doxorubicin was added into the reaction mix. The reaction was carried out for 1 h at room temperature in a light-protected area. A 25 μL portion of 4 X Laemmli sample buffer was added to stop the reaction. The samples were mixed thoroughly and set aside for 5 min at room temperature. A 25 μL portion (50 μg of membrane protein) of the reaction mixture was then analyzed by SDS-PAGE using a 10% polyacrylamide gel, followed by Western blot analysis using either anti-DrrA or anti-DrrB antibodies. Detection was done by a chemiluminiscent assay using Immun-Star AP, BioRad (Hercules, CA).

RESULTS

Cysteine-less DrrB: Previous studies have suggested that DrrA and DrrB interact with each other in a very specific manner (13). This interaction is essential for the maintenance of DrrB and for the function of DrrA, indicating that the two proteins are biochemically coupled. The purpose of the present study was to analyze domains in DrrB that are involved in interaction with DrrA. A model for the membrane topology of DrrB is now available (17). This model suggests that DrrB contains eight transmembrane domains with both the N-terminal and the C-terminal ends directed in the cytoplasm (17). On the basis of this model, several single-cysteine substitutions in the proposed cytosolic as well as the transmembrane domains of DrrB were made (Figure 1). Cross-linking between a defined cysteine in the DrrB protein and an amine in the DrrA protein was analyzed. The DrrA protein contains 43 primary amines which are spread evenly over the entire length of the protein. Of the 43 amines, 5 are lysines, which may be preferentially involved in cross-linking. The lysines are present at amino acid positions 16, 46, 137, 226, and 327 in DrrA, which contains a total of 329 residues. The cysteine to amine cross-linking approach was possible because DrrB protein contains a single cysteine at position 260, whereas DrrA protein contains none. Using site-directed mutagenesis, the single cysteine in DrrB was altered to a serine residue. To rule out if the C260S mutation has an adverse effect on interaction between DrrA and DrrB, the levels of DrrA and DrrB in the mutant C260S were compared to those in the wild type C260 (Figure 2). Comparable levels of DrrA (Figure 2A) and DrrB (Figure 2B) were seen in the membrane fractions prepared from the wild type and the mutant cells. Since the stability of DrrA and DrrB is a good indicator of interaction (13), these results suggest that the cysteine-less DrrB is not affected in its interaction with DrrA. Single Cysteine Substitution Mutants of DrrB. Twenty single cysteine substitution mutants in DrrB were then created using

C260S as the starting material (Figure 1). The residues chosen for cysteine substitutions were selected so that they would result in conservative changes. Western blot analysis of the cell membranes showed that both DrrA (Figures 3-5) and DrrB (not shown) are expressed in cells containing cysteine substitution mutants. Some amount of variation in the amounts of DrrA and DrrB was seen in the substitution mutants, as compared to the wild-type cells (Figures 3-5). Experimental variation in the levels of DrrA or DrrB is also routinely seen in the wild-type cells, as expected in a physiological system.

Secondary Structure Analysis of the Cysteine Substitution Mutants: The membrane topology of the DrrB protein has been determined experimentally, and it has been shown to contain eight transmembrane helices with both the N- and the C-terminal tails in the cytoplasm (17). The predicted secondary structure of DrrB was determined by the Chou-Fasman method. By this method, the DrrB protein is seen to contain two helical stretches in regions of DrrB that are exposed to the cytoplasm. The first helical region, extending from amino acids 24 to 53, lies within the N-terminal cytoplasmic tail, and the second lies in the third cytoplasmic loop (C3), extending from amino acids 226-248. Since the Chou-Fasman method does not predict transmembrane helices, the secondary structure prediction of DrrB was verified by the PROF method employed by the Predictprotein server (www.predictprotein.org). PROF not only predicted the helices corresponding to the transmembrane domains of DrrB, but more significantly, it predicted the same two helical segments as were shown by the Chou-Fasman method in the cytoplasmic regions of DrrB. These regions lie between amino acids 32 and 49 in the N-terminal domain and between 222 and 245 in the C-terminal domain. Secondary structure prediction was also done for the 20 single-cysteine substitutions and other point mutants used in this study. Three out of 20 cysteine substitution mutants showed some change in the secondary

structure of the protein by the Chou-Fasman prediction, while the others remained unchanged. Those with the altered secondary structure include S35C, A44C, and S236C. Of these, only S236C was seen to affect doxorubicin resistance phenotype, as described below. The PROF method of prediction showed no significant change in the secondary structure of any of the substitutions or point mutants used in the study.

Doxorubicin Resistance: To determine if cysteine substitutions in DrrB have an effect on the function of the transporter, doxorubicin resistance assays were carried out. Most of the strains containing single-cysteine substitutions showed levels of doxorubicin resistance comparable to that of the wild-type strain (Table 1), suggesting that the function of the complex is not significantly affected by the single-cysteine substitutions constructed in this study. However, a few substitutions, including V53C, T70C, V92C, A129C, S236C, and S249C, showed a decrease in resistance to doxorubicin (Table 1). The possible significance of these observations is discussed later.

Heterobifunctional Cross-Linking: Heterobifunctional cross-linking using GMBS was performed between the 20 single cysteine substitution mutants of DrrB (as well as the wild-type C260) and DrrA. GMBS is an NHS-ester cross-linker. It interacts with a free sulfhydryl group, provided by a cysteine residue on one arm and an amine residue on the other, thus forming a cross-linked product. The N-terminal mutant S23C was the first mutant where a cross-linked product of DrrA and DrrB was identified (Figure 3). Western blot analysis of the cross-linked sample identified a species of about 60 kDa when probed with either anti-DrrA (Figure 3B, lanes 2-5) or anti-DrrB (Figure 3D, lanes 2-5) antibodies. On the basis of its size, this species would correspond to one subunit of DrrA and one subunit of DrrB. Cross-linking could be seen at GMBS concentrations as low as 0.2 mM (Figure 3B,D, lane 2). No significant increase in the cross-linking efficiency

was observed when higher concentrations of GMBS were used (Figure 3B,D, lanes 2-5); however, at concentrations higher than 2 mM, a significant drop in the intensity of the 60 kDa species with a concomitant increase in the higher species with molecular mass greater than 200 kDa was seen (not shown). Since high concentrations of the cross-linker can result in nonspecific aggregates, the maximum concentration of GMBS used in this study was 1 mM.

The 60 kDa cross-linked species did not appear in the cysteine-less (C260S) sample on addition of the cross-linker (Figure 3A,C) or in the S23C control sample where DMSO alone was added instead of the cross-linker (Figure 3B,D, lane 1). To further verify if the same cross-linked species was detected by both anti-DrrA and anti-DrrB antibodies, a lane containing the cross-linked S23C sample was spliced vertically into halves. Each half was probed with either the anti-DrrA or the anti-DrrB antibodies. The reaction was developed by the chemiluminescence assay, and the halves of the nitrocellulose membrane were then aligned with the help of internal protein markers. Results in Figure 3E show that the same cross-linked species reacted with both antibodies, suggesting that it consists of both DrrA and DrrB.

Both anti-DrrA and anti-DrrB antibodies were also seen to cross-react with some other proteins nonspecifically (Figure 3). This is not unexpected, since the cross-linking experiments reported here are carried out with the cell membrane preparations containing many other proteins in addition to DrrA and DrrB. Furthermore, the antibodies used for detection of the cross-linked species are polyclonal in nature, thus resulting in cross-reactivity with certain other epitopes (2). The addition of the cross-linker also appeared to change the mobility of some of these unrelated proteins. For example, a 43 kDa protein picked up nonspecifically with the anti-DrrA antibody (Figure 3B, lane 1) is decreased or is not seen in the cross-linked samples (Figure 3B, lanes 2-5). It should be pointed out that the disappearance of the 43 kDa band happens in all the samples,

irrespective of the presence (S23C) or absence (C260S) of a cysteine in DrrB (Figure 3A). Since the 60 kDa cross-linked species is not seen in C260S (even though the 43 kDa band disappears), it clearly indicates that the cross-linked species seen in S23C is not the result of cross-linking between DrrB and this 43 kDa unrelated protein. Thus, the 43 kDa protein cross-links with another unknown protein in the membrane. Since our focus in this study is on specific cross-linked species of DrrA and DrrB, further analysis of the 43 kDa protein was not carried out. S23C, which showed a specific 60 kDa cross-linked species of DrrA and DrrB (described above), was used as a positive control in further cross-linking experiments. The remaining 19 cysteine substitution mutants and the wild-type C260 were analyzed for the cross-linked product of DrrA and DrrB by Western blot analysis using both antibodies; however, only the blots obtained with the anti-DrrA antibody are shown (Figures 4 and 5). As seen with S23C, all the other cysteine substitution mutants tested in the N-terminal tail, S4C, S15C, S35C, and S44C, also showed the appearance of the 60 kDa species on cross-linking with GMBS by Western blot analysis (Figure 4A,B). The effect of addition of ATP (Figure 4A) or doxorubicin on cross-linking was also determined. No significant effect of addition of either substrate alone or together on cross-linking was observed (not shown). Analysis of the mutants in TM1 (V53C and T70C) and TM2 (V92C and S107C) also showed the 60 kDa cross-linked species containing DrrA and DrrB (Figure 4B). However, S80C, a cysteine substitution in the first periplasmic loop (P1), did not show cross-linking with DrrA (not shown). V116C located in the first cytoplasmic loop also showed cross-linking with DrrA (Figure 4B). Analysis of mutants in TM's 3, 4, 5, and 6 and the intervening cytoplasmic loops C2 and C3 did not show the 60 kDa cross-linked species (Figure 5A,B). Wild-type DrrB, which according to the topological model contains residue C260 in the seventh transmembrane domain, cross-linked with DrrA (Figure 5C), although another

substitution mutant, S249C, also in the seventh transmembrane domain, did not cross-link with DrrA (Figure 5B). Finally, both A270C in the eighth transmembrane domain (Figure 5C) and A282C at the C-terminal end of DrrB showed cross-linked products with DrrA (Figure 5C). Together, the chemical cross-linking data presented above show that DrrA cross-links with both the N-terminal and the C-terminal domains of the DrrB protein, suggesting that these regions may be involved in interaction. At the N terminus, the interaction involves the first 50 amino acids of the N-terminal cytoplasmic tail and includes the first and second transmembrane domains extending up to the first cytoplasmic loop of the DrrB protein. At the C-terminal end, the interaction between DrrA and DrrB involves the seventh and the eighth transmembrane helices of DrrB and it extends to the short cytosolic C-terminal tail. The intensity of the cross-linked species varies, depending on the location of the cysteine in the DrrB protein. The best cross-linking was seen with cysteines in the N-terminal cytosolic tail, suggesting that this may be the major site of interaction with DrrA.

Identification of a Conserved Motif in DrrB: As described above, the Chou-Fasman and the PROF methods of secondary structure prediction showed that the DrrB protein contains two helical stretches that are present in regions exposed to the cytoplasm. The first helical region, extending from amino acids 24 to 53, lies within the N-terminal cytoplasmic tail and is part of the N-terminal domain that cross-links with DrrA; the second lies in the third cytoplasmic loop (C3), extending from amino acids 226 to 248. On further analysis, it was found that the helical region present in the N-terminal cytoplasmic tail of DrrB contains an amino acid sequence similar to the L-loop motif present in BtuC (18), which is the membrane component of the BtuCD system involved in VitB12 uptake in E. coli (Figure 6). The L-loop in BtuC is present in a helical stretch of the cytoplasmic loop between TM6 and TM7. On the basis of the crystal

structure of the BtuCD complex, the L-loop of BtuC forms extensive contacts with the ABC component, BtuD. It has also been previously suggested that the L-loop of BtuC shows similarity to a certain sequence in the first cytoplasmic loop of exporters, including the drug exporters MDR1 and LmrA, the lipid exporter MsbA, and the chloride channel CFTR (18), all members of the ABC superfamily.

An alignment of the N-terminal region of DrrB with the L-loop in BtuC and several other export and import proteins is shown in Figure 6. This alignment is different from that reported earlier by Locher et al. (18); thus, a clarification is needed at this point about the basis used for the alignment shown in Figure 6 in this study as well as about the relationship between the sequence of the L-loop (18) and the EAA-loop (19). Even though Locher et al. stated that there is a limited similarity of the L-loop of BtuC with the EAA-loop (18) of the binding protein-dependent importers (19), their sequence alignments did not reflect such a similarity. The alignment shown in Figure 6 in the present study uses the sequence analysis carried out by Saurin et al. (22) as the basis for the identification of the EAA-loop motif. In the analysis carried out by Saurin et al., 61 integral membrane proteins belonging to the binding protein dependent importers were classified on the basis of the similarities between their EAA motifs. It was shown that these proteins can be classified into eight clusters. The sequences belonging to the main cluster were called the "EAA cluster". Members of this cluster contain conserved sequences almost identical with the $E_1AA_3...G_7...I.LP$ motif; however, other clusters show some differences compared to the original EAA motif. Within the EAA motif, the central part A_3RALG_7 is the most conserved-of these, the flanking A_3 and G_7 being highly conserved and the middle residues RAL less conserved (22). According to this classification (22), BtuC is assigned to the cluster of iron-siderophore transporter proteins, which contain the central $A_3...G_7$ sequence; however, they lack the E residue

at position 1 and instead contain an E or a D at position -1 (Figure 6). We have based our alignment shown in Figure 6 on the information described above. Since BtuC contains a well-defined $A_3...G_7$ central domain, we have placed the A of the central domain A...G of BtuC at position 3 as described in (22). Thus, the E in BtuC falls in the -1 position, as for the members of the iron-siderophore cluster. Once BtuC was thus properly aligned with the EAA domain of other importers, DrrB and other exporters were then aligned with BtuC to obtain the alignment in Figure 6.

As seen in BtuC, the drug exporters, including DrrB, LmrA, MDR1 (N-terminal domain), and MDR1 (C-terminal domain), and other exporters shown in Figure 6 also contain the E residue at the -1 position and a somewhat less conserved $A_3...G_7$ central domain. The G at position 7 in the exporters does not seem to be very highly conserved; however, this group of proteins, along with BtuC, contains a highly conserved G at the -2 position and a positively charged residue R/K at position 4, which may be derived from the central domain A_3RALG_7 of the original EAA motif. Thus, it appears that the conserved sequence in DrrB and other exporters also bears a similarity to the EAA domain. From the sequence analysis described above and the alignment shown in Figure 6, we conclude that DrrB and other exporters contain a conserved motif bearing the sequence $GE_{-1}..A_3R/K..G_7$, which appears to be a modified version of the original EAA motif ($E_1AA_3RALG_7$). Furthermore, the motif present in the BtuC protein, a binding protein dependent importer, has characteristics of both the EAA motif of importers and the motif present in the exporters.

Site-Directed Mutagenesis of Residues in Domains of DrrB That Cross-Link with DrrA: To determine if residues within the interaction domains, identified by chemical cross-linking, are important for the function of the DrrB protein, conservative changes in certain residues in each

domain were made. These changes include S23A, G25A, E26D, and S35A in the N-terminal domain and C260A and A270S in the C-terminal domain. Doxorubicin resistance assays showed that S23A, G25A, and E26D mutations in the N-terminal domain confer sensitivity to between 4 and 6 μg/mL of doxorubicin while the cells containing the wild-type DrrA and DrrB grow up to 8-10 μg/mL of doxorubicin (Table 2). Since S35A mutation in the N-terminal domain and C260A and A270S in the C-terminal domain showed no change in the doxorubicin resistance phenotype as compared to the wild type, nonconservative mutations of these three residues, including S35I, C260E, and A270Y, were created. S35I mutation conferred doxorubicin sensitivity, while cells containing C260E and A270Y still remained relatively unaffected (Table 2). Protein expression analysis by SDS-PAGE showed that most mutations, except S23A, S35A, and A270Y show varying degrees of reduction in the levels of DrrA and DrrB. The most severe reduction in the levels of both DrrA and DrrB is seen with S35I mutation (Figure 7). G25A and E26D also showed significantly reduced levels of DrrA and DrrB, although these are less affected as compared to S35I. No significant change in the predicted secondary structure of any of the mutated proteins was seen by the Chou-Fasman or by the PROF method of secondary structure prediction.

DISCUSSION

The aim of the present study was to characterize domains in the DrrB protein that are involved in interaction with the ABC component DrrA. It has previously been shown that the DrrA and DrrB proteins are biochemically coupled for their function and stability, although they form separate subunits in the transporter (13). To understand how these two proteins regulate the stability and function of each other and result in the formation of a functional transporter, it is necessary to understand their molecular interactions. The strategy employed to study interaction between DrrA and DrrB made use of a cysteine to amine cross-linking approach. This study was facilitated by the availability of a model for the membrane topology of DrrB (17). Thus, it was possible to introduce cysteine residues in DrrB at the potential sites of interaction with DrrA. Since DrrA is a soluble protein, the sites of interaction are expected to lie in the domains of DrrB exposed in the cytoplasm. Cysteine-less DrrB was first created by replacing the single cysteine in DrrB at position 260 with a serine residue. Twenty single cysteine substitution mutants were then created at desired locations in the cysteine-less DrrB (Figure 1). Cross-linking between DrrA and DrrB was then carried out by using the chemical cross-linker GMBS, which enables the formation of a cross-link between a primary amine in one protein (DrrA) and a free sulfhydryl group in another (DrrB) (23, 24).

Doxorubicin resistance assays showed that the cysteine-less DrrB C260S as well as most of the single cysteine substitutions in DrrB did not affect the function of the transporter. Six (V53C, T70C, V92C, A129C, S236C, S249C) out of 20 substitutions created in this study, however, showed varying levels of doxorubicin-sensitive phenotype (Table 1). All of the affected residues, except S236C, lie in the predicted membrane spanning helices of DrrB. Both DrrA (Figures 4 and 5) and DrrB (not shown) are still expressed in all of the six strains. Secondary structure

analysis by the Chou-Fasman method showed that five (V53C, T70C, V92C, A129C, S249C) of these six mutants, which resulted in doxorubicin sensitivity, showed no change at all in their predicted secondary structure, the exception being S236C, which showed a split in the helical stretch predicted between residues 226 and 248 in the C terminus of DrrB. Thus, we can conclude that doxorubicin sensitivity in V53, T70, V92, A129, and S249C is not the result of a change in the secondary structure, whereas doxorubicin sensitivity in S236C may possibly be due to such a change. Since most of the affected residues, except S236C, occur in the membrane domains, it is possible that these residues may be involved in substrate recognition and thus may be crucial for the transport function of the DrrB protein. Studies to determine the role of these residues in the function of the transporter will be carried out in the future.

From the chemical cross-linking studies presented in this paper, we can conclude that DrrA cross-links with cysteines introduced in both the N-terminal and the C-terminal ends of DrrB. At the N-terminal end, the best cross-linking is seen with residues in the N-terminal cytoplasmic tail, even though it extends to residues in the first and second transmembrane domains and the first cytoplasmic loop. Interaction at the C-terminal end includes the seventh and the eighth transmembrane domain as well as the short C-terminal cytoplasmic tail of DrrB. It is intriguing that DrrA also cross-links with residues in the transmembrane domains of DrrB. This might indicate that DrrA embeds itself into the membrane during its interaction with DrrB. A similar phenomenon has been observed with other peripheral membrane proteins involved in transport, most significantly with SecA (25). It has been shown that some part of SecA is permanently embedded in the membrane (26-28) and that it may also play a significant role in the formation of the channel for the secretion of proteins (25).

Two alternate explanations (shown in the model in parts A and B of Figure 8) can account for the

observation that DrrA cross-links simultaneously with both the N- and C-terminal ends of DrrB. The models shown in Figure 8 depict the complex of DrrA and DrrB as a tetramer. On the basis of the cross-linking studies carried out earlier, it has been suggested that the stoichiometry of the functional complex of DrrAB may be A_2B_2 (13). Tetramers containing DrrA and DrrB were not seen in the present study and are not expected to form in this situation, because cross-linking with GMBS specifically requires a cysteine. Each subunit of DrrB has only one cysteine; thus, it can form a cross-link with only one subunit of DrrA. The possible mechanism of interaction between DrrA and DrrB by each of these models can be explained as follows (1). According to the model in Figure 8A, one subunit of DrrA binds to the N terminus of one subunit of DrrB and to the C terminus of the other subunit (2). According to the model in Figure 8B, the halves of a subunit of DrrB fold upon each other such that the N- and C-terminal ends of DrrB are close to each other, and one subunit of DrrA is then able to interact with both ends simultaneously. We currently favor the second model (Figure 8B), because suppressor analyses presently being carried out in this laboratory suggest that the N- and the C-terminal ends of DrrB may be on the same interface (unpublished results). However, further biochemical and genetic analyses are required to clearly determine whether the interaction between DrrA and DrrB occurs by the mechanism depicted in model A or B in Figure 8. It will also be important in future studies to determine if a single region in DrrA interacts with both termini in DrrB or whether the interaction with DrrB occurs to two separate domains in DrrA. Even though the cross-linking seen in this study is likely to occur between subunits within a tetramer, the possibility of cross-linking between tetramers cannot be ruled out. Both intra- and intermolecular cross-linking between cysteines in Pgp, where all four domains are present in a single molecule, has been seen (29). However, DrrA and DrrB form separate subunits that are held together by noncovalent

interactions within a tetramer of $DrrA_2B_2$; thus, at this time it is not possible to distinguish between cross-links within a tetramer vs those between tetramers. Crystal structure information for three ABC transporters, including E. coli BtuCD, E. coli MsbA, and V. cholera MsbA, has recently become available (18, 30, 31). This information provides valuable insights into the structure of the complex and into the domains involved in interaction between the membrane component and the ABC component in these systems. Interestingly, we find that present within the N-terminal domain of DrrB, which shows cross-linking with DrrA, is a sequence which has significant similarity to a sequence in the "L-loop" motif recently identified in BtuC by crystal structure analysis (18) (Figure 6). According to the crystal structure of the BtuCD complex, the L-loop in BtuC forms extensive contacts with the ABC component BtuD. It has also been reported that the sequence of the L loop bears local similarity to a sequence present in the first cytoplasmic loop of drug exporters, MDR1 and LmrA, and the lipid exporter, MsbA, and to the fourth cytoplasmic loop in CFTR (18). In the present study, we find similarity of the L-loop to a sequence in the N-terminal cytoplasmic tail of DrrB and biochemically demonstrate that this region may be involved in interaction with DrrA. In both DrrB and BtuC, this sequence lies in a helical stretch in a cytoplasmic domain of the protein; in DrrB, it is present in the N-terminal cytoplasmic tail, while in BtuC, it is present in the cytoplasmic loop between TM6 and TM7 (18).

From the analysis carried out in this study (Figure 6), we conclude that the L-loop of BtuC is actually similar to the EAA loop of other importers. We further conclude that DrrB and other exporters (as well as the importer BtuC) contain a conserved motif with the sequence $GE_1..A_3R/K..G_7$ and that it is actually a modified version of the original EAA motif ($E_1AA_3RALG_7$) present in the binding protein dependent permeases. Our results thus indicate for the first time

that the EAA motif or a modified version of this motif may be present at the interaction interfaces in both uptake and efflux systems, suggesting that the sequences involved in interaction are derived from an ancestor before the importers and exporters of the ABC family might have diverged.

A conserved motif, similar to the one identified in the N-terminal domain, was not identified in the C-terminal interacting domain of DrrB in this study. It should be mentioned, however, that a second helical region was identified in the third cytoplasmic loop, between residues 226 and 248, of DrrB. It is possible that, in the three-dimensional structure, this region (extending up to the C-terminal end of DrrB) may actually lie close to the conserved motif present in the N-terminal domain of DrrB and thus may contribute to forming the interface with DrrA, as is indicated by the cross-linking data (Figure 5C). Such architecture for DrrB would also be suggested by the model in Figure 8B. However, further biochemical and genetic studies are needed to answer some of these questions. Mutagenesis of certain residues in and around the conserved motif in the N terminus of DrrB, including S23A, G25A, E26D, and S35I, resulted in sensitivity to doxorubicin, although mutagenesis of C260 and A270 in the C terminus did not confer doxorubicin sensitivity significantly. These findings indicate that the motif in the N terminus is required for the function of the DrrB protein, whereas the domain in the C terminus may not be directly involved in function but may be at the same interface of interaction, as was suggested above. G25A, E26D, and S35I mutations also resulted in reduced levels of DrrA and DrrB. Since the stability of DrrB is known to be dependent on its interaction with DrrA, such a phenotype might indicate a direct role for these residues in interaction between DrrA and DrrB. Second-site suppressor analysis of the S23A, G25A, E26D, and S35I mutations will be carried out in the future to verify if these residues are indeed directly involved in interaction with DrrA, as is

suggested by the cysteine cross-linking studies reported here. Mutagenesis of certain residues in the conserved motif in MDR1 was also previously shown to result in loss of drug resistance (32); however, these residues were never biochemically shown to be directly involved in interaction with the ABC domain of MDR1. The only system where biochemical characterization has previously been carried out is the maltose uptake permease, where a typical EAA-loop (33), present in the membrane subunits MalF and MalG, has been shown to be involved in interaction with MalK by chemical cross-linking studies (34).

In summation, this study identifies two domains in DrrB that may be involved in interaction with DrrA and identifies a motif in the N-terminal cytoplasmic tail of DrrB. This motif has similarities to the EAA motif of binding protein dependent importers and the L-loop motif of BtuC. Other interactions between DrrA and DrrB, if present, could not be identified by the strategy employed in this study. Further studies, including the crystal structure analysis of the complex, would be required to identify other interactions and to determine the overall structure of the complex. Not only is the present study important for understanding the mechanism of interaction and function of the DrrAB complex, but it is also a necessary step toward elucidation of the temporal sequence of events leading to the biogenesis of the complex. Since the specific binding of DrrA to DrrB protects DrrB from proteolysis, we have previously suggested that DrrA may act like a chaperone to facilitate the proper assembly of the complex in the membrane (13). Furthermore, DrrB regulates the catalytic activity of DrrA via precise, but not yet understood, conformational changes. Future studies in this laboratory will identify the interacting domains in DrrA and will also try to unravel the concomitant conformational changes that are essential for the function of the complex as a transporter.

REFERENCES

1. Guilfoile, P. G., and Hutchinson, C. R. (1991) A bacterial analogue of the mdr gene of mammalian tumor cells is present in Streptomyces peucetius, the producer of daunorubicin and doxorubicin, *Proc. Natl. Acad. Sci. USA 88*, 8553-7.

2. Kaur, P. (1997) Expression and characterization of DrrA and DrrB proteins of Streptomyces peucetius in Escherichia coli: DrrA is an ATP binding protein, J. Bacteriol. 179, 569-75.

3. Fath, M. J., and Kolter, R. (1993) ABC transporters: bacterial exporters, Microbiol. Rev. 57, 995-1017.

4. Gottesman, M. M., and Pastan, I. (1993) Biochemistry of multidrug resistance mediated by the multidrug transporter, Annu. Rev. Biochem. 62, 385-427.

5. Ambudkar, S. V., Lelong, I. H., Zhang, J., Cardarelli, C. O., Gottesman, M. M., and Pastan, I. (1992) Partial purification and reconstitution of the human multidrug-resistance pump: characterization of the drug-stimulatable ATP hydrolysis, Proc. Natl. Acad. Sci. USA 89, 8472-8476.

6. Loo, T. W., and Clarke, D. M. (1995) P-glycoprotein. Associations between domains and between domains and molecular chaperones, J. Biol. Chem. 270, 21839-21844.

7. Ostedgaard, L. S., Rich, D. P., DeBerg, L. G., and Welsh, M. J. (1997) Association of domains within the cystic fibrosis transmembrane conductance regulator, Biochemistry 36, 1287-1294.

8. van Veen, H. W., Venema, K., Bolhuis, H., Oussenko, I., Kok, J., Poolman, B., Driessen, A. J., and Konings, W. N. (1996) Multidrug resistance mediated by a bacterial homologue of the human multidrug transporter MDR1, Proc. Natl. Acad. Sci. USA 93, 10668-10672.

9. Gileadi, U., and Higgins, C. F. (1997) Membrane topology of the ATP-binding cassette transporter associated with antigen presentation (Tap1) expressed in Escherichia coli, J. Biol.

Chem. 272, 11103-11108.

10. Klein, I., Sarkadi, B., and Varadi, A. (1999) An inventory of the human ABC proteins, Biochim. Biophys. Acta 1461, 237-262.

11. Gentschev, I., and Goebel, W. (1992) Topological and functional studies on HlyB of Escherichia coli, Mol. Gen. Genet. 232, 40-48.

12. Dean, M., Hamon, Y., and Chimini, G. (2001) The human ATP-binding cassette (ABC) transporter superfamily, J. Lipid Res. 42, 1007-1017.

13. Kaur, P., and Russell, J. (1998) Biochemical coupling between the DrrA and DrrB proteins of the doxorubicin efflux pump of Streptomyces peucetius, J. Biol. Chem. 273, 17933-17939.

14. Bass, R. B., Locher, K. P., Borths, E., Poon, Y., Strop, P., Lee, A., and Rees, D. C. (2003) The structures of BtuCD and MscS and their implications for transporter and channel function, FEBS Lett. 555, 111-115.

15. Welsh, M. J., Anderson, M. P., Rich, D. P., Berger, H. A., Denning, G. M., Ostedgaard, L. S., Sheppard, D. N., Cheng, S. H., Gregory, R. J., and Smith, A. E. (1992) Cystic fibrosis transmembrane conductance regulator: a chloride channel with novel regulation, Neuron 8, 821-829.

16. Wang, W., He, Z., O'Shaughnessy, T. J., Rux, J., and Reenstra, W. W. (2002) Domain-domain associations in cystic fibrosis transmembrane conductance regulator, Am. J. Physiol. Cell Physiol. 282, C1170-C1180.

17. Gandlur, S. M., Wei, L., Levine, J., Russell, J., and Kaur, P. (2004) Membrane topology of the DrrB protein of the doxorubicin transporter of streptomyces peucetius, J. Biol. Chem. 279, 27799-27806.

18. Locher, K. P., Lee, A. T., and Rees, D. C. (2002) The E. coli BtuCD structure: a framework

for ABC transporter architecture and mechanism, Science 296, 1091-1098.

19. Dassa, E., and Hofnung, M. (1985) Sequence of gene malG in E. coli K12: homologies between integral membrane components from binding protein-dependent transport systems, Embo J. 4, 2287-2293.

20. Sambrook, J., Fritsch, E. F., Maniatis, T. (1989) Molecular Cloning: A Laboratory Manual, 2nd ed., Cold Spring Harbor Laboratory Press, New York.

21. Nakamura, H., Tojo, T., and Greenberg, J. (1975) Interaction of the expression of two membrane genes, acrA and plsA, in Escherichia coli K-12, J. Bacteriol. 122, 874-879.

22. Saurin, W., Koster, W., and Dassa, E. (1994) Bacterial binding protein-dependent permeases: characterization of distinctive signatures for functionally related integral cytoplasmic membrane proteins, Mol. Microbiol. 12, 993-1004.

23. Brinkley, M. (1992) A brief survey of methods for preparing protein conjugates with dyes, haptens, and cross-linking reagents, Bioconjug. Chem. 3, 2-13.

24. Peeters, J. M., Hazendonk, T. G., Beuvery, E. C., and Tesser, G. I. (1989) Comparison of four bifunctional reagents for coupling peptides to proteins and the effect of the three moieties on the immunogenicity of the conjugates, J. Immunol. Methods 120, 133-143.

25. Wang, H. W., Chen, Y., Yang, H., Chen, X., Duan, M. X., Tai, P. C., and Sui, S. F. (2003) Ring-like pore structures of SecA: implication for bacterial protein-conducting channels, Proc. Natl. Acad. Sci. USA 100, 4221-4226.

26. Eichler, J., and Wickner, W. (1998) The SecA subunit of Escherichia coli preprotein translocase is exposed to the periplasm, J. Bacteriol. 180, 5776-5779.

27. Chen, X., Brown, T., and Tai, P. C. (1998) Identification and characterization of protease-resistant SecA fragments: secA has two membrane-integral forms, J. Bacteriol. 180, 527-537.

28. Ramamurthy, V., and Oliver, D. (1997) Topology of the integral membrane form of Escherichia coli SecA protein reveals multiple periplasmically exposed regions and modulation by ATP binding, J. Biol. Chem. 272, 23239-23246.

29. Urbatsch, I. L., Gimi, K., Wilke-Mounts, S., Lerner-Marmarosh, N., Rousseau, M. E., Gros, P., and Senior, A. E. (2001) Cysteines 431 and 1074 are responsible for inhibitory disulfide cross-linking between the two nucleotide-binding sites in human P-glycoprotein, J. Biol. Chem. 276, 26980-26987.

30. Chang, G., and Roth, C. B. (2001) Structure of MsbA from E. coli: a homologue of the multidrug resistance ATP binding cassette (ABC) transporters, Science 293, 1793-1800.

31. Chang, G. (2003) Structure of MsbA from Vibrio cholera: a multidrug resistance ABC transporter homologue in a closed conformation, J. Mol. Biol. 330, 419-430.

32. Currier, S. J., Kane, S. E., Willingham, M. C., Cardarelli, C. O., Pastan, I., and Gottesman, M. M. (1992) Identification of residues in the first cytoplasmic loop of P-glycoprotein involved in the function of chimeric human MDR1-MDR2 transporters, J. Biol. Chem. 267, 25153-25159.

33. Mourez, M., Hofnung, M., and Dassa, E. (1997) Subunit interactions in ABC transporters: a conserved sequence in hydrophobic membrane proteins of periplasmic permeases defines an important site of interaction with the ATPase subunits, Embo J. 16, 3066-3077.

34. Hunke, S., Mourez, M., Jehanno, M., Dassa, E., and Schneider, E. (2000) ATP modulates subunit-subunit interactions in an ATP-binding cassette transporter (MalFGK2) determined by site-directed chemical cross-linking, J. Biol. Chem. 275, 15526-15534.

TABLES

Table 1: Doxorubicin Resistance of *E. coli* N43 Cells Expressing Wild Type DrrA with DrrB Containing Different Cysteine Substitutions[a]

domain of DrrB	location of cysteine	amt of dox, μg/mL			
		0	4	6	8
(wild type)	C260	+++	+++	+++	++
N-terminus	S15C	+++	+++	+++	++
N-terminus	S23C	+++	+++	+++	++
N-terminus	S35C	+++	+++	++	++
N-terminus	A44C	+++	+++	++	+
TM 1	V53C	+++	++	++	−
TM 1	T70C	+++	+	+	+
P 1	S80C	+++	++	+	−
TM 2	V92C	+++	±	−	−
TM 2	S107C	+++	+++	++	++
C 1	V116C	+++	+++	+++	++
TM 3	A129C	+++	++	+	−
TM 4	T149C	+++	++	++	+
C 2	A160C	+++	+++	++	+
TM 5	V173C	+++	+++	++	+
TM 6	S213C	+++	+++	++	+
C 3	S236C	+++	++	+	−
TM 7	S249C	+++	+	+	−
TM 8	A270C	+++	+++	++	++
C-terminus	A282C	+++	+++	++	++
cysteine-less DrrB	C260S	+++	+++	+++	+++
vector only	pSU2718	++++	±	−	−

[a] Legend: +++, very good growth; ++, good growth; +, some growth; −, no growth.

TABLE 1: Doxorubicin Resistance of E. coli N43 Cells Expressing Wild Type DrrA with DrrB Containing Different Cysteine Substitutions[a]: [a] Legend: +++, very good growth; ++ good growth; + some growth; -, no growth.

Table 2: Doxorubicin Resistance of *E. coli* N43 Cells Expressing Wild-Type DrrA with DrrB Containing Mutations in the N-Terminal Cytoplasmic Tail or the C-Terminal End[a]

domain of DrrB	location of cysteine	amt of dox, μg/mL			
		0	4	6	8
(wild type)	C260	+++	+++	+++	++
N-terminus	S23A	+++	++	−	−
N-terminus	G25A	+++	±	−	−
N-terminus	E26D	+++	±	−	−
N-terminus	S35A	+++	+++	+++	+++
N-terminus	S35I	+++	±	−	−
C-terminus	C260A	+++	+++	+++	−
C-terminus	C260E	+++	+++	+++	−
C-terminus	A270S	+++	+++	+++	+
C-terminus	A270Y	+++	+++	++	++
vector only	pSU2718	+++	±	−	−

[a] Legend: +++, very good growth; ++ good growth; + some growth; −, no growth.

TABLE 2: Doxorubicin Resistance of E. coli N43 Cells Expressing Wild-Type DrrA with DrrB Containing Mutations in the N-Terminal Cytoplasmic Tail or the C-Terminal End[a]: [a]

Legend: +++, very good growth; ++ good growth; + some growth; -, no growth.

FIGURES

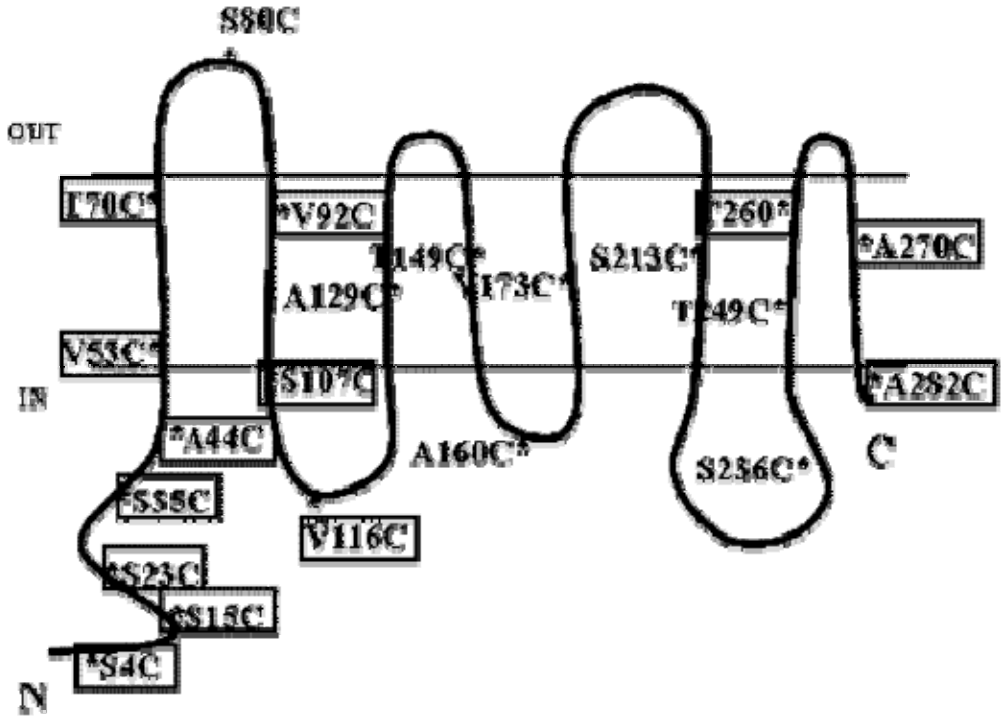

FIGURE 1: Topological depiction of the DrrB protein in the membrane showing the location of various cysteine substitutions: This drawing for the topology of DrrB in the membrane is based on a previously published model of the DrrB protein (*17*). The topological model of DrrB, which is based on gene fusion analysis, suggests that the DrrB protein contains eight transmembrane α-helices, with both the N and the C termini in the cytoplasm. To determine domains in DrrB that may be involved in interaction with DrrA, various single-cysteine substitutions were created in the DrrB protein. The location of these cysteines in DrrB is shown. The cysteine substitutions were made in the N- and C-terminal tails, the cytoplasmic loops, and

the transmembrane domains of DrrB. S80C is the only cysteine substitution in a periplasmic domain. Since DrrA was found to cross-link with the residues in the N-terminal cytoplasmic tail as well as with residues in TM1 and TM2, S80C was created specifically to map the entire N-terminal domain for its interaction with DrrA. The locations of various cysteines that showed cross-linking with DrrA are marked with rectangles.

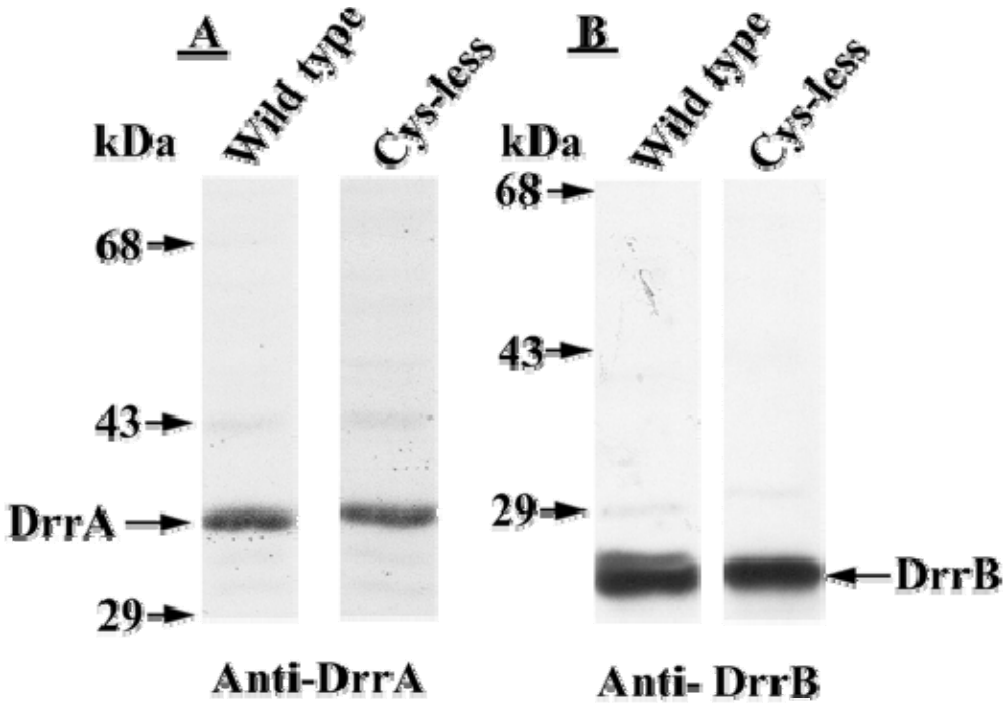

FIGURE 2: Levels of DrrA and DrrB in cells containing wild-type (C260) or cysteine-less DrrB (C260S): *E. coli* cells containing C260 or C260S were induced with IPTG. The lysates were prepared by French press, followed by ultracentrifugation to prepare the membrane fractions, as described in Materials and Methods. Twenty micrograms of membrane protein was analyzed by SDS-PAGE on 10% gels, followed by Western blot analysis using anti-DrrA or anti-DrrB antibodies. A chemiluminescence detection kit was used for detection of the bands. Migration of the standard proteins is shown on the left. (A) Probed with anti-DrrA. (B) Probed with anti-DrrB. Lanes: lane 1, wild-type C260; lane 2, cysteine-less mutant C260S.

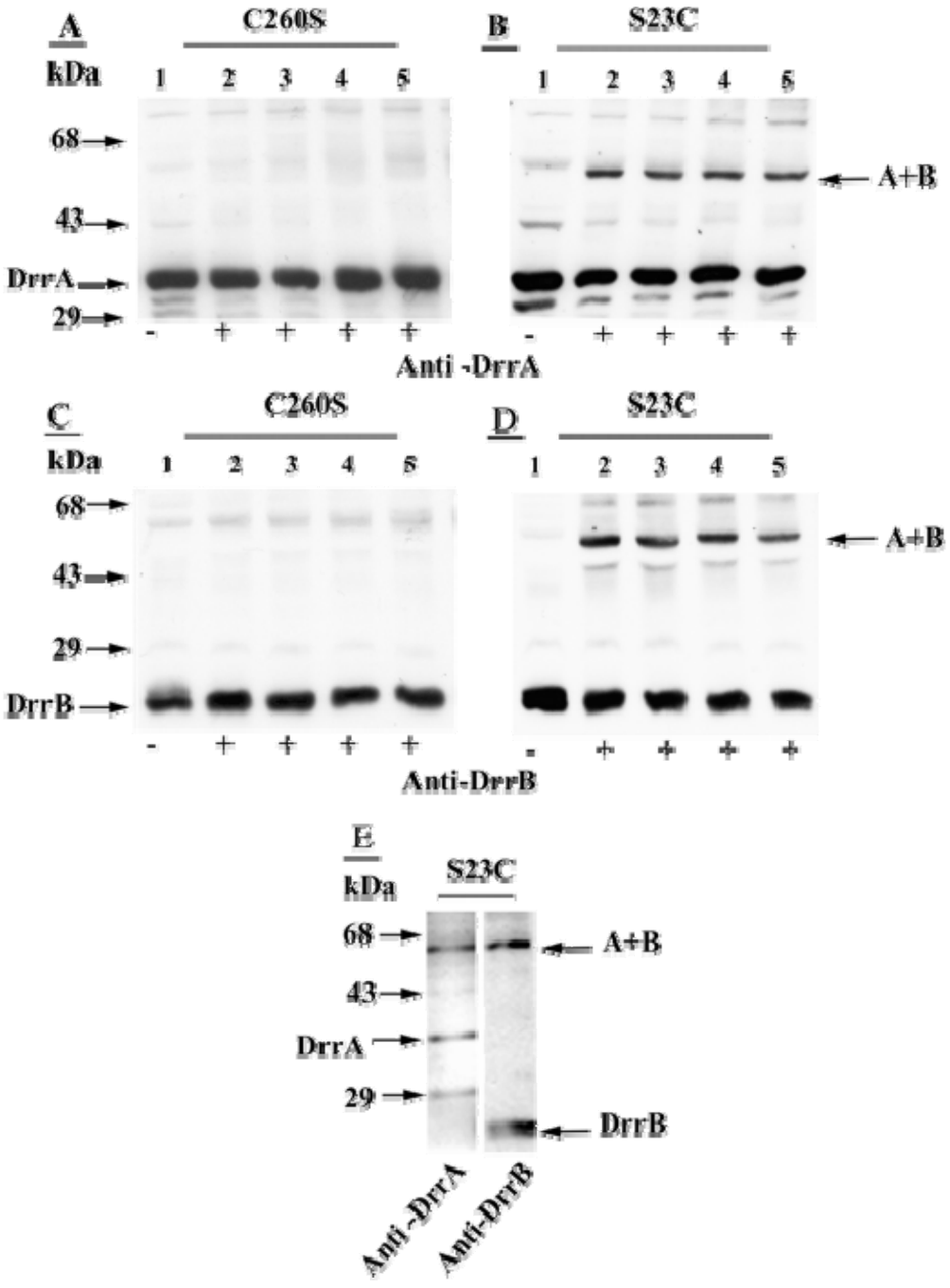

FIGURE 3: Chemical cross-linking between wild-type DrrA and DrrB containing cysteine substitution C260S or S23C: The cell membrane fraction containing the DrrA and DrrB

(C260S or S23C) proteins was subjected to chemical cross-linking using different concentrations of GMBS, as described in Materials and Methods. Fifty micrograms of protein was resolved by SDS-PAGE, followed by Western blot analysis using anti-DrrA or anti-DrrB antibodies. The "minus" and "plus" at the bottom of the lanes indicate the absence and presence of the cross-linker in the reaction, respectively. The migration of the protein standards is shown on the left. The location of the cross-linked species is marked as A+B. (A and B) Probed with anti-DrrA. (C and D) Probed with anti-DrrB. Lanes: lane 1, no GMBS; lane 2, 0.2 mM GMBS; lane 3, 0.4 mM GMBS; lane 4, 0.6 mM GMBS; lane 5, 0.8 mM GMBS. (E) A reaction containing the cross-linked S23C sample was analyzed by SDS-PAGE, as described above. The prestained high-molecular-weight protein marker from GibcoBRL was added to the sample before electrophoresis. The resolved proteins were transferred to the nitrocellulose membrane. The lane containing the S23C sample was vertically spliced into halves. Each half was then probed with either the anti-DrrA or anti-DrrB antibodies. Detection was done by the chemiluminescence method. After detection, the vertical halves were aligned using the prestained internal protein marker.

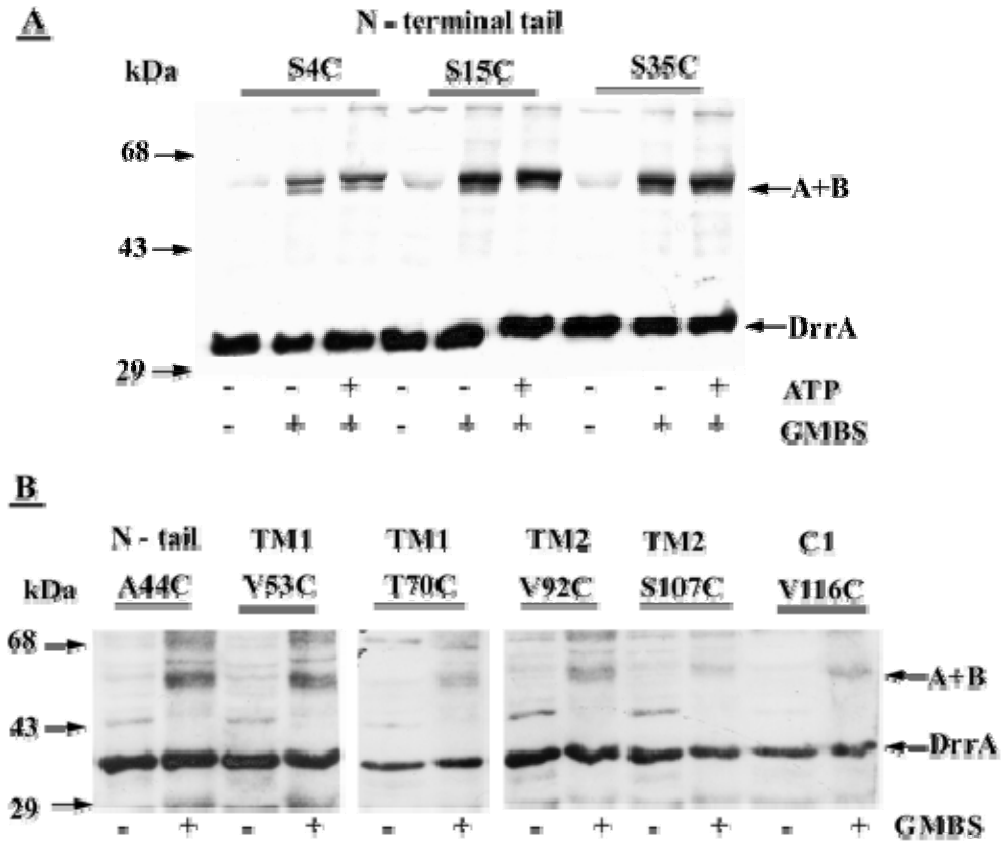

Figure 4: Chemical cross-linking between wild-type DrrA and DrrB containing cysteine substitutions in the N-terminal cytoplasmic tail, the transmembrane domains TM1 and TM2, and the cytoplasmic loop C1: The conditions used for chemical cross-linking between DrrA and DrrB were same as described in the legend to Figure 3. The proteins were resolved by SDS-PAGE, followed by Western blot analysis using anti-DrrA antibodies. The "minus" and "plus" at the bottom of the lanes indicate the absence and presence, respectively, of the cross-linker or ATP in the reaction. The migration of the protein standards is shown on the left. The location of the cross-linked species is marked as A+B. (A) S4C, S15C, S35C. (B) A44C, V53C,

T70C, V92C, S107C, and V116C. Figure 5 Chemical cross-linking between wild-type DrrA and DrrB containing cysteine substitutions in various transmembrane domains (TM3-TM8) or cytoplasmic loops C2 and C3. The conditions used for chemical cross-linking between DrrA and DrrB were same as described in the legend to Figure 3. The proteins were resolved by SDS-PAGE, followed by Western blot analysis using anti-DrrA antibodies. The "minus" and "plus" at the bottom of the lanes indicate the absence and presence of the cross-linker in the reaction, respectively. The migration of the protein standards is shown on the left. The location of the cross-linked species is marked as A+B. (A) S23C (positive control), A129C, T149C, A160C. (B) V173C, S213C, S236C, S249C. (C) C260 (wild type), A270C, A282C.

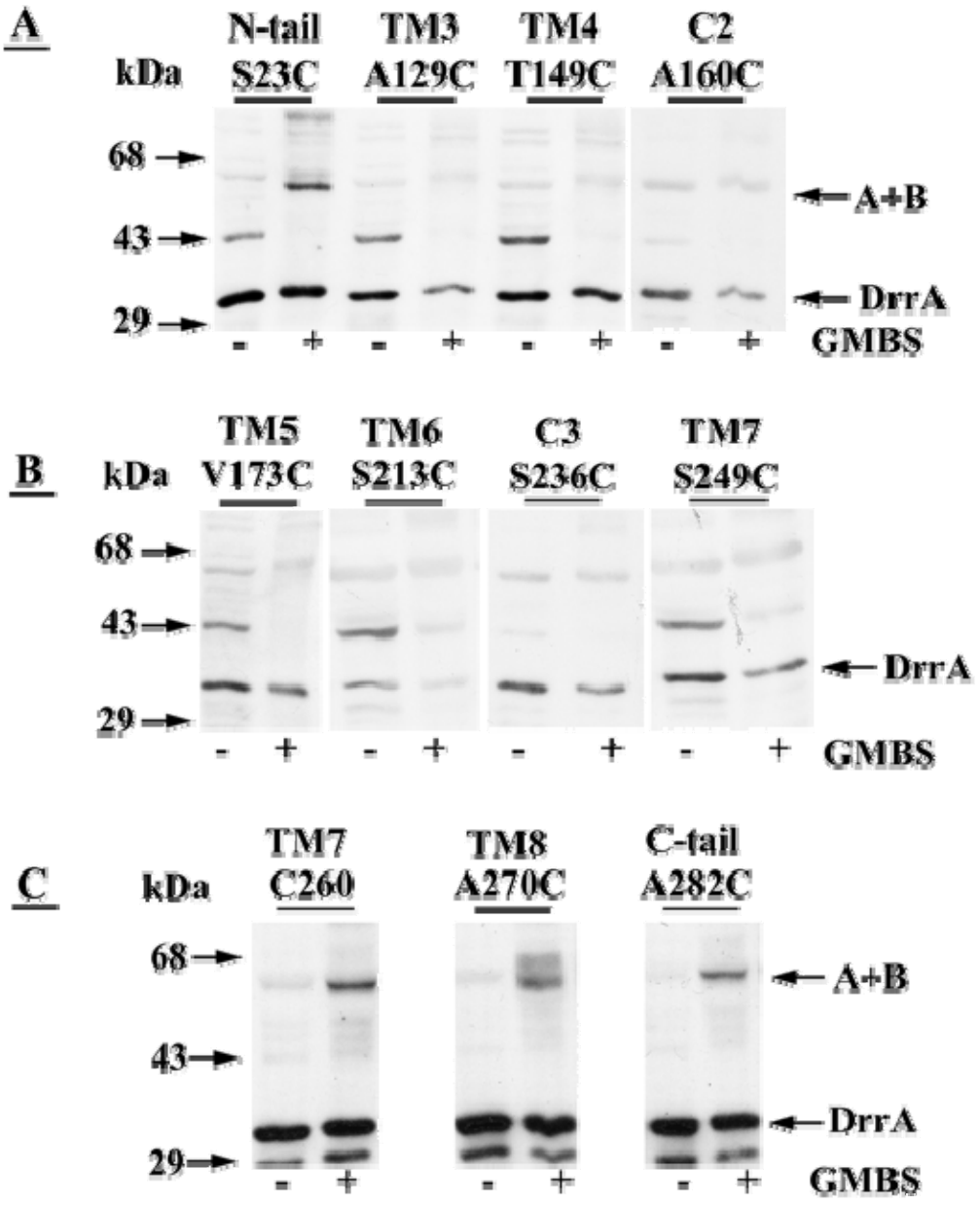

FIGURE 5: Chemical cross-linking between wild-type DrrA and DrrB containing cysteine substitutions in various transmembrane domains (TM3-TM8) or cytoplasmic loops C2 and C3: The conditions used for chemical cross-linking between DrrA and DrrB were same as described in the legend to Figure 3. The proteins were resolved by SDS-PAGE, followed by

Western blot analysis using anti-DrrA antibodies. The "minus" and "plus" at the bottom of the lanes indicate the absence and presence of the cross-linker in the reaction, respectively. The migration of the protein standards is shown on the left. The location of the cross-linked species is marked as A+B. (A) S23C (positive control), A129C, T149C, A160C. (B) V173C, S213C, S236C, S249C. (C) C260 (wild type), A270C, A282C.

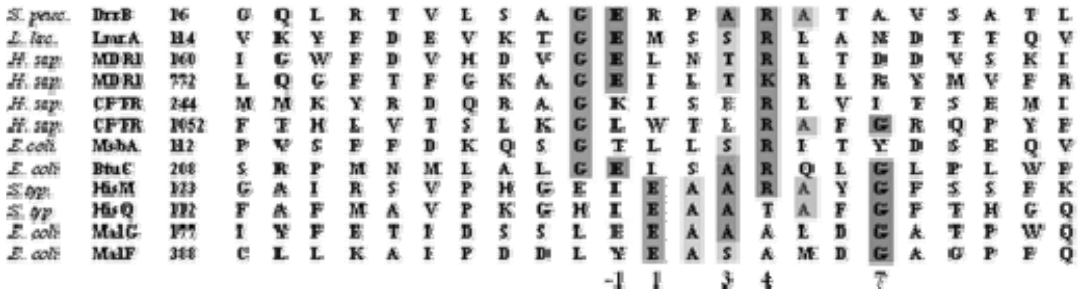

FIGURE 6: Alignment of the amino acid sequence of regions of DrrB, LmrA, MDR1 (N domain), MDR1 (C domain), CFTR (N domain), CFTR (C domain), MsbA, BtuC, HisM, HisQ, MalG, and MalF predicted to interact with their ABC domains/subunits: The dark gray regions show residues that are highly conserved, whereas the residues in light gray are less conserved. The first amino acid in the sequence of each protein is shown. The position of certain residues of the EAA domain is marked at the bottom. The E of the EAA loop is marked as position 1, and the E of the EAA loop in BtuC is marked as position -1.

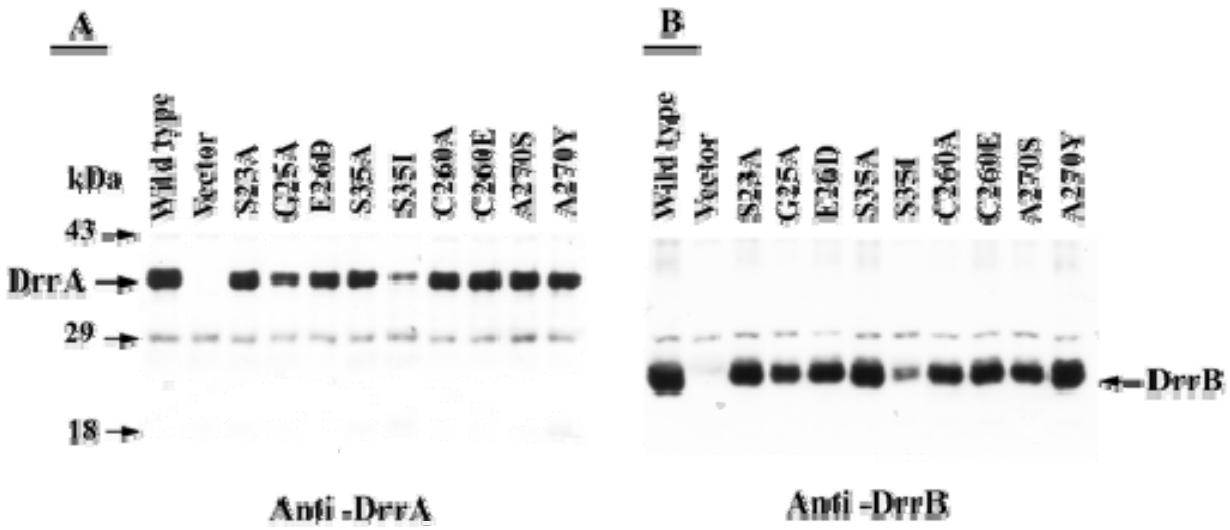

FIGURE 7: Levels of DrrA and DrrB in cells containing point mutations in the N-terminal cytoplasmic tail or the C-terminal end of DrrB: *E. coli* cells containing the indicated plasmids were induced with IPTG. The lysates were prepared by French press, followed by ultracentrifugation to prepare the membrane fractions. Twenty micrograms of membrane protein was analyzed by SDS-PAGE on 10% gels, followed by Western blot analysis using anti-DrrA or anti-DrrB antibodies. A chemiluminescence detection kit was used for detection of the bands. Migration of the standard proteins is shown on the left. (A) anti-DrrA. (B) anti-DrrB.

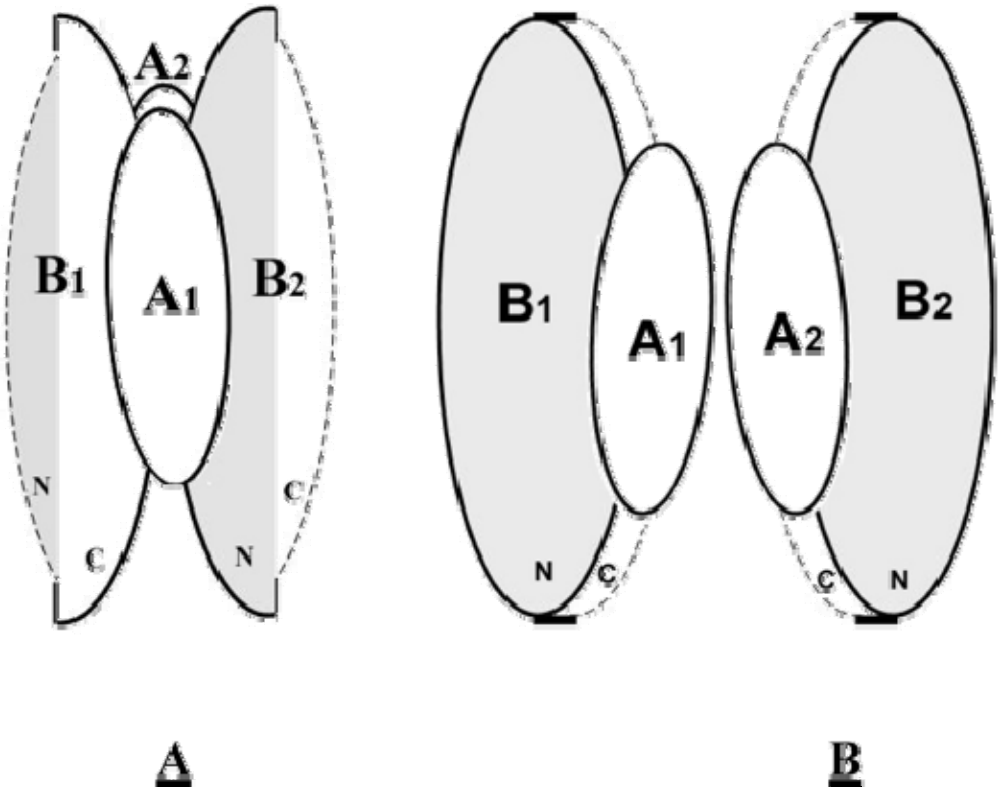

FIGURE 8: Models showing two possible mechanisms of interaction between DrrA and DrrB: The complex of DrrA and DrrB is shown as a tetramer consisting of two subunits of DrrA (A_1 and A_2) and two subunits of DrrB (B_1 and B_2). Further, each subunit of DrrB is shown as containing the N half and the C half (B_1N, B_1C and B_2N, B_2C). On the basis of the observation that DrrA interacts with both the N- and C-terminal ends of DrrB, two alternate models for interaction are proposed. (A) One subunit of DrrA interacts with two subunits of DrrB simultaneously. Thus, $DrrA_1$ contacts B_1C and B_2N. Similarly, $DrrA_2$ contacts B_1N and B_2C. (B) One subunit of DrrA interacts with both the N- and C-termini of the same subunit of DrrB. This

is possible if the halves of DrrB fold upon each other, allowing the N- and C-termini to come together on an interface. Thus, $DrrA_1$ binds to the interface of B_1N and B_1C. Similarly, $DrrA_2$ binds to the interface of B_2N and B_2C.

CHAPTER 2

Conformational changes in the Q-loop region of DrrA: Role of Q-loop in Dimerization of DrrA and in interactions with DrrB

ABSTRACT

DrrA and DrrB proteins form an ATP-dependent efflux pump for doxorubicin and daunorubicin in *Streptomyces peucetius*. DrrA, the catalytic subunit, forms a complex with the integral membrane protein DrrB. Previous studies have provided evidence for strong interaction between these two proteins, which was found to be critical for ATP binding to DrrA and for stability of DrrB. Chemical cross-linking experiments carried out previously showed that in the resting state of the complex DrrA and DrrB are in contact with each other. Use of a cysteine-to-amine crosslinker then allowed identification of the N-terminal cytoplasmic tail of DrrB (residues 1-53) as being the primary region of contact with DrrA. In this study single cysteine substitutions were introduced in different domains of DrrA in a strain already containing S23C substitution in the N-terminal tail of DrrB. By using different arm-length disulfide cross-linkers, we found that a cysteine placed in the Q-loop region of DrrA traps DrrA in the closed conformation. Furthermore, the same region of DrrA was also found to interact with DrrB, although the A-A interaction was much more prominent than the A-B interaction under these conditions. Based on additional data shown here, we propose that the A-B interaction identified here is specific to the closed state of DrrA and that this interaction identifies an important step in the communication of conformational changes between the N-terminal region of DrrB and the Q-loop region of DrrA. Significance of these findings in the mechanism of the DrrAB complex is discussed, and a model based on analyses of different conformations of DrrA and DrrB is presented.

INTRODUCTION

Self-resistance to doxorubicin and daunorubicin, two anticancer antibiotics, in the producer organism *Streptomyces peucetius* is conferred by DrrA and DrrB proteins (*1*). Together, these two proteins are proposed to form an ATP-driven drug pump for the export of these antibiotics, in the process conferring resistance (*1, 2*). We are interested in understanding the mechanism by which this prototype drug transporter carries out efflux of these antibiotics. This is important for a variety of reasons - the most important being that drug resistance is an emerging clinical problem and an understanding of the mechanism of resistance can help in designing effective strategies to combat drug resistance. Furthermore, the DrrAB system exhibits similarities with P-glycoprotein (Pgp), an MDR protein overexpressed in cancer cells. Pgp confers multidrug resistance by carrying out ATP-dependent efflux of a variety of structurally unrelated drugs, including doxorubicin and daunorubicin (*3*). Both DrrAB and Pgp also belong to the ABC family of proteins, therefore they share not only functional, but also sequence similarity. Thus, the DrrAB system can shed light on the mechanism and origin of multidrug resistance.

Most ABC transporters are composed of four domains: two transmembrane (TMD) and two nucleotide-binding domains (NBD). In Pgp, all four domains are present on a single polypeptide (*3*), while in DrrAB the domains are present on separate subunits (*1, 2, 4-6*). The functional complex of DrrAB is believed to consist of two subunits of DrrA and two of DrrB (*4*). Crystal structure data for several ABC proteins and intact ABC transporters are now available(*7-21*). These structures depict the structure of an NBD monomer to be L-shaped having two arms (*7-15*). Arm I contains the Walker A and Walker B motifs and is known as the RecA-like core ATP domain, while Arm II contains the signature motif as part of the α-

helical domain. A flexible Q-loop, which contains a highly conserved glutamine at its N-terminus, joins the RecA-like core domain to the α-helical domain. More recent crystal structures, especially of *E. coli* MalK (*17*) and *M. jannaschii* MJ0796 proteins (*8*), have also facilitated identification of the head-to-tail dimeric intermediates of the NBDs. In a head-to-tail dimer, the Walker A domain of one subunit is aligned with the signature domain from the opposing subunit, thus producing two nucleotide binding interfaces in a dimer. This conformation is achieved in the presence of ATP and is referred to as the closed conformation. In the nucleotide-free or the open conformation, the NBDs are no longer in close proximity with one another. The crystal structure of Sav1866, an MDR protein from *S. aureus*, however, implies a more limited movement of the NBD's. This could result from constraints on the structure caused by domain swapping and subunit twisting that have been noted in this structure (*21*). The Sav1866 structure captures the protein in the ADP-bound, outward-facing conformation, which resembles the state after release of the substrate into the extracellular space. The structure of this protein in the inward-facing conformation has so far not been visualized. Although availability of structural data from many different ABC proteins (both soluble and intact transporters) has already provided many important insights, still crystal structures present only snapshots. The biochemical characterization of these and other ABC transporters will thus be essential to complement structural studies and to develop a full understanding of the mechanisms by which energy is transduced between the ABC domains and the transmembrane domains. Characterization of the DrrAB drug export system can therefore provide a valuable understanding of the efflux systems, especially drug efflux systems.

The *drrAB* locus of *S. peucetius* has been subcloned and the proteins expressed in *E. coli* (*2*). The expression of these two proteins confers doxorubicin resistance in this host, indicating that the complex is assembled properly (2). Initial characterization of this system showed that DrrB is an integral membrane protein, and it contains eight transmembrane helices (*6*). DrrA, a peripheral membrane protein, forms a complex with DrrB in the cell membrane, and it functions as the catalytic subunit (*2*). Furthermore, DrrA and DrrB are biochemically dependent on each other for stability and function (*4*). For example, DrrA binds ATP/GTP only if it is in a complex with DrrB in the membrane, and DrrB is unstable if DrrA is absent. While many of these factors make the study of this system quite challenging; at the same time, because of its separate subunit architecture and tight inter-subunit interactions, it makes for an ideal system to study NBD: NBD and NBD: TMD interactions.

In a recent study conducted in this laboratory, we introduced several single cysteine substitutions in DrrB and then by using a cysteine to amine hetero-bifunctional cross-linker showed that DrrA interacts predominantly with the N-terminal cytoplasmic tail (residues 1-53) of DrrB (*5*). Within this region of DrrB, we also identified a sequence with similarities to the EAA motif found in importers of the ABC family of proteins, thus leading to the proposal that the EAA or the EAA-like motif may be involved in forming a generalized interface between the ABC and the TMD of both uptake and export systems. The goal of the present study was to characterize DrrA and to further our understanding of interactions between DrrA and DrrB. By using a combination of approaches, including point mutations, cysteine substitutions in the conserved domains of DrrA, and disulfide cross-linking analysis, we show here that the Q-loop region of DrrA plays an important role in dimerization of DrrA as well as in interactions with DrrB. We provide evidence showing that DrrA can be trapped in the closed conformation by

placing a cysteine substitution in the Q-loop region, thus implying that in the closed conformation two Q-loops from opposing subunits are in close proximity with each other. Furthermore, we also show that the interaction of the Q-loop with the N-terminus of DrrB is involved in transmitting conformational changes between DrrA and DrrB. Implications of these findings in the mechanism of the DrrAB complex are discussed, and a model depicting different conformations of DrrA and DrrB is presented. While this manuscript was being completed, a similar study carried out with the maltose system was published. This study supports and complements the conclusions of the present study by showing that in the closed state distance between the Q-loops of MalK is significantly reduced (*22*). Findings of this study will also be discussed.

EXPERIMENTAL PROCEDURES

Bacterial Strains and Plasmids: The bacterial strains used in this study were E.coli TG1 (23), N43 (*24*), HMS174 (*23*), and XL1 Blue (*23*). The plasmids used in this study included pDx101 (*drrAB* in pSU2718) and pDX121 (*drrAB* in pET28a).

Media and Growth conditions: The cells were grown in LB medium (*25*) at 37^{o}C, unless mentioned otherwise. Chloramphenicol was added to 20 μg/ml, and kanamycin was added to 30 μg/ml, where needed.

Site-directed mutagenesis of drrA: Single and double cysteine variants of DrrA were constructed by site-directed mutagenesis using a strategene QuikChange multisite-directed mutagenesis kit (La Jolla, CA). The strategy involved the use of complimentary primers that incorporated the change at the required position. The templates used included pDx101 and pDx121, and the primers were designed as described earlier (*5*). The single cysteine present in DrrB was first mutagenized to serine (C260S). Cysteine substitution mutants were then created at amino acid positions 45, 89, 140, 174, 195 and 198 in DrrA. These mutants were named A45CA(A)/C260S(B), Y89C(A)/C260S(B), Y140C(A)/C260S(B), S174C(A)/C260S(B), T195C(A)/C260S(B), and Y198C(A)/C260S(B). For double-cysteine mutants, cysteine substitutions of DrrA were created in the DrrB S23C background. Double substitutions were created at amino acid positions 89, 91,174,195 and 198 of DrrA. These mutants were named Y89C(A)/S23C(B), S91C(A)/S23C(B), S174C(A)/S23C(B), T195C(A)/S23C(B) and Y198C(A)/S23C(B). Conservative and non-conservative point mutations in certain residues in different domains of DrrA were also made. These changes include G44S, G44A, K47E, K47R (Walker A), L160A, D164A, E165Q (Walker B), Q88E (Q-loop), and S141R and G143S (signature domain).

Doxorubicin Resistance Assay: Doxorubicin resistance assays were carried out on M9 (*23*) plates supplemented with 0.25% casamino acids. The plates were layered with 4 mL of top agar (0.8% agar in M9 medium) containing the desired concentration of doxorubicin. Briefly, 4 mL of top agar containing 0, 6, 8, or 10 μg/mL of doxorubicin (Sigma Chemicals) and 1 mM thiamine-HCl was poured on top of M9 plates. The plates were covered with foil to prevent exposure to light. N43, a doxorubicin-sensitive strain of *E. coli*, was transformed with the indicated plasmids. Freshly transformed cells were grown for 8 hours in 3 mL of LB with the appropriate antibiotics. 1 μL of the 8 hour old N43 culture from above was streaked on plates containing doxorubicin. N43 containing the plasmid pSU2718 was used as a negative control. The plates were then incubated at 37^{o}C overnight, and growth was recorded after 24 hours of incubation.

Nucleotide binding properties of DrrA mutants: To study nucleotide binding, photolabeling of the various mutants of DrrA with [α-^{32} P] ATP was carried out (*2, 4*). A 50 mL culture of *E.coli* TG1 cells containing the indicated plasmids was grown to mid-log phase and induced with 0.25 mM IPTG. Growth was continued for an additional 3 hours at 37^{o}C. The cells were spun down and resuspended in 1.5 ml QAE buffer (25 mM Tris.Cl, pH 8.0, 20% glycerol, 2 mM EDTA) containing 1 mM DTT and lysed by a single passage through a French pressure cell at 20,000 psi. The cell lysates were then centrifuged at 10,000 g for 15 minutes to remove unbroken cells. The supernatant was centrifuged at 100,000 g for 1 hour to prepare membrane protein. ATP binding assay was carried out in a 100 μl reaction volume containing 0.1 mg membrane protein, 25 mM Tris.Cl, pH 8.0, 20% glycerol, 2 mM EDTA, 10 μM ATP, 250 μM Mg^{2+}, 35 μM dox, and 10 μCi [α-^{32} P] ATP. The mixture was exposed to UV light at 254 nm for 30 minutes on ice. Proteins were precipitated with 400 μl of 10% TCA on ice for 30

minutes. Samples were spun down at 14,000 g for 15 minutes and the supernatant was resuspended in 20 µl 4X Laemmli sample buffer containing 5 µl of 1 M unbuffered Tris. The samples were solubilized by heating at 55^{o}C for 10 minutes and analyzed by SDS-PAGE using a 10% polyacrylamide gel, followed by autoradiography.

Purification of wild-type and mutant DrrAB proteins: DrrAB proteins were purified using pDx121, which introduces his-tags at the N-terminus of DrrA and the C-terminus of DrrB. HMS174 cells containing the indicated plasmid were induced with IPTG, and membrane fractions were prepared, as described above. DrrAB proteins were solubilized from the membrane and purified as a complex using Ni-NTA column. The proteins were analyzed by SDS-PAGE using a 10% polyacrylamide gel, followed by Western blot analysis with anti-DrrA or anti-DrrB antibodies. Details of the method used for solubilization and purification of the DrrAB proteins are being reported elsewhere (unpublished data). The yield of the DrrAB proteins was roughly 0.43 µg/ul.

Homobifunctional (disulphide) and Heterobifunctional (cysteine to amine) Cross-Linking: For homobifunctional cross-linking, a 100 µl reaction volume containing 250 µg of membrane protein in 0.1 M phosphate buffer, pH 7.4, was treated with thiol-specific reagents copper phenanthroline (CuPhe) (3 mM $CuSO_4$/9 mM 1, 10 phenanthroline), DTME (Dithio-bis-maleimidoethane) (1 mM) (Pierce chemicals), or MTS (3,6,9,12,15-Pentaoxaheptadecane-1methanethiosulfonate) (0.2 mM) (Toronto Research Chemicals) for 30 minutes at room temperature. For heterobifunctional cross-linking, a 100 µl reaction volume containing 250 µg of membrane protein in 0.1 M phosphate buffer, pH 7.4, was treated with GMBS (*N*-[γ-maleimidobutyryloxy]succinimide ester) (1 mM) (Pierce Chemicals) for 1 hour at room temperature in a light-protected area. The reactions were terminated by the addition of 25 µl

4X non-reducing Laemmli sample buffer. The samples were mixed thoroughly and set aside for 5 minutes at room temperature. A 25 µL portion (50 µg of membrane protein) of the reaction mixture was then analyzed by SDS-PAGE using a 10% polyacrylamide gel, followed by Western blot analysis using either anti-DrrA or anti-DrrB antibodies. To study the effect of ATP and ATPγS on cross-linking, 35 µg purified wild-type or mutant DrrAB proteins were incubated with or without 10 µM ATPγS, 10 µM ATP, or 1 mM DTME for 30 minutes at room temperature. Prior to incubation, purified proteins were reduced with 1 mM DTT and immediately passed through a 10K Nanosep centrifugal column (Pall Corporation) to remove DTT. The reaction was terminated by the addition of 4X non-reducing Laemmli sample buffer. 15 µg protein was analyzed by SDS-PAGE, followed by western blot analysis.

Determination of composition of the 78 kDa cross-linked species by SELDI: DrrAB proteins containing a cysteine at position 89 in DrrA (labeled Y89C(A)/C260S(B)) were purified by using a Ni-NTA column. The purified sample was subjected to disulphide cross-linking using DTME as described above. The samples were analyzed by SDS PAGE using 10% polyacrylamide gel, followed by Coomassie Blue staining (*23*). The band of interest was excised and subjected to in-gel digestion with 100 ng trypsin. The mass of the trypsin-generated peptide fragments was determined by Surface Enhanced Laser Desorption/Ionization (SELDI) using the CIPHERGEN Protein Chip® Technology in the core facility of the Department of Biology at Georgia State University.

Fourier resonance energy transfer (FRET): In separate reactions, 5 mg of membrane protein prepared from A45C(A)/C260S(B) or Y140C(A)/C260S(B) was incubated with either 1mM NBD-Cl (7-chloro-4-nitrobenzo-2-oxa-1, 3-diazole) for 2 hours at 22^{o}C or with 30 µM MIANS [2-(4'-maleimidylanilino) naphthalene-6-sulfonic acid] for 30 minutes at 22^{o}C. Unreacted

probes were quenched with 1 mM dithioerythritol (DTE), and the samples were passed through a desalting column (Zeba TM Desalt Spin column, Pierce). NBD or MIANS-labeled DrrAB proteins were solubilized and purified from the cell membrane, as described earlier. For FRET analysis, 250 µL MIANS-labeled, purified A45C(A)/C260S(B) (approx. 100 µg of protein) proteins were mixed with 250 µL NBD-labeled, purified Y140C(A)/C260S(B) and incubated for 30 minutes at 22^{o}C to obtain doubly-labeled MIANS-NBD-A45C/Y140C DrrAB dimers. As controls, MIANS-labeled A45C(A)/C260S(B) was mixed with NBD-labeled A45C(A)/C260S(B), and MIANS labeled Y140C(A)/C260S(B) was mixed with NBD labeled Y140C(A)/C260S(B) for 30 minutes to obtain doubly-labeled MIANS-NBD-A45C DrrAB and MIANS-NBD-Y140C DrrAB, respectively. For clarity, the controls and the experimental set-up are shown below in the form of a table.

MIANS A45C + NBD A45C	Control 1
MIANS Y140C+ NBD Y140C	Control 2
MIANS A45C + NBD Y140C	Experiment

Fluorescence spectra were recorded on an Alphascan-2 spectrofluorimeter (Photon Technology International, London, Ontario, Canada). The excitation and emission slits were set at 4 nm. The excitation wavelengths for MIANS and NBD fluorophores were 322 nm and 465 nm, respectively, while emission was monitored at 420 nm and 523 nm, respectively for individual probes. However, for the energy transfer experiment (table above), samples were excited at 322 nm (for MIANS) while emission was monitored between 350 nm and 600 nm to include both MIANS and NBD.

RESULTS

Characterization of point mutations in DrrA: DrrA, the ABC subunit of the DrrAB pump, contains several conserved domains, as shown in the alignment of the amino acid sequence of DrrA with 5 other importers and exporters belonging to the ABC family (Figure 1A). The alignment was determined by ClustalW, and the secondary structure was analyzed by the PHD method of prediction. The alignment highlights the conserved domains within the ATPase domain of each transporter and shows high sequence similarity between each of them. These domains in DrrA have been diagrammatically represented in Figure 1B. To study the effect of mutations within the conserved domains on function of the DrrAB transporter, both conservative and non-conservative changes in residues within each domain were made. These include G44S, G44A, K47E and K47R in Walker A; L160A, D164A and E165Q in Walker B; Q88E in Q-loop; and S141R and G143S in the signature motif. Protein expression analysis showed that mutations in the conserved domains caused varying degrees of reduction in the levels of DrrA and DrrB (Figure 2A, left panels) as compared to the wild-type. Nucleotide binding properties of DrrA in each of these mutants was analyzed by [α-32P] ATP cross-linking experiments. These data are shown in Figure 2A, right panels. As expected, Walker A mutations significantly reduced ATP binding to DrrA. Interestingly, E165Q, a Walker B mutant, showed slightly higher levels of ATP binding as compared to the wild-type. The conserved glutamate in the Walker B domain is known to be crucial for hydrolysis of ATP but not for ATP binding, thus the ATP binding phenotype observed for E165Q is consistent with that role. (Preliminary studies conducted in this laboratory have shown that the Kd for ATP binding in both wild type and E165Q is in the range of 250-350 μM (data not shown)). A non-conservative mutation in the adjoining residue, D164A, showed drastic reduction in expression levels of DrrA and DrrB and thus prevented ATP binding. Q88E mutation in the Q-loop

reduced ATP binding but did not completely abolish it, while the signature domain mutant, G143S, had no effect on binding of ATP. A non-conservative mutation, S141R, in the signature domain affected expression and completely abolished ATP binding.

It was previously shown that [α-32P] ATP binding to wild type DrrA is competed by unlabeled ATP (2). To determine if this is true for the [α-32P] ATP binding seen in the mutants, competition experiments using 10-fold and 50-fold higher concentration of unlabeled ATP were carried out using K47R, Q88E, E165Q, S141R. Data in Figure S3 show that 10-fold higher concentration of unlabeled ATP is sufficient to completely prevent labeling with [α-32P] ATP in all of the mutants tested. Finally, ATP binding to DrrA is known to be stimulated by doxorubicin (2). The ATP binding experiments shown in Figure 2A, 2B and 2C were carried out in the presence of doxorubicin, as indicated in Material and Methods. The data in Fig. 2D, however, show [α-32P] ATP binding to a selected set of mutants both in the absence and presence of doxorubicin. These data show that doxorubicin stimulates ATP binding to these mutants, as seen with the wild type protein. E165Q, however, binds ATP well even in the absence of doxorubicin, indicating that this mutation traps the DrrA protein in the closed conformation. The experiments shown in Figure 2A-2C were repeated three times. . The intensities of the bands in both Western blots (left panels) and the autoradiograms (right panels) were determined by densitometric scanning using Quantity one analysis software (Biorad). The averages (from 3 or 4 experiments) of the ratio of ATP bound/protein concentration for selected mutants used for further experiments in this article were plotted in a histogram shown in Figure S2. The error bars reflect standard deviations.

To determine if mutations in DrrA have an effect on the overall function of the transporter, doxorubicin resistance assays were carried out. The data show that while cells

containing wild-type DrrA and DrrB grow up to 10 μg/ml of doxorubicin (Table 1), the Q-loop mutant Q88E grows up to 6-8 μg/ml and all other mutants grow up to 4-6 μg/ml of doxorubicin. Two non-conservative changes in the Q88 residue (Q88S and Q88N) were also made. These two changes conferred greater sensitivity to doxorubicin as compared to Q88E. Some of these mutations described in Figure 2 were used in the following experiments described in this paper.

Head-to- tail conformation of DrrA dimers: To determine if DrrA undergoes head-to-tail dimerization, as reported for other ABC proteins (*8, 16, 17, 20, 26-29*), fourier resonance energy transfer (FRET) experiments were carried out. In a head-to-tail dimer, the Walker A domain of one subunit is expected to interact with the signature domain of the other. To determine such a conformation, a single cysteine substitution was introduced within the Walker A (A45C(A)/C260S(B)) or the ABC signature motif (Y140C(A)/C260S(B)) of DrrA. The expression levels of DrrA and DrrB proteins in both of these mutants were unaffected (data not shown). The membrane fractions prepared from strains containing these mutations were then labeled with either MIANS or NBD-Cl. Following incubation with either probe, the DrrAB proteins were immediately purified. MIANS and NBD-Cl are fluorophores that become fluorescent only on binding to cysteine residues within a protein. The fluorescent emission spectra were measured spectrofluorimetrically to determine whether binding of the probe to cysteines in DrrA took place. Data in Figure 3A, panels A and B show that both A45C and Y140C could be labeled with either MIANS or NBD-Cl. It has previously been shown that the fluorescence emission spectrum of MIANS overlaps fairly well with the absorbance spectrum of NBD-Cl (*30*). Thus MIANS and NBD-Cl form a good donor-acceptor pair. Once the labeling of DrrA with these probes was successfully achieved, we wanted to

determine if the energy transfer would occur between them. If the DrrA dimer is a head-to-tail dimer, we would expect energy transfer between A45C-MIANS and Y140C-NBD-Cl. Thus, in this experiment, excitation was carried out at 322 nm for MIANS, while emission was carried out between 350 nm and 600 nm to be able to observe fluorescence emission of both MIANS and NBD-Cl. The data are shown in Figure 3A, panel E. When excitation is carried out at 322 nm, MIANS-A45C protein shows an emission peak at 420 nm (Panel E, curve 1) as is also seen in panel A, (curve 1). NBD-Y140C gives no signal under these conditions, (Panel E, curve 2), as expected. When these proteins were mixed, excitation at 322 nm resulted in significant (about 90%) quenching of the MIANS emission peak (Panel E, curve 3). This quenching is simultaneously accompanied by an emission peak at 530 nm (Panel E, curve 3) from NBD-Y140C. These data show that fluorescence energy transfer occurred between MIANS bound to A45C and NBD-Cl bound to Y140C. Control experiments, where A45C-MIANS was mixed with A45C-NBD-Cl, or Y140C-MIANS was mixed with Y140C-NBD-Cl, are shown in Figure 3A, panels C and D, respectively. When excitation was carried out at 322nm, the fluorescence property of either probe in these situations remained unaltered (curve 3), indicating that FRET did not occur between two probes in the Walker A domains or the signature domains. These data indicate that the Walker A motif of one DrrA molecule lies in close proximity to the signature motif of another DrrA molecule in the DrrA dimer. The three dimensional model of DrrA dimers was built based on MalK dimer, the closest homologue whose structure had been published in the PDB (PDB accession code: 1Q12) (Figure 3B).The model shows a similar head-to-tail dimeric arrangement of the DrrA dimers compared to that of the MalK dimers.

Characterization of subunit interactions by use of disulphide cross-linkers: The N-terminal cytoplasmic tail of DrrB, including residues 1- 53, was previously shown by GMBS-mediated (cysteine to amine) cross-linking experiments to be involved in interaction with DrrA (5). To determine regions in DrrA that may be involved in interaction with the N-terminal region of DrrB, cysteine substitutions were made in DrrA. Wild-type DrrA contains no cysteine, while wild-type DrrB contains one at position 260, which was modified to a serine (5). Cysteine substitutions in DrrA were made in a plasmid already containing S23C substitution in DrrB, or in the cys-less DrrB background, unless indicated otherwise. The residues chosen for cysteine substitutions in DrrA were selected so that they were positioned either within or at close proximity to conserved domains in DrrA, and that they would result in conservative changes. While ten double mutants were originally constructed, five mutations showed significantly reduced levels of DrrA and DrrB expression and thus were not used for further investigation. The remaining five double cysteine mutants (Y89C(A)/S23C(B), S91C(A)/S23C(B), S174C(A)/S23C(B), T195C(A)/S23C(B) and Y198C(A)/S23C(B)) were analyzed by cross-linking with a 0 Å disulphide cross-linker, CuPhe. Cross-linking between S23C in DrrB and a cysteine in DrrA is expected to result in a 65 kDa species. The data in Figure 4 show, that in two cysteine mutants, namely Y89C(A)/S23C(B) and S91C(A)/S23C(B), both in the Q-loop region, a major cross-linked species migrating at about 78 kDa (marked as *) was produced instead. This species was only seen in the blots probed with anti-DrrA antibody (Figure 4A), but was absent in the blots probed with anti-DrrB antibody (Figure 4B). In addition, a minor 65 kDa species (also marked as *) was also produced, which could be detected by both anti-DrrA (Fig. 4A) and anti-DrrB (Fig. 4B) antisera, indicating that it is a complex of DrrA and DrrB. In the blot shown in Fig. 4B (probed with anti-DrrB antibody), we also see DrrB dimers

in samples treated with CuPhe. Since DrrB dimers are produced in all cysteine variants tested (not shown), this species results from non-specific association of DrrB monomers in the presence of a disulfide cross-linker. Such non-specific association of cysteine variants of DrrA is clearly not seen (shown in Fig. 4A), thus we conclude that DrrB, being a membrane protein, is more prone to this kind of aggregation.

When another disulfide cross-linker DTME was used, we found that once again the major cross-linked species with Y89C DrrA corresponded to 78 kDa in size (Fig. 5, lanes 3-4). To determine whether the 78 kDa cross-linked species was formed between two monomers of DrrA (Y89C(A)/Y89CDrrA) or between DrrA and DrrB (Y89C(A)/S23C(B)), two other variants of DrrB were tested. One contained C260 as the only cysteine in DrrB (Y89C(A)/C260(B)) and the other contained no cysteine (Y89C(A)/C260S(B)). DTME-mediated disulphide cross-linking showed that the location of a cysteine in DrrB (whether S23C (Figure 5A, lanes 3-4) or C260 (Figure 5A, lanes 5-6)) made no difference to the Y89C-mediated disulphide cross-linking. Furthermore, the 78 kDa cross-linked species was formed even in the absence of a cysteine in DrrB (Figure 5A, lanes 7-8), suggesting that the cross-linked species may be a homodimer of DrrA.

To determine the exact composition of the 78 kDa cross-linked species and to verify that it represents DrrA dimer, the DrrAB proteins were purified from the single cysteine mutant (Y89C(A)/ C260S(B)) cloned in a pET vector (Figure 6). The purified Y89C protein contained the 78 kDa species even without addition of the cross-linker (Figure 6, lane 9), indicating that the two cysteines are at very close proximity with one another and were therefore spontaneously oxidized to yield a disulphide cross-linked species. The formation of the cross-linked species was further enhanced on addition of DTME (Figure 6, lane 10). The

gel slice containing the 78 kDa species was excised from the gel shown in Figure 6, lane 9, and subjected to SELDI analysis using the CIPHERGEN Protein Chip ® Technology, as described under Experimental Procedures. Analysis of the peptide map of the 78 kDa species showed that 96.4% of the peptides generated by the 78 kDa species matched that of the DrrA protein. Therefore, all of the above data together suggest that the 78 kDa species is a multimer, most likely a dimer, of DrrA. The DrrA monomer is 36.5 kDa in size, thus the dimer should migrate at 73 kDa on SDS-PAGE. However, the cross-linked species migrates at about 78 kDa. This may be due to the specific conformation of the dimer resulting from cross-linking. To determine if formation of the 78 kDa DrrA dimeric species is DrrB-dependent, purified DrrA or DrrAB proteins were subjected to DTME cross-linking (Fig. 6B). As reported earlier, both DrrA and DrrB proteins are dependent on each other for stability (*4*). The expression of DrrA in the absence of DrrB is about 50-60% of the DrrAB-containing system, while the expression of DrrB protein is undetectable in the absence of DrrA (*4*). The densitometric analysis of the monomeric and dimeric species seen in Fig. 6B show that while the yield of purified DrrA in DrrA-alone system is half of the DrrAB system, the yield of the cross-linked 78 kDa species is almost 10-fold reduced, indicating that DrrB is required for efficient dimerization of DrrA.

Effect of ATP and ATPγS on dimer formation: To study the effect of nucleotide binding on DrrA homodimer formation, cysteine-less DrrAB and Y89C(A)/C260S(B) proteins were purified. The purified proteins were incubated with ATP or the non- hydrolyzable analog ATPγS. Since the purified Y89C DrrA protein spontaneously forms the 78 kDa species, the samples were first reduced with DTT to break up the disulphide bonds (Figure 7A, lane 1). On addition of DTME (Figure 7A, lane 4), or ATPγS (Figure 7A, lane 3) to this reduced protein,

the 78 kDa species was again seen. Addition of ATP to the Y89C protein (Fig. 7A, lane 2) or ATPγS to the cysteine-less mutant did not induce dimerization (Figure 7A, Lane 7). To determine the role of the nucleotide binding domain in Y89C-mediated dimerization, a K47R mutation in the Walker A domain was constructed in the existing Y89C(A)/C260S(B) mutant. K47R mutation completely abolished ATP binding to DrrA (Figure 3, panel A). The resulting mutant protein (Y89C, K47R(A)/C260S(B)) was purified and cross-linked with the disulphide cross-linker DTME (Figure 7B). The DrrA protein in this mutant failed to dimerize in the presence of DTME even though it contained the Y89C mutation (Figure 7B, lanes 5-6). Further characterization was done by using E165Q, a mutation in the Walker B domain. Since E165Q binds ATP very well (Figure 3B, right panel), this mutation was introduced in the existing Y89C(A)/C260S(B) mutant. This protein was able to form disulphide cross-linked species in the presence of DTME (Figure 7C, lane 8). Furthermore, this protein also showed significant dimerization on addition of either ATP or ATPγS, even without addition of DTME (Figure 7C, lanes 5-7). E165Q alone, in the absence of Y89C mutation, did not show dimerization in the presence of DTME, ATP or ATPγS (Figure 7C, lanes 1-4). Together, the data from Figures 7B and 7C suggest that an intact ATP binding Walker A domain is required for the formation of DrrA dimers and that the Y89C dimers can be held together either by use of the disulfide cross-linker or by binding of ATPγS to the dimer interface. The data shown in this Figure were quantitated, as described for Figure. 2. The averages of the ratio of cross-linked dimer/monomeric DrrA protein were plotted in a histogram shown in Figure S4. The error bars represent standard deviation.

Effect of DrrB on conformation of DrrA: As shown in the previous experiments, disulphide cross-linking using DrrAB containing one cysteine in DrrA (Y89C(A)/C260S(B)), or two

cysteines - one each in DrrA and DrrB (Y89C(A)/S23C(B)), results predominantly in the 78 kDa DrrA homo-dimeric species, indicating that Y89C is in close contact with Y89C from another subunit of DrrA. A minor 65 kDa species, consisting of DrrA and DrrB, is also seen when S23C in DrrB is simultaneously present. To further characterize DrrA-DrrB interaction, a cysteine to amine cross-linker GMBS was used. GMBS cross-linking of six different cysteine substitutions in DrrA with DrrB was analyzed. These included A45C(A)/C260S(B), Y89C(A)/C260S(B), Y140C(A)/C260S(B), S174C(A)//C260S(B), T195C(A)/C260S(B) and Y198C(A)/C260S. Of these, only Y89C and Y140C, both in the helical domain of DrrA, showed cross-linking with GMBS. Moreover, they produced identical cross-linking patterns. Only the data obtained with GMBS cross-linking of Y89CDrrA are shown in Fig. 8A. In this experiment, (A)/S23C(B) served as a control. GMBS cross-linking of S23C with an amine in DrrA produces a major 65 kDa DrrA + DrrB species (Figure 8A and 8B, lanes 1 and 2), as was also reported earlier (5). Y89C(A)/C260S(B) showed a different cross-linking pattern, however (Figure 8A, lanes 3-4). Three cross-linked species were seen: a minor 65 kDa species, and two major species of 78 kDa and around 100 kDa. The 65 kDa species corresponds to a heterodimer of A + B and is detected by both anti-DrrA (Fig. 8A, lane 4) and anti-DrrB antisera (Fig. 8B, lane 4), while the 78 kDa species is a homodimer of DrrA and is detected only by anti-DrrA antibodies (Fig. 8A, lane 4) and not by anti-DrrB serum (Fig. 8B, lane 4). The third 100 kDa species is again detected by anti-DrrA antibodies (Fig. 8A, lane 4), but not by anti-DrrB antibodies (Fig. 8B, lane 4). The significance of the 100 kDa species is not clear at this moment. Since it is not detected by anti-DrrB, it is likely that it represents a different conformation of the Y89C DrrA homodimer that has been doubly cross-linked through GMBS-mediated cysteine-amine cross-links, thus resulting in a different mobility.

The composition of this species will be analyzed further in the future studies. However, the most important conclusion that can be drawn from the GMBS cross-linking experiment shown in Figure 8A, lanes 3-4 (as is also seen with disulfide cross-linkers) is that once a cysteine is placed in the Q-loop/helical domain of DrrA, the predominant interaction is between DrrA monomers. Since a minor 65 kDa DrrA-DrrB species is also produced, it indicates that the same region of DrrA is also involved in interaction with DrrB. GMBS cross-linking experiments also provided another interesting insight. It was noted that the presence of S23C (DrrB) simultaneously with Y89C (DrrA) interfered with the formation of the DrrA homodimers as well as the 100 kDa species (Figure 8A, lane 6), suggesting that the introduction of S23C in DrrB affects Y89C mediated A-A interaction. Furthermore, these data indicate that the three situations, S23C, Y89C, and Y89C-S23C represent three different conformations of DrrA and DrrB.

The effect of S23C in DrrB on Y89C in DrrA was analyzed further by use of the disulphide cross-linkers. In Figure 9A, results obtained with three cross-linkers of different arm lengths are compared. These include CuPhe (0 Å), DTME (13.3 Å) and MTS (24.0 Å). All three cross-linkers showed the formation of the 78 kDa cross-linked species with equal efficiency when Y89C (A)/C260S (B) is used (Figure 9A, lanes 1-4). Interestingly, however, when S23C is also present, MTS-mediated cross-linking between Y89C-Y89C is prevented (lane 9), even though cross-linking by CuPhe (lane 7) and DTME (lane 8) was unaffected. These data indicate that S23C did not prevent DrrA-DrrA interaction but somehow altered it so that it is not picked up by the long arm-length cross-linker MTS. In the MTS-treated samples, the only species seen is the 65 kDa (A+B) species (Figs. 9 A and 9B, lane 9), as is also seen in the CuPhe (lane 7), and to a lesser extent in the DTME-treated, samples. (A smaller species of

about 55 kDa, picked up by anti-DrrA antibodies in the CuPhe sample, has not been characterized further in this study.) The data shown in this Figure were quantitated, as described earlier for Figure. 2. The averages (cross-linked dimer/monomeric DrrA protein) were plotted in a histogram shown in Figure S5. The error bars reflect standard deviation.

To determine if presence of any other cysteine in DrrB could have a similar inhibitory effect on Y89C-Y89C cross-linking, Y89C(A)/C260(B) was tested. Data in Figure 9C (lanes 1-4) show that MTS-mediated Y89C-Y89C cross-linking was not prevented by C260. Thus, this effect was specific to S23C (N-terminal tail) of DrrB. Furthermore, if S23C in DrrB is replaced by S23A, once again MTS-mediated Y89C-Y89C cross-linking occurs normally (lanes 5-8), indicating that a cysteine residue at position 23 in DrrB is required for this effect.

DISCUSSION

A major unresolved question that intrigues investigators in the field of ABC transporters is the mechanism by which their nucleotide binding domains interact with the membrane domains, a step essential for transduction of energy to bring about import or export. In this laboratory, our focus is an ABC drug transporter, DrrAB, which carries out efflux of the anticancer drugs doxorubicin and daunorubicin. In previous studies conducted in this laboratory, we found that the NBD and the TMD of the DrrAB system, even though present on separate subunits, are tightly coupled for their function and stability, implying specific interaction between the subunits (*4*). Recently our efforts have focused on understanding the molecular basis of interaction between DrrA and DrrB (*5*). In the present study, cysteine substitutions were made near the conserved domains of DrrA to understand interactions between subunits by using cysteine-cysteine or cysteine-amine cross-linking approaches. We show here that the Q-loop region of DrrA plays an important role in dimerization of the nucleotide binding domains, and it is also involved in mediating interactions between the NBD and the transmembrane subunit DrrB. Furthermore, we show that this interaction plays a role in communication of conformational changes between DrrA and DrrB. The critical role played by the Q-loop in the function of ABC transporters has been recognized before in structural studies carried out with MalK and BtuCD, among others (*17, 20*). Similarly, biochemical studies carried out previously with the maltose and the Bmr systems have also pointed to the importance of the Q-loop region (*22, 31-35*). The results obtained in the present study not only strengthen previous observations but also extend them further 1) by showing that the Q-loop plays a role in producing the closed conformation of DrrA and 2) by providing evidence for communication between the closed conformation of DrrA and the transmembrane domain via the N-terminal

region of DrrB. We present a model in Fig. 10, which attempts to interpret and summarize the data obtained in this study and presents this information in the context of information already available in literature on other ABC proteins.

Previous studies from this laboratory have shown that in the resting state of the complex, DrrA is in contact with DrrB. We showed that if membranes containing the wild type DrrA and DrrB proteins are treated with DTSSP, a general amine-to-amine cross-linker, only a heterodimeric species consisting of DrrA and DrrB is seen (*4*), implying that in the resting state DrrA is predominantly in contact with DrrB and not another monomer of DrrA. This state is represented as A-B in the model shown in Figure 10. The resting state complex of DrrA and DrrB could also be identified in GMBS (a cysteine to amine cross-linker) cross-linking experiments where it was shown that residues in the N-terminal cytoplasmic tail of DrrB (residues 1-53) are involved in interaction with DrrA (5). In the present study, we show that a cysteine substitution in the Q-loop of DrrA produces a conformational switch from A-B conformation to the A-A homodimeric state. An important step in the catalytic mechanism of ABC transporters is the dimerization of their nucleotide binding domains (*8, 14, 16, 17, 20*), however the dimeric state is transient (since hydrolysis of ATP immediately returns the protein to the open conformation) and thus is difficult to identify in solution or in the crystalline state . In some proteins (for example, MJ0796), mutation of the catalytic glutamate in the Walker B domain was shown to enhance stability of the dimer and was essential for crystallization of the protein in the dimeric state (*36*). In this study, we found that the Y89C or S91C substitution in the Q-loop traps DrrA in the dimeric conformation, which could be identified by use of a zero arm-length disulfide cross-linker, copper phenanthroline. Since cysteine substitutions in other regions of DrrA did not result in the same effect, our data suggest that the Q-loop region is

present at the interface of two monomers and is actively involved in dimerization of DrrA. Further, we propose that the Y89C-induced conformation of DrrA *resembles* the closed state, which normally results from binding of ATP to the ABC proteins (*8, 14, 16, 17, 20*). We found that Y89C-mediated cross-linking by DTME was independent of ATP binding (Fig. 5B, lanes 2 and 3) (presumably because most of the protein was already in the dimeric state); nevertheless, an intact ATP binding (Walker A) domain was required for achieving this conformation. Furthermore, on the addition of a non-hydrolysable ATP analog, ATPγS, a stable Y89C DrrA dimer was produced even in the absence of the cross-linker, suggesting that in this situation the ATP analog serves to hold the Y89C dimer together. If E165Q, a mutation in the Walker B domain that prevents hydrolysis of ATP, is simultaneously present along with Y89C, then either ATP or ATPγS could substitute for the disulfide cross-linker. Based on these observations, we can conclude that the Y89C-Y89C contact is sensitive to binding of ATP/ ATPγS so that the Y89C dimer can be stabilized either by the disulfide cross-linker acting directly on the Q-loop or by binding of ATPγS to the interface of the dimer. These data imply that the Y89C dimeric conformation indeed resembles the closed state. Thus the phenomenon noted here is physiologically significant and is likely to be part of a transport cycle. Information gleaned from the MalK structure also shows that the Q-loops move much closer together in the closed state and that the distance between Q-loops from opposing subunits changes from 52.5 Å (open) to 27.2 Å (closed) state (*17*). The most recent biochemical study from Schneider's group on the maltose system also strengthens the data and interpretations presented in this study (*22*). They show that distances between Q-loops of MalK are significantly reduced during transition from the open to the closed state and, furthermore, that MalK can be fixed in the closed state by a mutation of the catalytic glutamate

(E159Q) or in the open state by a mutation in the signature motif (Q140K) of MalK. Our studies show similar, though not identical, results. Even though we interpret our results slightly differently, both studies are consistent with the model proposed for the open and closed conformations of MalK (*22*). The biggest difference between the two studies is that we are proposing that Y89C DrrA protein is already trapped in the closed, *though flexible*, conformation (the maximum distance between Q-loops being in the viccinity of 24 Å, which is close to the distance reported for the closed conformation of MalK). We base this on the observation that most of the Y89C protein forms dimers in the presence of CuPhe or a cysteine-to-amine cross-linker GMBS. Binding of ATP to Y89C protein has no further effect on cross-linking. Furthermore, in the resting (open) state, we see only A-B and no A-A conformation. As soon as Y89C mutation is introduced, however, we see mostly A-A (and very little A-B) implying a switch in the conformation. The idea that Y89C-Y89C contact is flexible comes from the observation that several cross-linkers of different arm-lengths can cross-link Y89C with equal efficiency. This is discussed again later.

Another aspect of the work described in this study involves interaction between the Q-loop of DrrA and the N-terminal cytoplasmic tail of DrrB. When S23C, a cysteine substitution of the S23 residue in the N-terminus of DrrB, is simultaneously present along with Y89C in DrrA, a species corresponding to the heterodimer of DrrA and DrrB (65 kDa) is also observed, although the major interaction is between two DrrA monomers. Since Y89C represents the dimeric state of DrrA, the S23C-Y89C contact appears to be specific to the closed state and is represented as A-B* in Figure 10. (We believe that the A-B* conformation is different from the A-B conformation described earlier, even though both involve the N-terminal tail region of DrrB. This question will be resolved in the future studies). What might be the significance of

the contacts between the S23 region (N- terminal cytoplasmic tail) in DrrB and the Q-loop of DrrA? According to the prevalent models, the flexible nature of the Q-loop allows transition of the NBDs from the open to the closed state and at the same time, it allows it to act as a relay of conformational changes between the nucleotide binding domain and the transmembrane domain (*37*). Supporting these ideas is the crystal structure of the intact transporter BtuCD, which shows that the Q-loop is present in a cleft on the surface of BtuD where it forms extensive contacts with the L-loop (analogous to the EAA loop) of BtuC (*20*). Similarly, when the ATP-bound MalK structure was aligned with BtuC (TMD), it showed that the Q-loop of MalK is positioned to mediate tight binding to the L-loop of BtuC and it also reaches in towards the γ-phosphate of ATP in the closed conformation of MalK (*17*).

Based on our own data presented here, we propose that the interaction between the S23 region of DrrB and the Q-loop of DrrA is involved in communication of conformational changes between DrrA and DrrB. The direct evidence of communication comes from the interesting observation that substituting S23 residue with S23C produces a significant effect on the behavior of Y89C in DrrA. This effect becomes evident only when different arm-length disulfide cross-linkers are employed. As mentioned in the results, DrrA (Y89C) can be cross-linked with linkers varying in length from 0 (CuPhe) to 24 Å (MTS). Interestingly, when S23C is simultaneously present in DrrB, the results are strikingly different: copper and DTME (13.3 Å) can still cross-link DrrA and produce DrrA homodimers very well, but MTS is now not able to do so. These data indicate that placing a cysteine in this region of DrrB produces a conformational change in the helical domain of DrrA. How S23C achieves this effect is not completely clear at this time. However, it seems reasonable to suggest that it produces a more rigid conformation of DrrA so that Y89C can still be cross-linked with zero or short arm length

cross-linkers but not with the long arm length linker MTS. This leads us to propose that the two Y89C residues (or the Q-loops) from opposing monomers are in flexible contact until a conformational change in DrrB (produced by S23C substitution here) produces a change in DrrA which fixes it in one position. Since only a cysteine substitution of S23 results in this effect, it might indicate affinity between the two cysteines, S23C and Y89C; however, instead of resulting in opening of the NBD dimer, the result of this interaction seems to be to fix the distance between DrrA monomers at less than 13 Å. It seems that the overall effect of this conformation of DrrB is to facilitate the closed conformation of DrrA. This observation is consistent with earlier findings, namely that the isolated ABC domains do not form stable homodimers even in the presence of Mg-ATP or non-hydrolyzable analogs, indicating that interaction with the TM domains is required for stable association (14). Previous studies from this laboratory have also shown that DrrA is in an active conformation to bind ATP only when it is in complex with DrrB (*4*), further strengthening the idea that DrrB facilitates the closed conformation of DrrA. Since S23C lies in the region of interaction between DrrA and DrrB, the effect seen in the present study is likely to be physiologically significant and thus may provide clues to the path of transmission of conformational changes from DrrB to DrrA. One situation where events in DrrB will be transmitted to DrrA is substrate binding to DrrB. This kind of signaling has been proposed to occur in the maltose system where substrate binding to the TMDs is believed to be signaled to the NBDs, resulting in their closing (*38*). We have already shown that doxorubicin binding to DrrB produces a significant enhancement of ATP binding to DrrA (*4*). It can thus be speculated that doxorubicin binding to DrrB produces a conformational change in the N-terminal tail of DrrB which is then transmitted to the helical

domain of DrrA. Is it possible then, that the S23C substitution in the N-terminal tail of DrrB mimics the effect of substrate binding to DrrB?

In this study the role of the Q-loop region in formation of the closed conformation of the nucleotide binding domain has been clearly elucidated. Furthermore, the long-range effects of conformational changes in DrrB on DrrA are very intriguing and could provide important insights into the mechanism by which DrrA and DrrB communicate. In our future studies, we would like to further understand how DrrB influences DrrA and how the Q-loop region is involved in communication between the NBD and the TMD.

REFERENCES

1. Guilfoile, P. G. & Hutchinson, C. R. (1991) A bacterial analog of the mdr gene of mammalian tumor cells is present in Streptomyces peucetius, the producer of daunorubicin and doxorubicin, *Proc Natl Acad Sci U S A. 88*, 8553-7.

2. Kaur, P. (1997) Expression and characterization of DrrA and DrrB proteins of Streptomyces peucetius in Escherichia coli: DrrA is an ATP binding protein, *J Bacteriol. 179*, 569-75.

3. Gottesman, M. M. & Pastan, I. (1993) Biochemistry of multidrug resistance mediated by the multidrug transporter, *Annu Rev Biochem. 62*, 385-427.

4. Kaur, P. & Russell, J. (1998) Biochemical coupling between the DrrA and DrrB proteins of the doxorubicin efflux pump of Streptomyces peucetius, *J Biol Chem. 273*, 17933-9.

5. Kaur, P., Rao, D. K. & Gandlur, S. M. (2005) Biochemical characterization of domains in the membrane subunit DrrB that interact with the ABC subunit DrrA: identification of a conserved motif, *Biochemistry. 44*, 2661-70.

6. Gandlur, S. M., Wei, L., Levine, J., Russell, J. & Kaur, P. (2004) Membrane topology of the DrrB protein of the doxorubicin transporter of Streptomyces peucetius, *J Biol Chem. 279*, 27799-806.

7. Diederichs, K., Diez, J., Greller, G., Muller, C., Breed, J., Schnell, C., Vonrhein, C., Boos, W. & Welte, W. (2000) Crystal structure of MalK, the ATPase subunit of the trehalose/maltose ABC transporter of the archaeon Thermococcus litoralis, *Embo J. 19*, 5951-61.

8. Yuan, Y. R., Blecker, S., Martsinkevich, O., Millen, L., Thomas, P. J. & Hunt, J. F. (2001) The crystal structure of the MJ0796 ATP-binding cassette. Implications for the structural consequences of ATP hydrolysis in the active site of an ABC transporter, *J Biol Chem. 276*, 32313-21.

9. Smith, P. C., Karpowich, N., Millen, L., Moody, J. E., Rosen, J., Thomas, P. J. & Hunt, J. F. (2002) ATP binding to the motor domain from an ABC transporter drives formation of a nucleotide sandwich dimer, *Mol Cell. 10*, 139-49.

10. Schmitt, L., Benabdelhak, H., Blight, M. A., Holland, I. B. & Stubbs, M. T. (2003) Crystal structure of the nucleotide-binding domain of the ABC-transporter haemolysin B: identification of a variable region within ABC helical domains, *J Mol Biol. 330*, 333-42.

11. Verdon, G., Albers, S. V., Dijkstra, B. W., Driessen, A. J. & Thunnissen, A. M. (2003) Crystal structures of the ATPase subunit of the glucose ABC transporter from Sulfolobus solfataricus: nucleotide-free and nucleotide-bound conformations, *J Mol Biol. 330*, 343-58.

12. Hung, L. W., Wang, I. X., Nikaido, K., Liu, P. Q., Ames, G. F. & Kim, S. H. (1998) Crystal structure of the ATP-binding subunit of an ABC transporter, *Nature. 396*, 703-7.

13. Gaudet, R. & Wiley, D. C. (2001) Structure of the ABC ATPase domain of human TAP1, the transporter associated with antigen processing, *Embo J. 20*, 4964-72.

14. Karpowich, N., Martsinkevich, O., Millen, L., Yuan, Y. R., Dai, P. L., MacVey, K., Thomas, P. J. & Hunt, J. F. (2001) Crystal structures of the MJ1267 ATP binding cassette reveal an induced-fit effect at the ATPase active site of an ABC transporter, *Structure. 9*, 571-86.

15. Davidson, A. L. & Chen, J. (2004) ATP-binding cassette transporters in bacteria, *Annu Rev Biochem. 73*, 241-68.

16. Hopfner, K. P., Karcher, A., Shin, D. S., Craig, L., Arthur, L. M., Carney, J. P. & Tainer, J. A. (2000) Structural biology of Rad50 ATPase: ATP-driven conformational control in DNA double-strand break repair and the ABC-ATPase superfamily, *Cell. 101*, 789-800.

17. Chen, J., Lu, G., Lin, J., Davidson, A. L. & Quiocho, F. A. (2003) A tweezers-like motion of the ATP-binding cassette dimer in an ABC transport cycle, *Mol Cell. 12*, 651-61.

18. Lewis, H. A., Buchanan, S. G., Burley, S. K., Conners, K., Dickey, M., Dorwart, M., Fowler, R., Gao, X., Guggino, W. B., Hendrickson, W. A., Hunt, J. F., Kearins, M. C., Lorimer, D., Maloney, P. C., Post, K. W., Rajashankar, K. R., Rutter, M. E., Sauder, J. M., Shriver, S., Thibodeau, P. H., Thomas, P. J., Zhang, M., Zhao, X. & Emtage, S. (2004) Structure of nucleotide-binding domain 1 of the cystic fibrosis transmembrane conductance regulator, *Embo J. 23*, 282-93.

19. Lewis, H. A., Zhao, X., Wang, C., Sauder, J. M., Rooney, I., Noland, B. W., Lorimer, D., Kearins, M. C., Conners, K., Condon, B., Maloney, P. C., Guggino, W. B., Hunt, J. F. & Emtage, S. (2005) Impact of the deltaF508 mutation in first nucleotide-binding domain of human cystic fibrosis transmembrane conductance regulator on domain folding and structure, *J Biol Chem. 280*, 1346-53.

20. Locher, K. P., Lee, A. T. & Rees, D. C. (2002) The E. coli BtuCD structure: a framework for ABC transporter architecture and mechanism, *Science. 296*, 1091-8.

21. Dawson, R. J. & Locher, K. P. (2006) Structure of a bacterial multidrug ABC transporter, *Nature. 443*, 180-5.

22. Daus, M. L., Grote, M., Muller, P., Doebber, M., Herrmann, A., Steinhoff, H. J., Dassa, E. & Schneider, E. (2007) ATP-driven MalK Dimer Closure and Reopening and Conformational Changes of the "EAA" Motifs Are Crucial for Function of the Maltose ATP-binding Cassette Transporter (MalFGK2), *J Biol Chem. 282*, 22387-22396.

23. Sambrook, J., Fritsch, E. F., and Maniatis, T. (1989) *Molecular Cloning: A Laboratory Manual*, 2nd Ed., Cold Spring Harbor Laboratory, Cold Spring Harbor, NY.

24. Nakamura, H., Tojo, T. & Greenberg, J. (1975) Interaction of the expression of two membrane genes, acrA and plsA, in Escherichia coli K-12, *J Bacteriol. 122*, 874-9.

25. Miller, J. (1992) *Experiments in Molecular Genetics*, Cold Spring Harbor Laboratory, Cold Spring Harbor, NY.

26. Fetsch, E. E. & Davidson, A. L. (2002) Vanadate-catalyzed photocleavage of the signature motif of an ATP-binding cassette (ABC) transporter, *Proc Natl Acad Sci U S A. 99*, 9685-90.

27. Loo, T. W. & Clarke, D. M. (1995) P-glycoprotein. Associations between domains and between domains and molecular chaperones, *J Biol Chem. 270*, 21839-44.

28. Dalmas, O., Do Cao, M. A., Lugo, M. R., Sharom, F. J., Di Pietro, A. & Jault, J. M. (2005) Time-resolved fluorescence resonance energy transfer shows that the bacterial multidrug ABC half-transporter BmrA functions as a homodimer, *Biochemistry. 44*, 4312-21.

29. Guo, X., Chen, X., Weber, I. T., Harrison, R. W. & Tai, P. C. (2006) Molecular basis for differential nucleotide binding of the nucleotide-binding domain of ABC-transporter CvaB, *Biochemistry. 45*, 14473-80.

30. Qu, Q. & Sharom, F. J. (2001) FRET analysis indicates that the two ATPase active sites of the P-glycoprotein multidrug transporter are closely associated, *Biochemistry. 40*, 1413-22.

31. Hunke, S., Mourez, M., Jehanno, M., Dassa, E. & Schneider, E. (2000) ATP modulates subunit-subunit interactions in an ATP-binding cassette transporter (MalFGK2) determined by site-directed chemical cross-linking, *J Biol Chem. 275*, 15526-34.

32. Dalmas, O., Orelle, C., Foucher, A. E., Geourjon, C., Crouzy, S., Di Pietro, A. & Jault, J. M. (2005) The Q-loop disengages from the first intracellular loop during the catalytic cycle of the multidrug ABC transporter BmrA, *J Biol Chem. 280*, 36857-64.

33. Mourez, M., Jehanno, M., Schneider, E. & Dassa, E. (1998) In vitro interaction between components of the inner membrane complex of the maltose ABC transporter of Escherichia coli: modulation by ATP, *Mol Microbiol. 30*, 353-63.

34. Wilken, S., Schmees, G. & Schneider, E. (1996) A putative helical domain in the MalK subunit of the ATP-binding-cassette transport system for maltose of Salmonella typhimurium (MalFGK2) is crucial for interaction with MalF and MalG. A study using the LacK protein of Agrobacterium radiobacter as a tool, *Mol Microbiol. 22*, 655-66.

35. Mourez, M., Hofnung, M. & Dassa, E. (1997) Subunit interactions in ABC transporters: a conserved sequence in hydrophobic membrane proteins of periplasmic permeases defines an important site of interaction with the ATPase subunits, *Embo J. 16*, 3066-77.

36. Moody, J. E., Millen, L., Binns, D., Hunt, J. F. & Thomas, P. J. (2002) Cooperative, ATP-dependent association of the nucleotide binding cassettes during the catalytic cycle of ATP-binding cassette transporters, *J Biol Chem. 277*, 21111-4.

37. Jones, P. M. & George, A. M. (2002) Mechanism of ABC transporters: a molecular dynamics simulation of a well characterized nucleotide-binding subunit, *Proc Natl Acad Sci U S A. 99*, 12639-44.

38. Davidson, A. L., Shuman, H. A. & Nikaido, H. (1992) Mechanism of maltose transport in Escherichia coli: transmembrane signaling by periplasmic binding proteins, *Proc Natl Acad Sci U S A. 89*, 2360-4.

TABLES

Domain of DrrA	Mutation	Dox conc, µg/mL			
		0	6	8	10
(wild type)	C260	+++	+++	+++	++
cys-less	C260S	+++	+++	+++	++
Walker A domain	A45C	+++	+++	+	+
Walker A domain	G44A	+++	+/-	-	-
Walker A domain	K47R	+++	-	-	-
Walker B domain	L160A	+++	-	-	-
Walker B domain	D164N	+++	-	-	-
Walker B domain	E165Q	+++	-	-	-
Q-loop domain	Y89C	+++	+++	++	+
Q-loop domain	S91C	+++	+++	++	+
Q-loop domain	Q88E	+++	++	+	-
Q-loop domain	Q88S	+++	-	-	-
Q-loop domain	Q88N	+++	+	-	-
Signature domain	Y140C	+++	+++	+/-	+/-
Signature motif	S141R	+++	+	-	-
Signature motif	G143S	+++	+	-	-
N-ter tail (DrrB)	S23C	+++	++	++	++
Double mutant	Y89C/S23C	+++	+++	++	++
Double mutant	S91C/S23C	+++	++	++	++
Vector only	pSU2718	+++	+/-	-	-
aLegend: +++, very good growth; ++, good growth; +, some growth; -, no growth.					

TABLE 1: Doxorubicin Resistance of *E.coli* N43 Cells expressing different mutations in DrrA and wild type DrrB. N43 cells containing indicated plasmids were plated on M9 plates containing different concentrations of doxorubicin. The plates were incubated at 37 ^{o}C. Growth was scored after 24 hours of incubation. Legend: +++, very good growth; ++, good growth; +, some growth; -, no growth

FIGURES

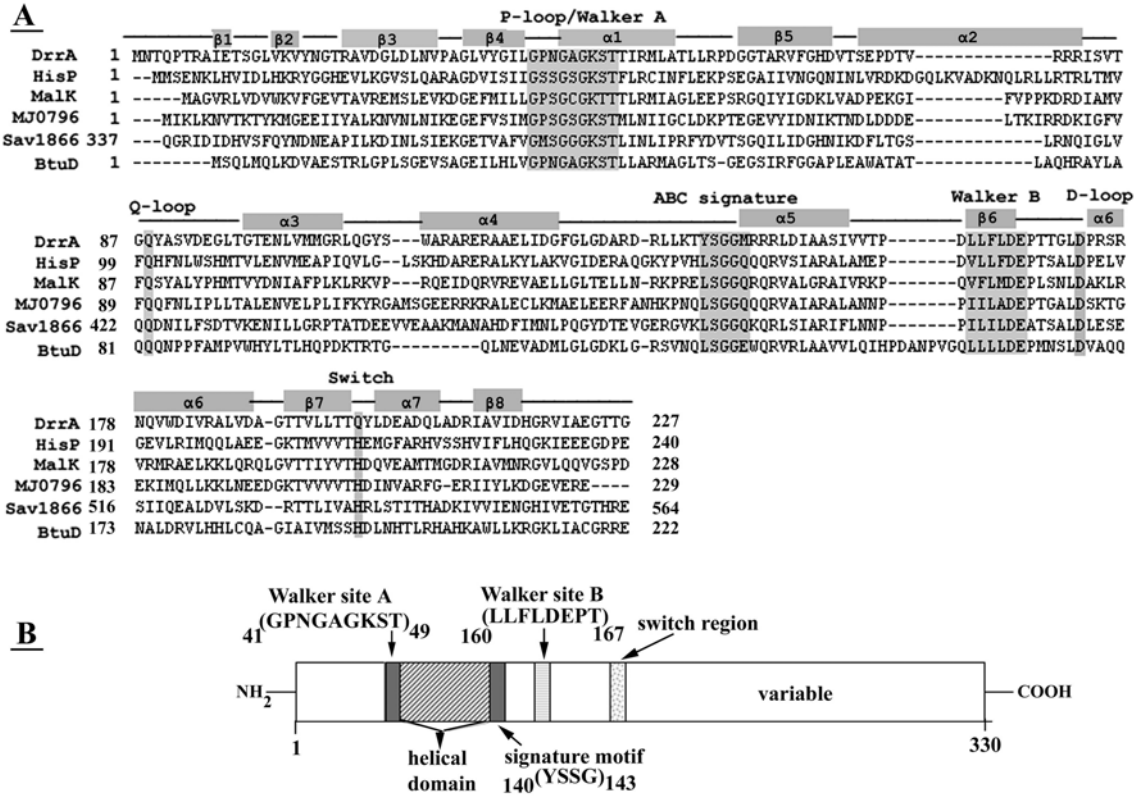

FIGURE 1: A, Nucleotide Binding Domains of different ABC transporters: Alignment of DrrA, HisP, MalK, MJO796, Sav1866 and BtuD was generated by ClustalW (http://www.ebi.ac.uk/clustalw/). Secondary structure was predicted by the PHD tool obtained on the ExPASy server (us.expasy.org/). Conserved domains mentioned in the text, namely Walker A, Walker B, signature motif, and Q-loop, have been highlighted in grey. Other highlighted domains include the D-loop and the switch region.

B A schematic representation of the conserved domains in DrrA: The location, length and consensus sequence of Walker A, Walker B, signature motif, helical domain, and the switch region are shown.

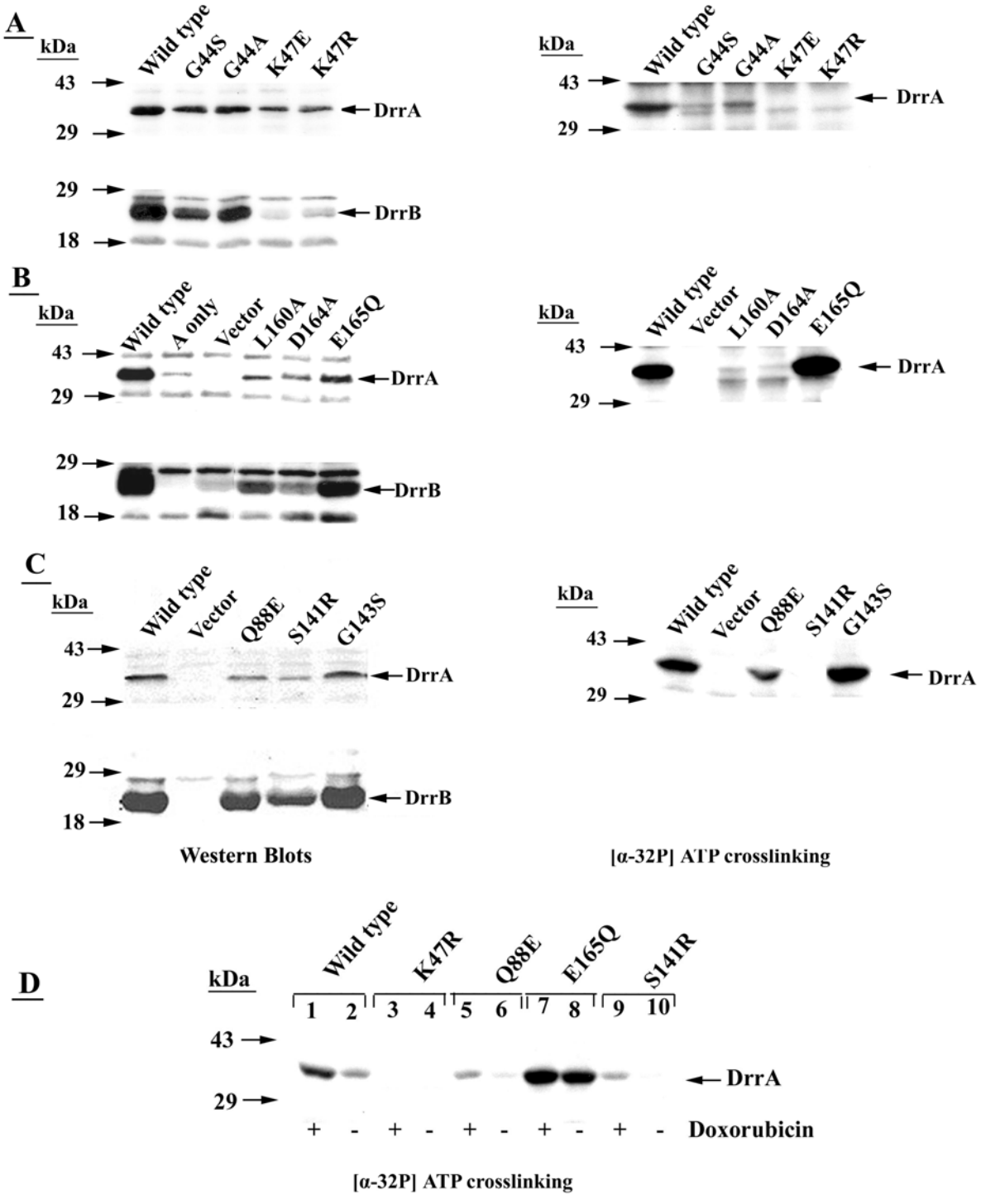
A
kDa
Wild type
G44S
G44A
K47E
K47R
43
29
DrrA
29
18
DrrB
B
kDa
Wild type
A only
Vector
L160A
D164A
E165Q
43
29
DrrA
29
18
DrrB
C
kDa
Wild type
Vector
Q88E
S141R
G143S
43
29
DrrA
29
18
DrrB
Western Blots
[α-32P] ATP crosslinking
D
kDa
Wild type
K47R
Q88E
E165Q
S141R
1 2 3 4 5 6 7 8 9 10
43
29
DrrA
+ - + - + - + - + - Doxorubicin
[α-32P] ATP crosslinking

FIGURE 2: Effect of various mutations in DrrA on expression levels of DrrA and DrrB and on ATP binding: *E. coli* cells containing the indicated plasmids were induced with IPTG. The cells were lysed by French press, followed by ultracentrifugation at 100,000g for 1hr to prepare membrane fractions. 25 μg of membrane protein was analyzed by SDS-PAGE on 10% gels, followed by Western Blot analysis using anti-DrrA (upper panel) or anti-DrrB (lower panel) antibodies. UV-catalyzed adduct formation between DrrA proteins and [α-^{32}P] ATP was performed as described under "Experimental Procedures". The proteins were resolved by SDS-PAGE on 10% gels, followed by autoradiography. Panels A-C, Left panels: Western blots; Right panels: [α-^{32}P] ATP binding. A: Walker A mutants, B: Walker B mutants, C: Q-loop and signature motif mutants. Panel D: [α-^{32}P] ATP binding in the presence or absence of doxorubicin. Experimental conditions were the same as described for panels A-C. The samples marked "+" contained 34 μM doxorubicin, while the samples marked "–" contained no doxorubicin. The experiments shown in Figure 2 were repeated three times. The data obtained with key mutants (those used in this work) were quantitated and plotted as histograms provided in the Supplementary information.

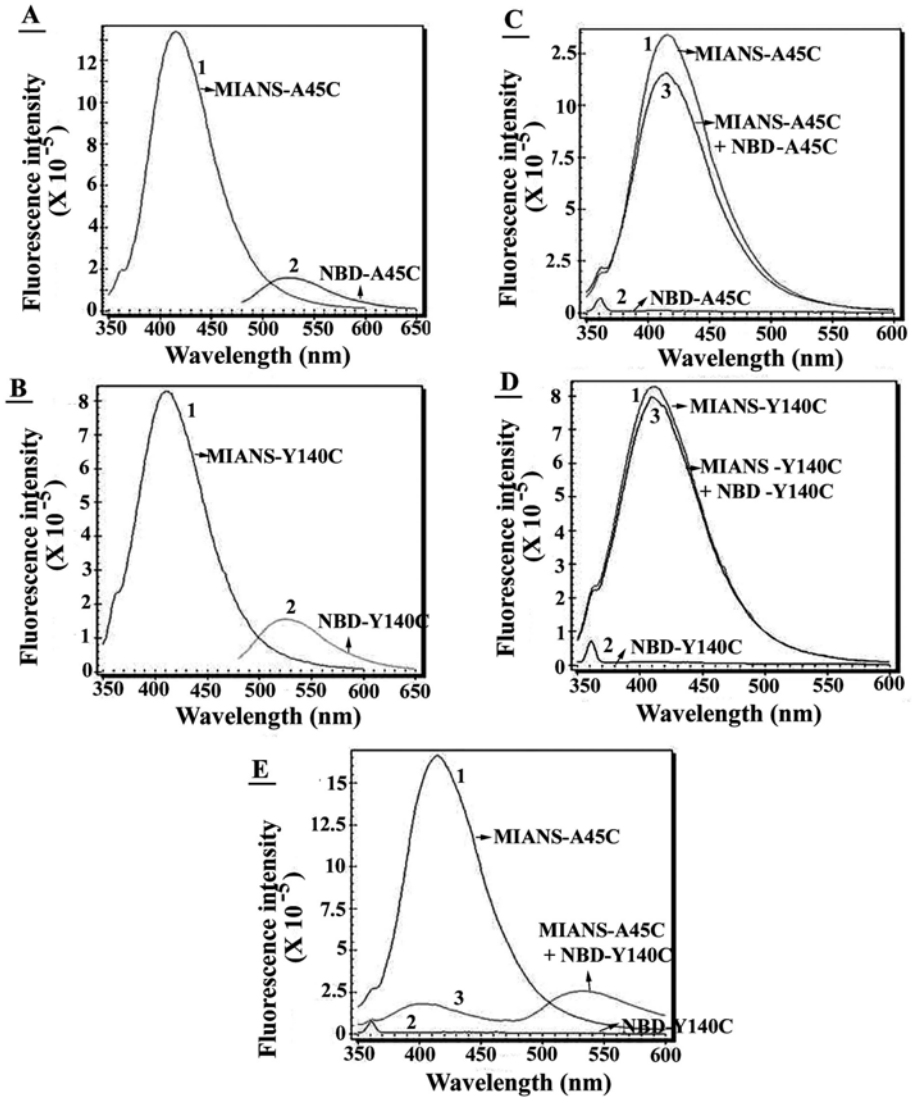

FIGURE 3A: Fourier Resonance Energy Transfer (FRET) analysis to determine the conformation of DrrA dimers: The membrane fractions prepared from cells containing A45C(A)/C260S(B) or Y140C(A)/C260S(B) were labeled with either MIANS or NBD-Cl. The labelled DrrAB proteins were purified as described in "Experimental Procedures". A and

B: Fluorescence spectra for individual proteins labeled with MIANS (excitation at 322 nm; emission at 420 nm) or NBD (excitation at 465 nm; emission at 523 nm). C: In separate reactions, A45C(A)/C260S(B) was labeled with either MIANS or NBD. The individually labeled proteins were then mixed. Excitation was carried out at 322 nm for MIANS and emission was monitored between 350nm and 600nm. D: In separate reactions, Y140C(A)/C260S(B) was labeled with either MIANS or NBD. The individually labeled proteins were then mixed. Excitation was carried out at 322 nm for MIANS and emission was monitored between 350nm and 600nm. E: A45C(A)/C260S(B) labeled with MIANS was mixed with Y140C(A)/C260S(B) labeled with NBD-Cl. These two labeled proteins were mixed. Excitation was carried out at 322 nm for MIANS and emission was monitored between 350nm and 600nm.

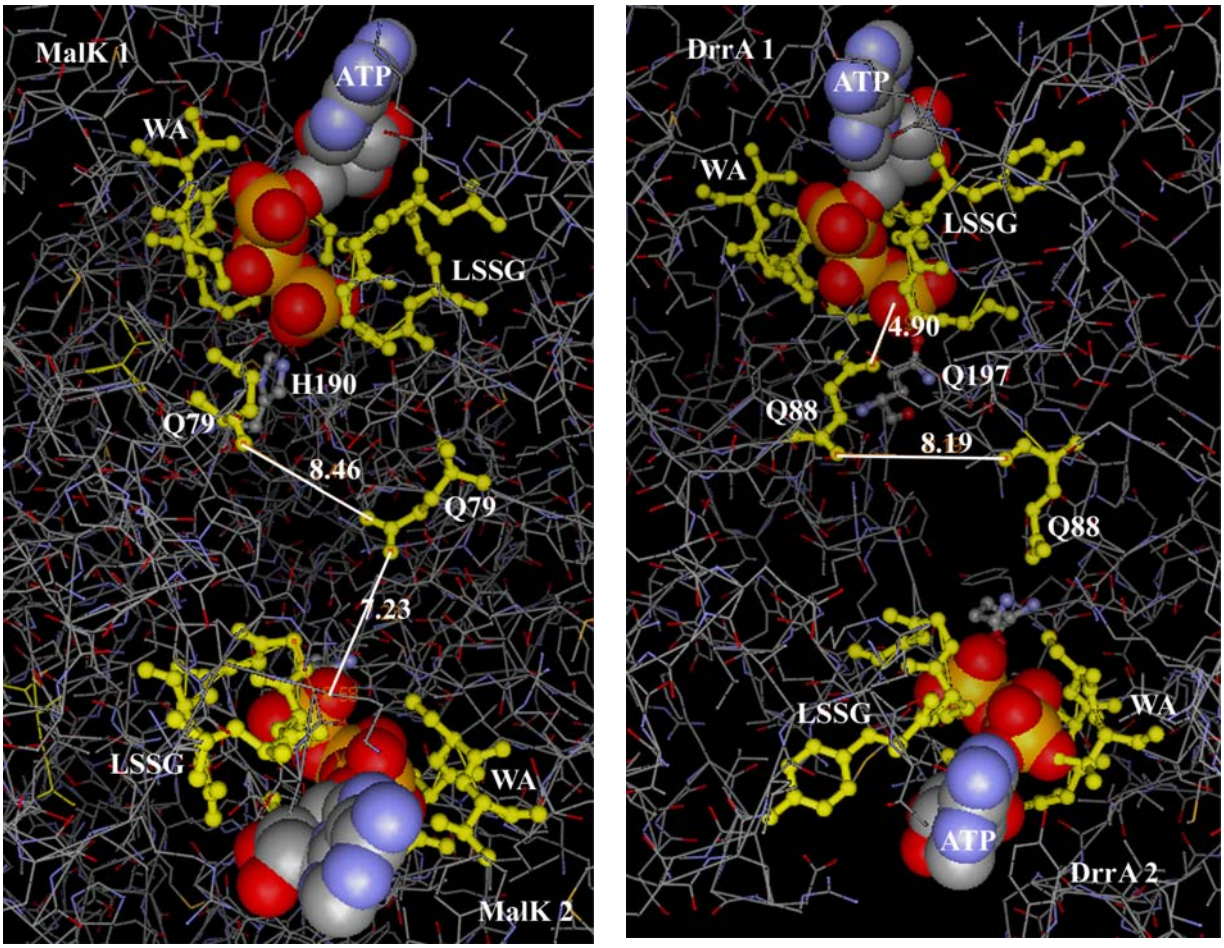

FIGURE 3B: Close-up view of the three-dimensional model of MalK dimer (A) and DrrA dimer (B): The three dimensional model of DrrA dimer built based on MalK dimer, the closest homologue whose structure had been published in the PDB (PDB accession code: 1Q12). The 3D model was built using Geno3D, a comparative molecular modeling program for proteins. The ATP co-ordinates were taken from the MalK model. The visualization of the models was performed using 3D Mol Viewer. Highlighted in the models are 1) the putative distances

between the Gln residues of the Q-loop (Q79-Q79 of MalK and Q88-Q88 of DrrA) 2) the putative distances between the Gln residue and ATP molecule. Also highlighted are the H190 (Malk) and Q197 (DrrA) residues of the switch region of the respective proteins.

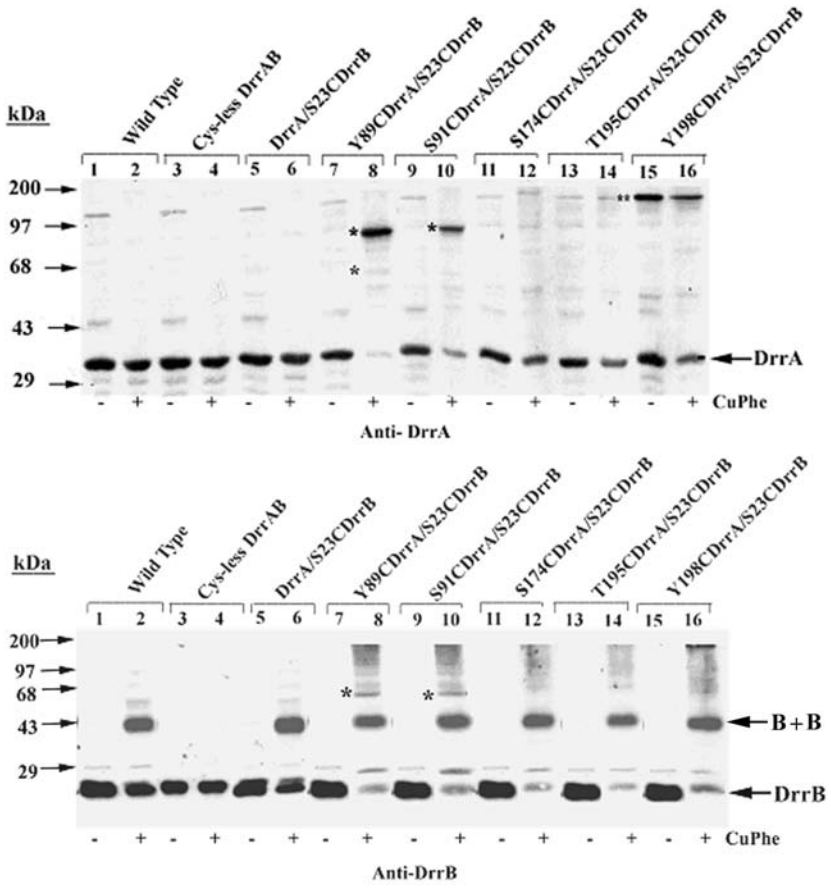

FIGURE 4: Copper phenanthroline-mediated disulphide cross-linking of DrrAB proteins: The cell membrane fractions were prepared and subjected to disulphide cross-linking using copper phenanthroline, as described under "Experimental Procedures". The reaction was terminated by the addition of 25 µL 4X non-reducing Laemmli sample buffer. 50 µg of protein was resolved by SDS-PAGE using 10% gels followed by Western blot using anti-DrrA or anti-DrrB antibodies. Lanes 1 and 2, Wild-type DrrAB; lanes 3 and 4, cysteine-less DrrAB; lanes 5 and 6, (A)/S23C(B); lanes 7 and 8, Y89C(A)/S23C(B); lanes 9 and 10, S91C(A)/S23C(B); lanes 11 and 12, S174C(A)/S23C(B); lanes 13 and 14, T195C(A)/S23C(B);

and lanes 15 and 16, Y198C(A)/S23C(B). Panel A, anti-DrrA; Panel B, anti-DrrB. The "minus" and "plus" at the bottom of the lanes indicate the absence and presence of the cross-linker in the reaction, respectively. The migration of the protein standards is shown on the left. The location of the 78kDa as well as the 65 kDa cross-linked species is marked as "*". A much larger species seen in Y198C (A)/S23C (B) in both absence and presence of the cross-linker (**) was not characterized further in this study.

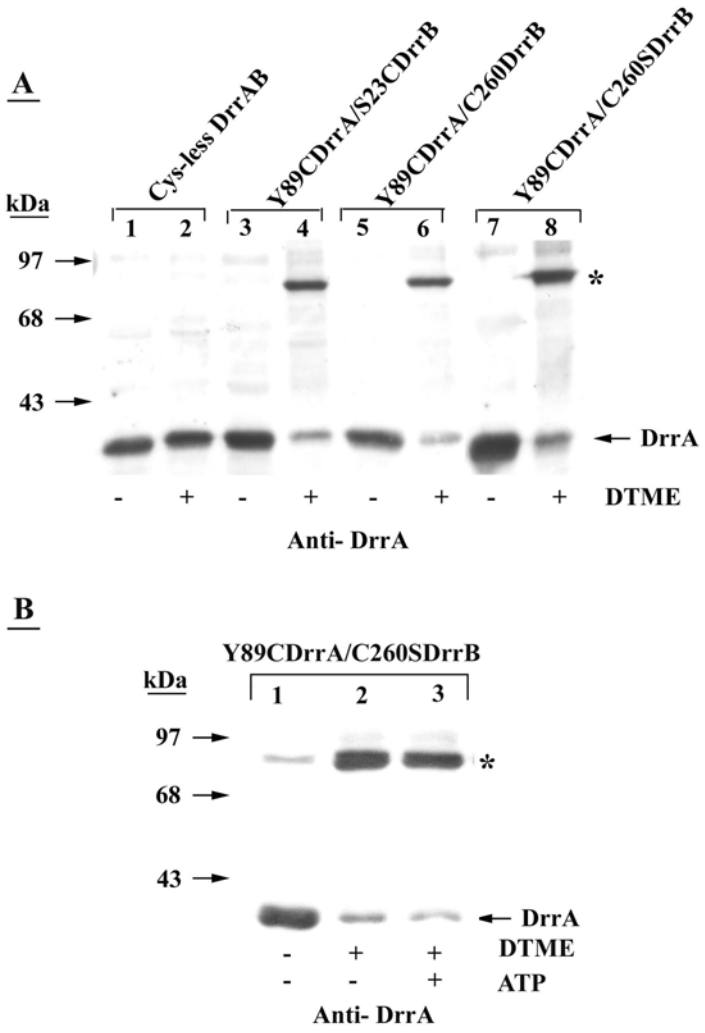

FIGURE 5: DTME-mediated disulphide cross-linking of Y89C (DrrA) and variants of DrrB: The conditions used for disulphide cross-linking were as described under legend to Figure 4. The reaction was terminated by the addition of 4X non-reducing Laemmli sample buffer. 50 µg of protein was resolved by SDS-PAGE followed by Western blot using anti-DrrA antibodies. Lanes 1 and 2, cysteine-less DrrAB; lanes 3 and 4, Y89C(A)/S23C(B); lanes 5 and 6, Y89C(A)/C260(B); lanes 7 and 8, Y89C(A)/C260S(B). The "minus" and "plus" at the bottom of the lanes indicate the absence and presence of the cross-linker in the reaction,

respectively. The migration of the protein standards is shown on the left. The location of the 78 kDa cross-linked species is marked as "*".

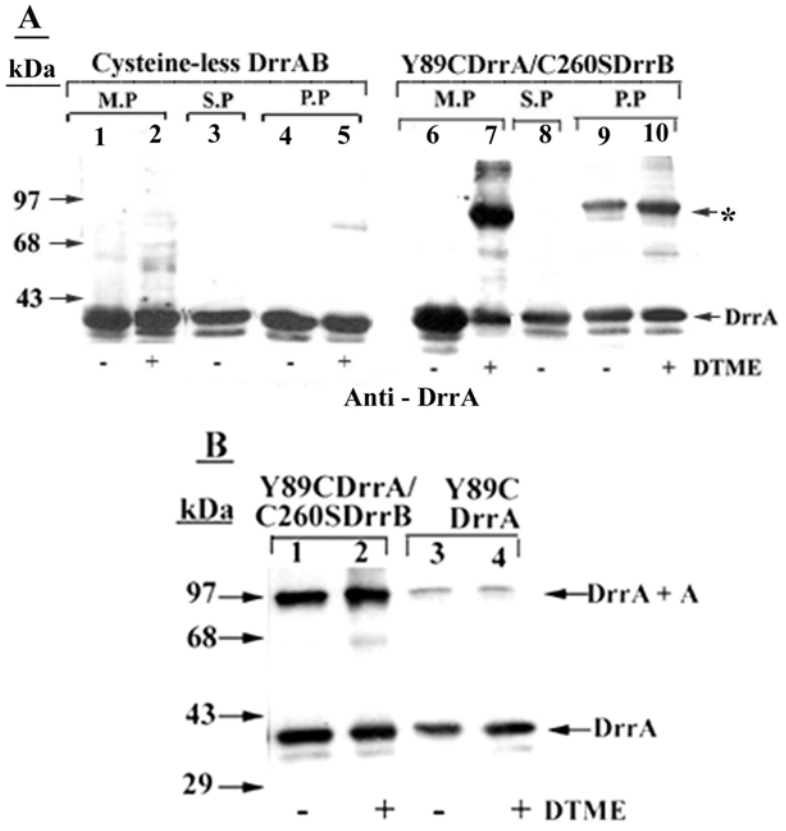

FIGURE 6: Purification of the DrrAB proteins and cross-linking by DTME: Membrane fraction was prepared as described in legend to Figure 3 and DrrAB purified as described in "Experimental Procedures". Samples were resolved by 10% SDS-PAGE followed by Western blot using anti-DrrA antibodies. Panel A: Lanes 1-5, cysteine-less DrrAB; lanes 6-10, Y89C(A)/C260S(B). Lanes 1 and 2, membrane proteins (MP); lane 3, solubilized protein (SP); and lanes 4 and 5, purified protein (PP). Panel B: Lanes 1 and 2, Y89C(A)/C260S(B); lanes 3 and 4, Y89C(A) alone.

The “minus” and “plus” at the bottom of the lanes indicate the absence and presence of the DTME cross-linker in the reaction, respectively. The migration of the protein standards is shown on the left. The location of the 78 kDa cross-linked species is marked as “*”.

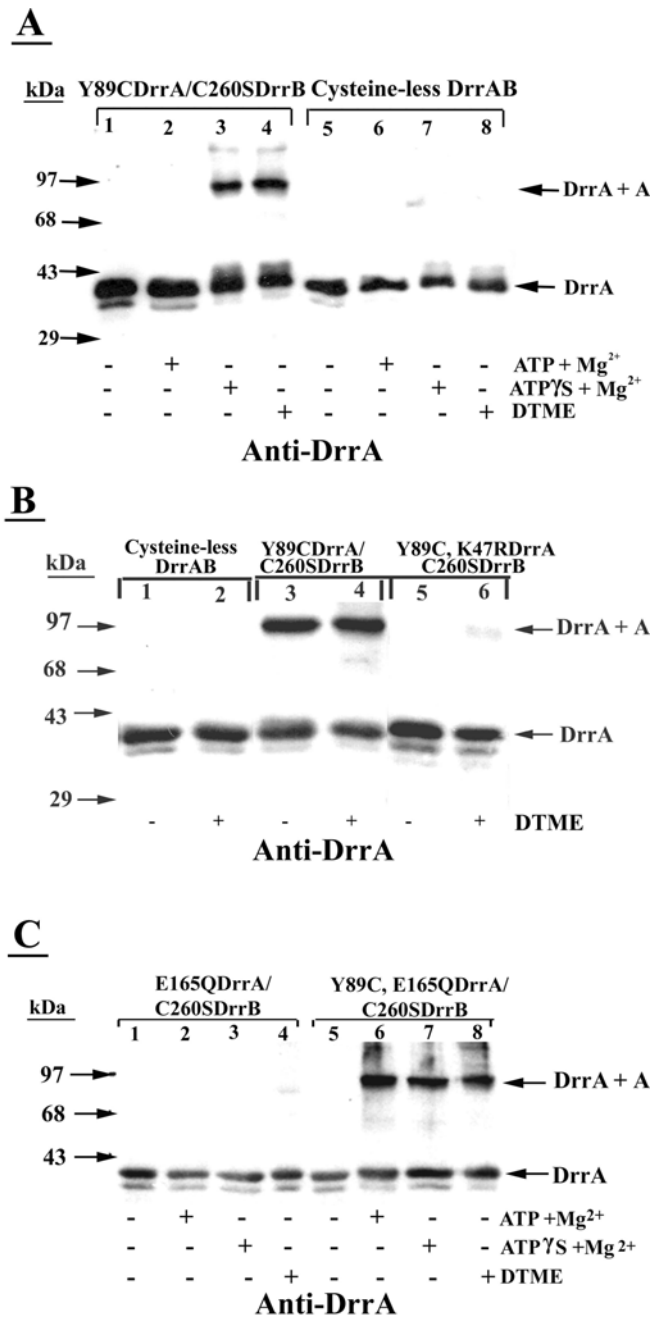

FIGURE 7: Effect of ATP and ATPγS on DrrA homodimer formation: DrrAB proteins were purified as described under "Experimental Procedures". Samples were reduced with 1mM DTT and passed through a 10K Nanosep centrifugal column. The reduced samples were

incubated with ATP, ATPγS, or DTME cross-linker. The reactions were terminated by the addition of 4X non-reducing Laemmli sample buffer. 15µg of each sample was analyzed by SDS-PAGE, followed by Western blot using anti-DrrA antibodies. Panel A: Lanes 1-4, Y89C(A)/C260S(B); lanes 5-8, Cysteine-less DrrAB. Panel B: Lanes 1 and 2, Cysteine-less DrrAB; lanes 3 and 4, Y89C(A)/C260S(B); lanes 5 and 6, Y89C, K47R(A)/C260S(B). Panel C: Lanes 1-4, E165Q(A)/C260S(B); lanes 5-8, Y89C, E165Q(A)/C260S(B). The "minus" and "plus" at the bottom of the lanes indicate the absence and presence of ATP, ATPγS, or the DTME cross-linker in the reaction. The migration of the protein standards is shown on the left. The location of the 78kDa cross-linked species is marked.

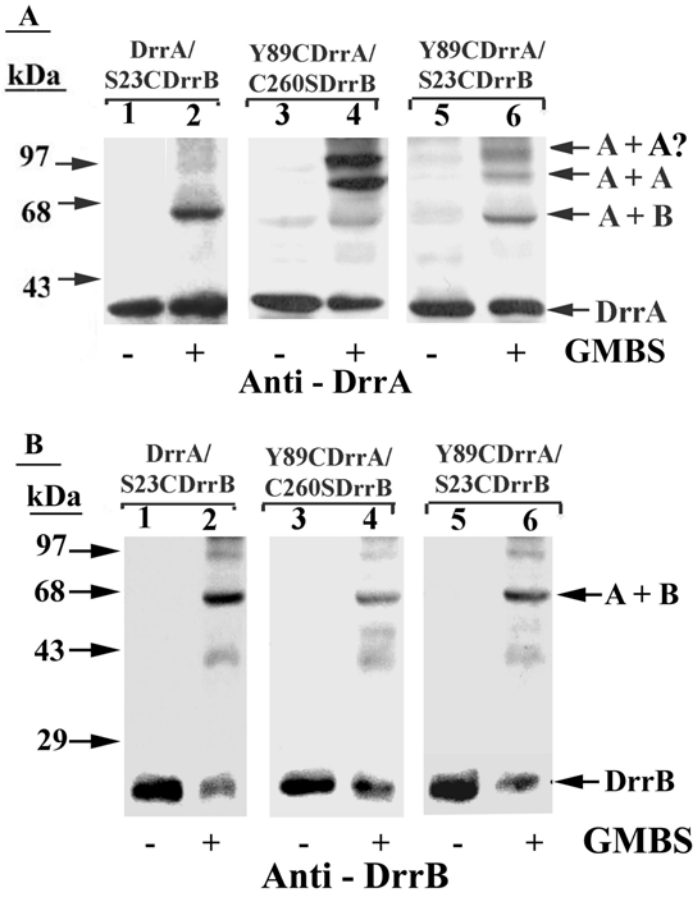

FIGURE 8: GMBS- mediated heterobifunctional cross-linking: The cell membrane fractions were prepared, as described earlier. Cross-linking was carried out as described under "Experimental Procedures". The reaction was terminated by the addition of 4X non-reducing Laemmli sample buffer. 50 µg of protein was resolved by SDS-PAGE, followed by Western blot using anti-DrrA or anti-DrrB antibodies. Lanes 1 and 2, (A)/S23C(B); lanes 3 and 4, Y89C(A)/C260S(B); lanes 5 and 6, Y89C(A)/S23C(B). Panel A, anti-DrrA; Panel B, anti-DrrB. The location of the cross-linked species is marked as "A + B", "A + A", and "A + A?"

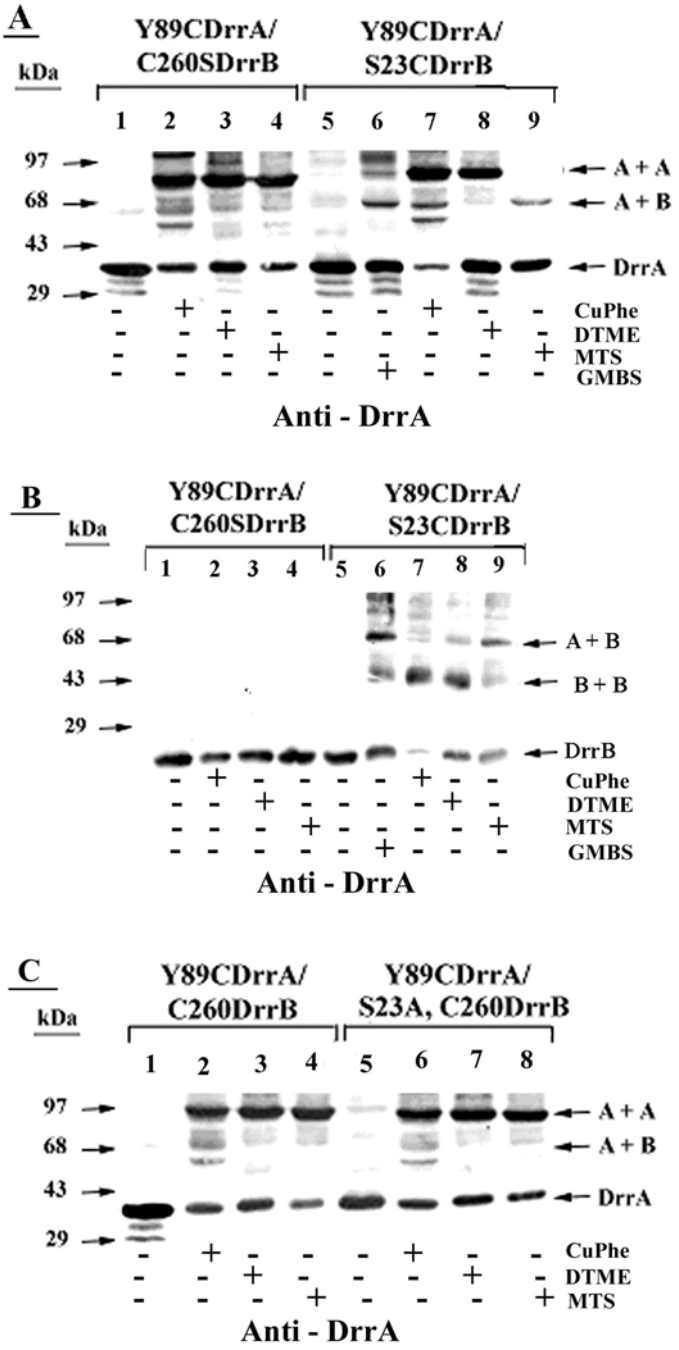

FIGURE 9: Use of disulphide cross-linkers of different arm-lengths: The protocols for membrane preparation and cross-linking analyses were same as described under legend to Fig.

3. Three cross-linkers of different am-lengths were used. These include 3 mM/9 mM CuPhe (0 Å), 1 mM DTME (13.3 Å), or 0.2 mM MTS (24.0 Å). Lanes 1-4, Y89C(A)/C260S(B); lanes 5-9, Y89C(A)/S23C(B). Cross-linked samples were probed with anti-DrrA or anti-DrrB antibodies. Panel A, anti-DrrA; Panel B, anti-DrrB. Panel C: Lanes 1- 4, Y89C(A)/C260(B); and lanes 5-8, Y89C(A)/S23A, C260(B). Cross-linked samples were probed with anti-DrrA antibodies.

The "minus" and "plus" at the bottom of the lanes indicate the absence and presence of the cross-linker in the reaction, respectively. The migration of the protein standards is shown on the left.

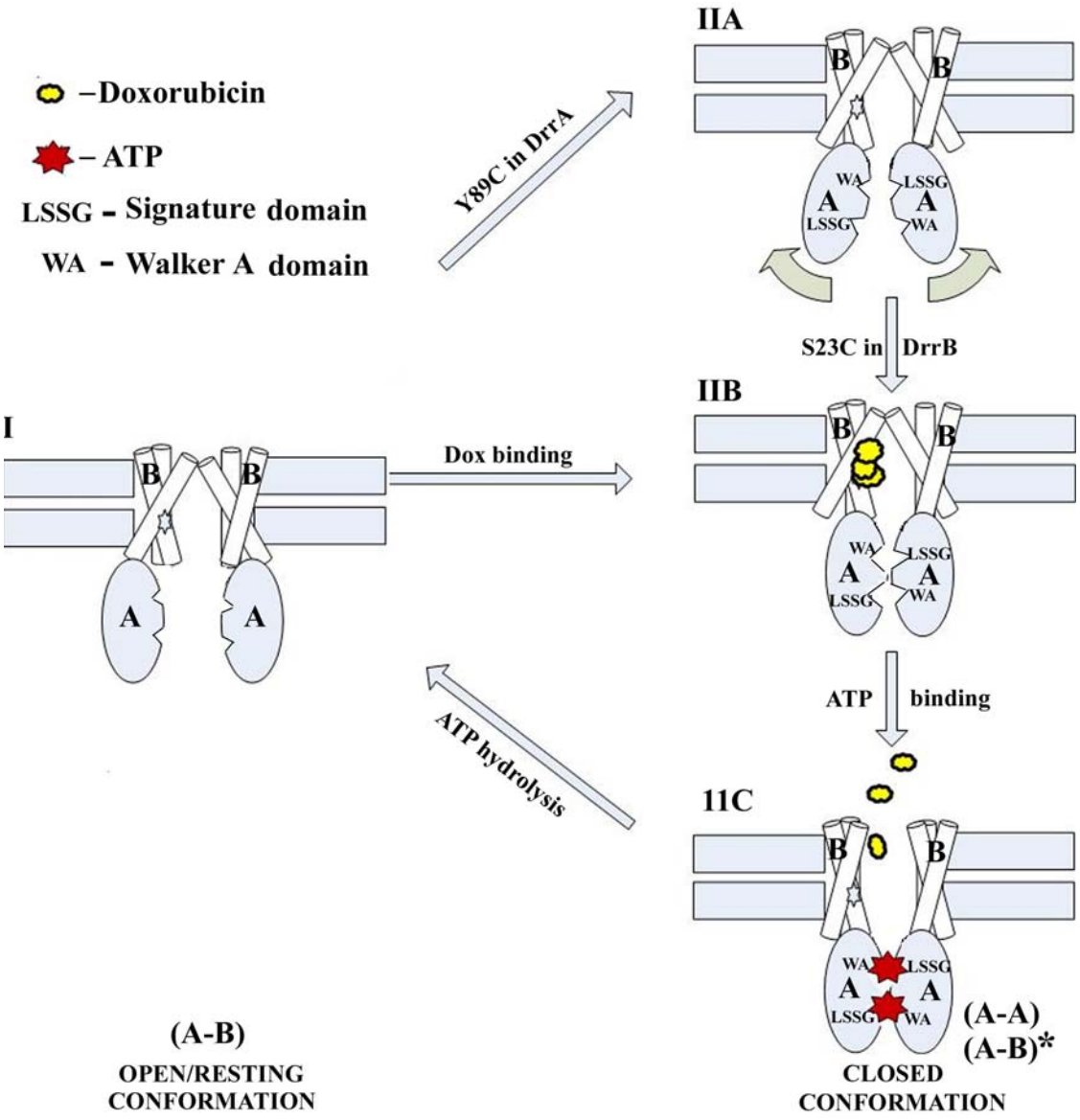

FIGURE 10: A model showing different conformations of DrrA and DrrB involved in the mechanism of doxorubicin efflux by the DrrAB pump. The model depicted here is based on analyses of Y89C and S23C substitutions in DrrA and DrrB, respectively. The resting-state complex of DrrA and DrrB (Confo. I, represented as A-B) is shown on the left. This state was

previously identified through DTSSP and GMBS cross-linking experiments (4,5). In this state, the DrrA monomers are away from each other, and the primary interaction occurs between the N-terminal cytoplasmic tail of DrrB and an unidentified region of DrrA (5). The helical domains of DrrA monomers are shown either facing towards each other (IA) (as seen in ref. 22), or away from each other (IB) (as proposed in ref. 32). Y89C substitution in DrrA changes the conformation to that resembling the closed conformation (Confo. IIA), as seen in disulfide cross-linking experiments presented in this study. In this conformation, the two Q-loops are close together (A-A), and they also form transient contacts with the N-terminal tail of DrrB (represented as A-B*). The Y89C-Y89C contact in this conformation is flexible (shown as a moving arrow), however simultaneous presence of S23C in DrrB produces a more rigid, closed conformation (Confo. IIB). This conformation resembles the conformation resulting from binding of doxorubicin to the wild type DrrB, and it is competent to bind ATP. This is consistent with previous studies conducted in this laboratory which show that ATP binding to DrrA occurs only when DrrA is in a complex with DrrB (4), and, furthermore, ATP binding to DrrA is stimulated by doxorubicin binding (2,4). Binding of ATP to this conformation then serves as the power stroke (Confo. IIC) for efflux of doxorubicin. Hydrolysis of ATP subsequently returns the pump to the resting state.

SUPPLEMENTARY DATA

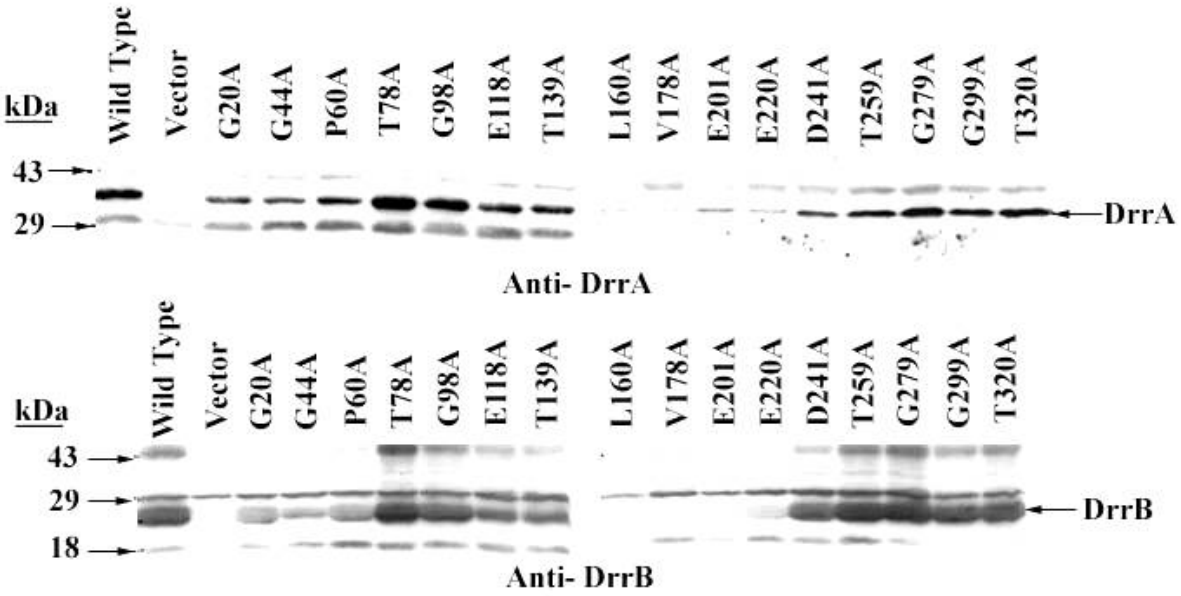

FIGURE S1: Alanine scanning mutagenesis of DrrA: To determine the domains in DrrA that have an effect on the expression and overall function of the DrrAB proteins, alanine substitutions were made all along the length of the DrrA proteins approximately 15 residues apart. The proteins were resolved by SDS-PAGE on 10% gels, followed by autoradiography.

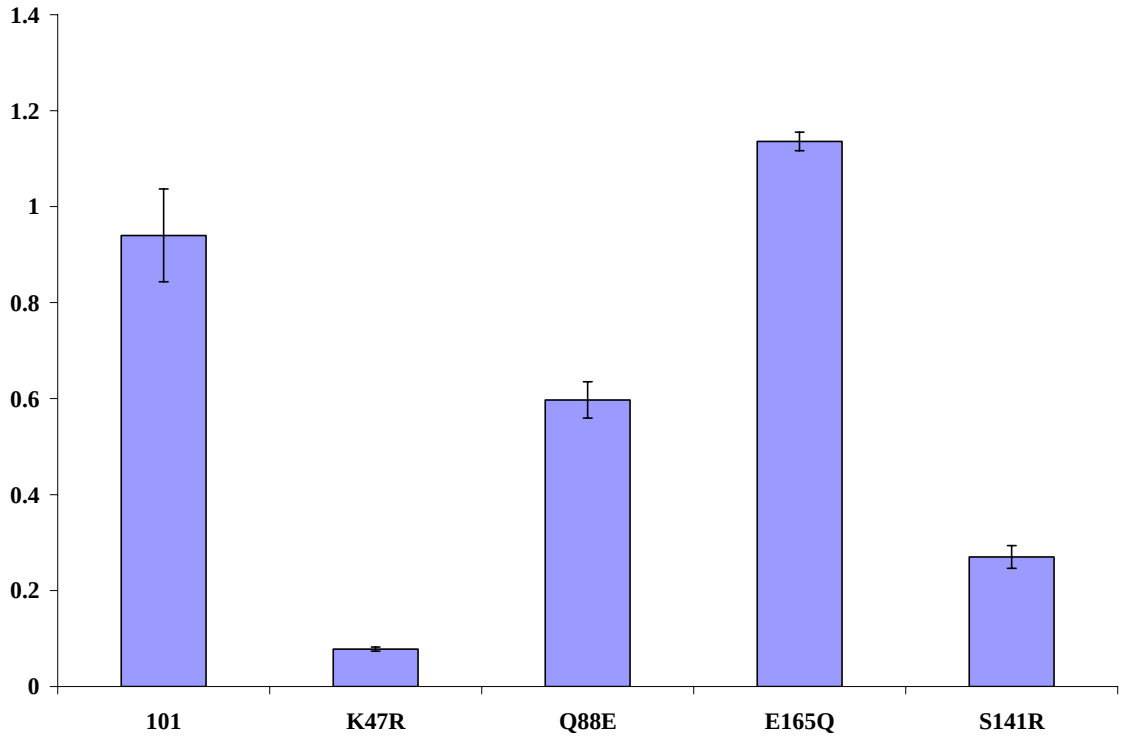

FIGURE S2: Quantitation of the ratio of ATP bound/protein concentration of point mutations in DrrA: The data shown in Figure 2 were quantitated. The averages of the ratio of ATP bound/protein concentration (from three experiments) were plotted in the histogram. The error bars reflect standard deviations.

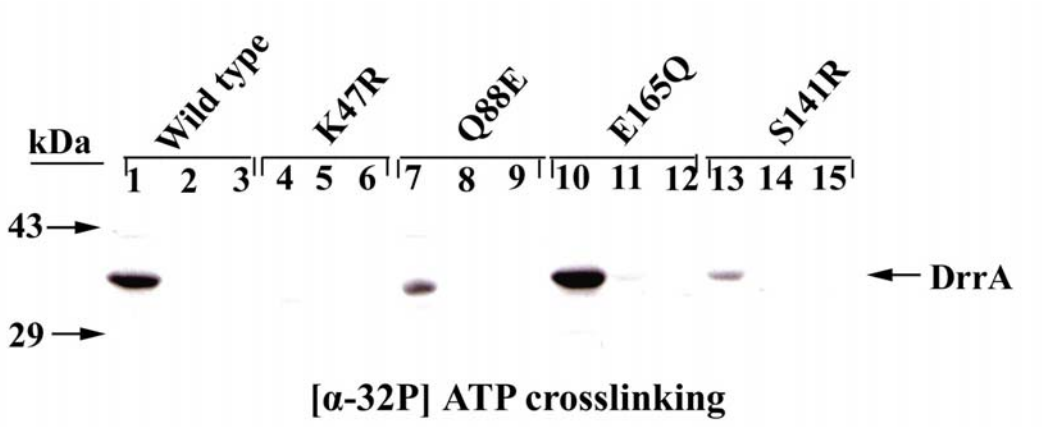

FIGURE S3: Competition with excess unlabeled nucleotides: Photoadduct formation between DrrA and [α-32P] ATP was carried out as described in the legend to Figure 2. The proteins were resolved by SDS-PAGE on 10% gels, followed by autoradiography. Lanes 1, 4, 7, 10, and 13-10μM unlabeled ATP; lanes 2, 5, 8, 11, and 14-100μM unlabeled ATP; lanes 3, 6, 9, 12, and 15-500μM

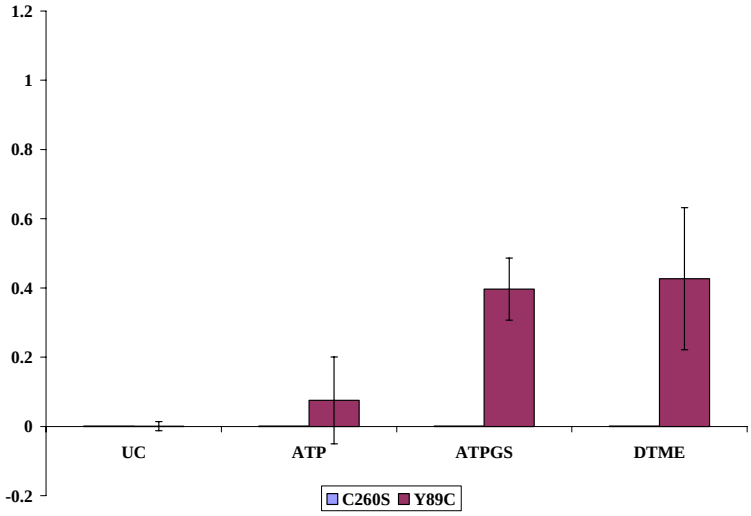
1.2
1
0.8
0.6
0.4
0.2
0
-0.2
UC
ATP
ATPGS
DTME
C260S
Y89C

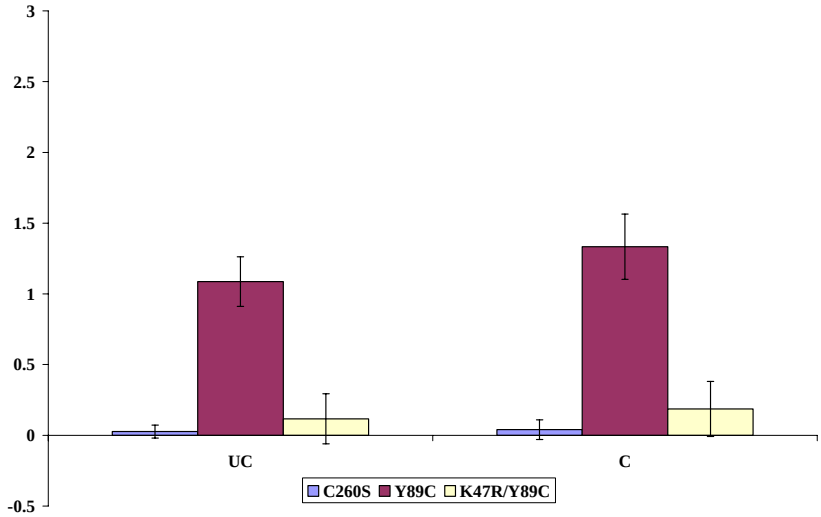
3
2.5
2
1.5
1
0.5
0
-0.5
UC
C
C260S
Y89C
K47R/Y89C

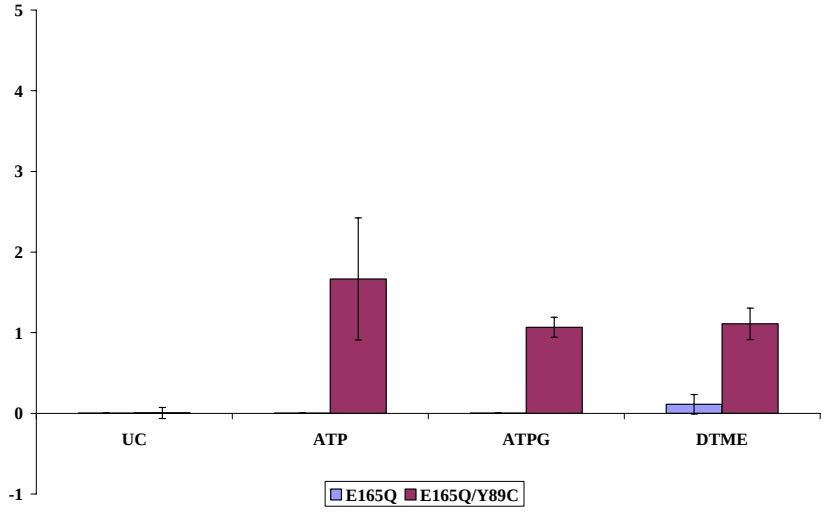
5
4
3
2
1
0
-1
UC
ATP
ATPG
DTME
E165Q
E165Q/Y89C

FIGURE S4: Quantitation of the ratio of cross-linked dimer/monomeric DrrA protein: The data shown in Figure 7 were quantitated. The averages of the ratio of cross-linked dimer/monomeric DrrA (from three experiments) were plotted in the histogram. The error bars reflect standard deviations.

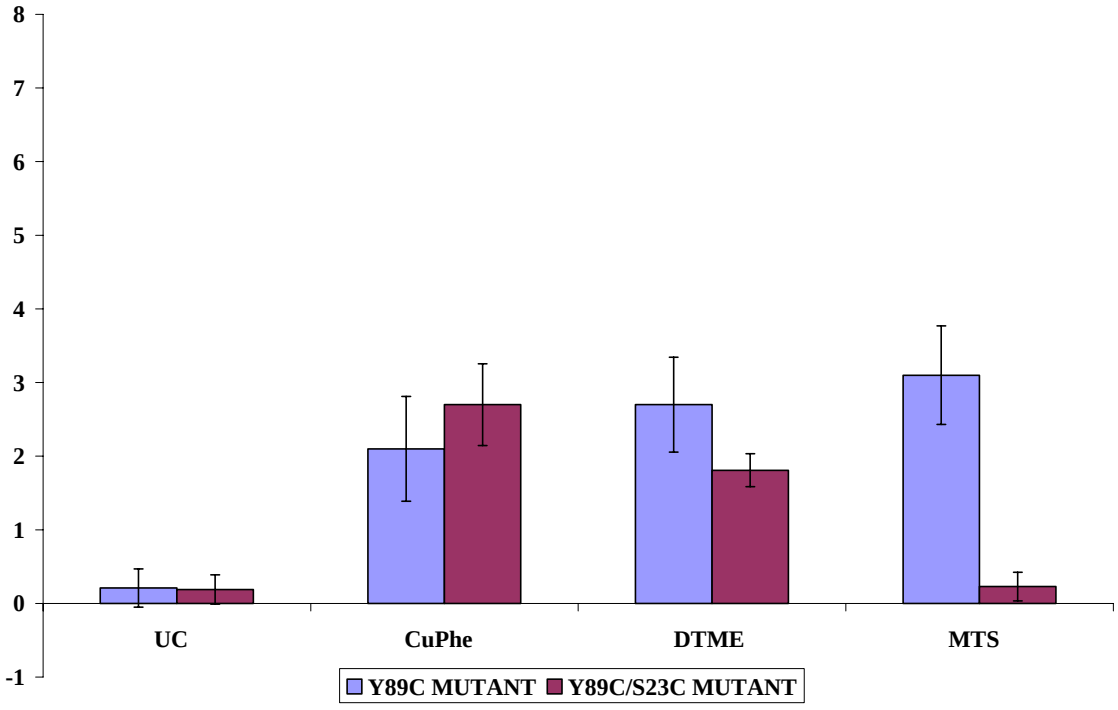

FIGURE S5: Quantitation of the ratio of cross-linked dimer/monomeric DrrA protein: The data shown in Figure 5 were quantitated. The averages of the ratio of cross-linked dimer/monomeric DrrA (from three experiments) were plotted in the histogram. The error bars reflect standard deviations.

CHAPTER III

Role of FtsH and GroEL in the Biogenesis of the DrrAB efflux pump

ABSTRACT

Streptomyces peucetius produces two anticancer agents, doxorubicin and daunorubicin, that belong to the anthracycline family of antibiotics. The organism is self-resistant to the potent effects of the antibiotics it produces due to the action of an efflux pump, DrrAB. The doxorubicin efflux pump is made up of two components: DrrA and DrrB. It has been shown that the two proteins are dependent on each other for stability and function. DrrB when expressed by itself (when DrrA is not simultaneously present) is rapidly degraded by a protease. Several known AAA metalloproteases have been known to degrade misassembled membrane proteins The goal of the present study is to determine the protease that is involved in the degradation of DrrB. This is expected to provide information about the biogenesis of the complex. Recent studies in this laboratory have shown that GroEL may also play a role in the biogenesis of the DrrAB complex. The present study investigates the role of FtsH and GroEL in the biogenesis of the DrrAB complex.

INTRODUCTION

Streptomyces peucetius produces two anticancer agents, doxorubicin and daunorubicin, that belong to the anthracycline family of antibiotics. The organism is self-resistant to the potent effects of the antibiotics it produces due to the action of an efflux pump, DrrAB (*1, 2*). The antibiotic synthesis and resistance genes are clustered together in the *dnr* operon (*1*). The doxorubicin efflux pump is made up of two components: DrrA and DrrB (*2*). The *drrAB* genes have been cloned into the heterologous *E. coli* expression system. Preliminary studies to determine the function and stability of the proteins in the expression system indicate that DrrA and DrrB are in their proper conformation (*2-5*). It has been shown that the two proteins are dependent on each other for stability and function (*3*). A Western blot analysis of cells containing the *drrB* gene alone shows a drastic reduction in the level of the DrrB protein (Figure 1, lane 3), implying that DrrA is required for stable expression of DrrB. When DrrA is introduced into the cells in *trans*, the expression level of DrrB is restored (lane 5). This suggests that DrrB depends on DrrA for maintaining its stability. Levels of DrrA are also reduced in cells containing the *drrA* gene alone, but not as dramatically as DrrB alone (lane 1 and 2). However, no ATP binding to DrrA is detected in cells containing DrrA alone, suggesting that DrrA is dependent on DrrB for maintaining its active conformation (*3*). The co-dependence of DrrA and DrrB on one another suggests biochemical coupling between the two proteins. Chemical cross-linking studies have shown that the two proteins interact with each other to form a tetramer with a stoichiometry of $DrrA_2B_2$.

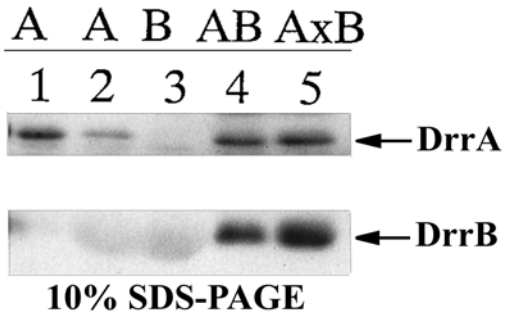

J BIOL CHEM, (1998). 273, 17933-17939

FIGURE 1: Effect of co-expression of DrrA and DrrB. *E. coli* cells, co-transformed with pDX103 and pDX108, were induced with IPTG and lysed as described under "Experimental Procedures". The total lysates were analyzed by SDS-PAGE followed by Western blot analysis using anti-DrrA or anti-DrrB serum. *Lane 1*, pDX108; *lane 2*, pDX102; *lane 3*, pDX103; *lane 4*, pDX101; *lane 5*, pDX103 and pDX108.

It has been observed previously that the accumulation of DrrB in the absence of DrrA (by gene fusions or expression from a strong promoter) can inhibit the growth of *E.coli* cells (Figure 2, curve with filled circles) (*2*). When DrrB is in complex with DrrA, no negative effect on growth is seen indicating that DrrA is able to stabilize DrrB and together they are able to form a healthy complex (Figure 2, open circles). Several known AAA metalloproteases have been known to degrade misassembled membrane proteins. Degradation of unassembled SecY (when SecE is absent), a subunit of the protein translocase, as well as the subunit 'a' of the F_o subunit of the H^+- ATPase has been shown to be brought about by FtsH. (*6, 7*). The goal of the present study is to determine the protease that is involved in the degradation of DrrB.

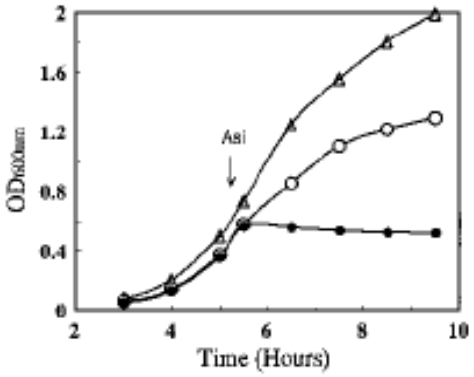

JOURNAL OF BACTERIOLOGY (1997), 569–575

FIGURE 2: Effect of induction of ArsD-DrrA or ArsD-DrrB fusion proteins. *E.coli* cells containing the indicated plasmids were grown to exponential phase andinduced with 10 mM sodium arsenite. Growth was monitored by recording the OD600 of the cultures. Triangles: DrrAB in *cis*; Empty circles: DrrA only; Filled circles: DrrB only.

Recent studies in this laboratory have shown that GroEL may play a role in the biogenesis of the DrrAB complex. It was found that when DrrA was purified by itself from the soluble fraction, it co-purifies with GroEL. GroEL did not co-purify with the complex of DrrAB. GroEL may have an important role to play in the folding state of the DrrA protein and in the overall assembly of the DrrAB pump. This molecular chaperone is believed to play a variety of roles, which include promoting folding, assembly, secretion, or membrane insertion of proteins (*8*). The present study investigates the role of GroEL in the biogenesis of the DrrAB complex.

To overcome the challenges in purification and reconstitution of the DrrA and DrrB proteins, it has become an important objective in this laboratory to study the factors involved in

stability, folding and and assembly of the DrrAB complex. This chapter involves the determination of the accessory proteins in the biogenesis of DrrAB, mainly, the protease/s involved in the degradation of DrrB and the role of GroEL in the assembly of the transporter.

EXPERIMENTAL PROCEDURES

Bacterial Strains and Plasmids: The bacterial strains are TG1, HMS174, SG110 (lon$^-$) ARK797 (*ftsH*$^-$), ARK796 (*ftsH*$^+$), MC4100 (GroEL$^+$) and NRK117 (GroEL$^-$). Plasmids used in this study are described below.

PLASMID	**GENOTYPE**
pDX101	P_{lac}*drrAB* in pSU2718
pDX103	P_{lac}*drrB* in pSU2718
pUC18drrAB	P_{lac}*drrAB* in pUC18
pDX203	P_{lac}*drrB* in pUC18
pDXFtsH	P_{lac}*ftsH* in pSU2718
pUCFtsH	P_{lac}*ftsH* in pUC18
pDXGroEL	P_{lac}*groEL* in pSU2718
pKYGroEL/ES	$P_{lac}P_{groE}$*groEL/ES* in pSU2718

Media and Growth conditions: The cells were grown in LB medium at 37^{o}C (9), unless mentioned otherwise. Chloramphenicol was added to 20 µg/ml, kanamycin was added to 30 µg/ml, ampicillin was added to 100 µg/ml, and tetracycline was added to 15 µg/ml, where needed.

DNA manipulations: The conditions for plasmid isolation, DNA endonuclease restriction analysis, ligation, and sequencing have been described elsewhere.

Construction of site-directed mutations in ftsH: *ftsH* mutants were constructed by site-directed mutagenesis using a strategene QuikChange multisite-directed mutagenesis kit (La Jolla, CA).

The strategy involved the use of complimentary primers that incorporated the change at the required position. The templates used included pUC18*ftsH* and pSU2718 *ftsH*, and the primers were designed as described earlier (*4*). Based on published data (*10, 11*), the conserved lysine residue at position 198 in the Walker A domain of *ftsH* was altered to arginine (K198R) and the conserved glutamate residue at position 415 in the Zn^{2+} binding motif was altered to glutamine (E415Q) respectively. All mutations were verified by nucleotide sequencing.

Growth experiments using protease- deficient strains: The effect of DrrAB and DrrB protein expression on the growth of protease deficient strains (AR797, *ftsH*$^-$; SG110, *lon*$^-$; SG1126, *clpA*$^-$ and AD1089, *clpP*$^-$) was analyzed. Different strains containing the appropriate plasmid were grown at 30^{o}C followed by induction at mid-log phase with 0.25mM isopropylthiogalactopyranoside (IPTG). Following induction, the samples were immediately shifted to 42^{o}C. Cell growth was monitored by measuring the O.D at 600nm at 0, 1, 2 and 3 hours after induction.

Effect of FtsH on DrrAB and DrrB protein expression: Growth and induction of AR797 (*ftsH*$^-$) and ARK796 (*ftsH*$^+$) strains containing the indicated plasmids was carried out as described in the previous section. Cells were collected at 3 hours after switch to 42^{o}C. The cells were spun down and resuspended in 1.5 ml QAE buffer (25 mM Tris.Cl, pH 8.0, 20% glycerol, 2 mM EDTA) containing 1 mM DTT and lysed by a single passage through a French pressure cell at 20,000 psi. The cell lysates were then centrifuged at 10,000 g for 15 minutes to remove unbroken cells. The supernatant was centrifuged at 100,000 g for 1 hour to prepare membrane protein. 50 μg of membrane protein of the reaction mixture was then analyzed by SDS-PAGE using a 10% polyacrylamide gel, followed by Western blot analysis using either

anti-DrrA or anti-DrrB antibodies. Similar studies were done using wild-type TG1 cells containing the indicated plasmids. Growth and induction were done at 37^{o}C unless mentioned otherwise. Levels of DrrAB and DrrB were analyzed as mentioned above.

Co-purification of GroEL and solubilized fraction of DrrA: Purification DrrA in complex with DrrB and DrrA alone: DrrAB proteins were purified using pDx121, which introduces his-tags at the N-terminus of DrrA and the C-terminus of DrrB. DrrA was purified using pDX132, which introduces a his-tag at the N terminus of DrrA. HMS174 cells containing the indicated plasmid were induced with IPTG. Membrane and cytosolic fractions were prepared, as described above. DrrA protein was purified from the cytosolic fraction by using a Ni-NTA column, while the DrrAB proteins were solubilized from the membrane fraction and purified as a complex using Ni-NTA. 5 mg membrane protein was solubilized in 5ml buffer containing Buffer A(75mM KPi pH 7.4, 200mM NaCl, 20%Glycerol) containing 1mM DTT, and 1X Protease Buffer and 1% n-OG. Reaction was incubated for 1 hr on ice. The solubilized reaction was ultracentrifuged for 1 hr and loaded onto a Ni-column that was pre-equilibrated with 2 column volumes (20 ml) of freshly prepared Buffer B (75mM KPi pH 7.4, 200mM NaCl, 20 % Glycerol and 0.05% n-OG) followed by incubation for 1hr at 4^{o}C. The column is washed with 3 column volumes (30 ml) of Buffer B containing 10mM Imidazole and eluted with Buffer A (75mM KPi pH 7.4, 200mM NaCl, 20% glycerol) containing 1% n-OG and 500mM Imidazole. 20µl of the sample was resuspended in 5µl 4X Laemmli sample buffer and solubilized by heating at 55^{o}C for 10 min. The samples were analyzed by SDS-PAGE followed by Western blot analysis with anti-DrrA or anti-DrrB antibodies.

Identification of the unknown 68 kDa protein by amino acid sequencing: The purified DrrA protein samples were run on a 10% polyacrylamide gel for electrophoresis. The 68 kDa protein

band was transferred onto a polyvinylidene difluoride membrane. The band was excised and subjected to N-terminal sequencing using a Beckman model LF3000 solid phase amino acid sequencer in the core facility of the Department of Biology at the Georgia State University. Following identification, the protein samples were separated by electrophoresis followed by western blot analysis using anti-DrrA and anti-GroEL antibodies.

Effect of GroEL/ES on DrrAB and DrrB expression: The expression of proteins was analyzed by growth of NRK117 (*groEL*$^-$) and MC4100 (*groEL*$^+$) strains containing the indicated plasmids at 37^{o}C to a mid-log phase followed by induction at mid-log phase with 0.25mM isopropylthiogalactopyranoside (IPTG). Samples were collected at 3 hours post induction. The cells were spun down and resuspended in 1.5 ml QAE buffer (25 mM Tris.Cl, pH 8.0, 20% glycerol, 2 mM EDTA) containing 1 mM DTT and lysed by a single passage through a French pressure cell at 20,000 psi. The cell lysates were then centrifuged at 10,000 g for 15 minutes to remove unbroken cells. The supernatant was centrifuged at 100,000 g for 1 hour to prepare membrane protein. 50 μg of membrane protein of the reaction mixture was then analyzed by SDS-PAGE using a 10% polyacrylamide gel, followed by Western blot analysis using either anti-DrrA or anti-DrrB antibodies. To study the effect of GroEL on DrrAB or DrrB alone, in the presence or absence of FtsH, studies were done with the wild-type (AR796) and ts mutant strains (AR797) of FtsH. Cells containing plasmid containing *drrAB* or *drrB* were co-transformed with a plasmid carrying *groEL*. Cells were grown to a mid-log phase followed by induction at with 0.25mM isopropylthiogalactopyranoside (IPTG). Following induction, the samples were immediately shifted to 42^{o}C. Levels of DrrAB and DrrB were analyzed as mentioned above.

RESULTS

Effect of expression of DrrAB or DrrB protein on growth of protease deficient strains: Plasmids carrying *drrAB* (pDx101) and *drrB* (pDx103) genes were transformed into different strains of *E.coli* carrying mutations for known proteases, namely *ftsH* (*12-14*), *lon* (*15*), *clpA* (*16*) and *clpP* (*17*). Cells were grown to exponential phase and induced with IPTG, followed by a temperature shift to 42^{o} C to inactivate FtsH. Optical Density (O.D) of cells was measured for 3 hours following induction as an indication of growth. Results show that while *lon*, *clpA* and *clpP* protease deficient strains showed no inhibition of growth (data not shown), ftsH^{-} strains showed an inhibition of growth (Figure 3). Results in Figure 3A show that cells expressing DrrB proteins alone as well as cells expressing DrrAB showed significant inhibitory effect on growth. Over-expression or the misassembly of membrane proteins has been shown to be harmful or toxic to the growth of cells in other studies (*18, 19*). Expression of DrrB in a protease-deficient strain might have a similar effect. Previous studies showed that when DrrB is in complex with DrrA, no negative effect on growth is seen indicating that DrrA is able to stabilize DrrB and together they are able to form a complex (*2*). Our results were therefore unexpected i.e. the growth defect in the ftsH^{-} strain caused by over-expression of the DrrAB complex. This might indicate that 1) the temperature shift to 42 ^{o}C might have destabilized the proteins, consequently causing the complex to come apart or become misassembled, or 2) FtsH in addition to degrading membrane proteins may play an additional role in the chaperone activity of the DrrAB transporter (*12, 14, 20, 21*). The growth experiment was also performed with FtsH^{+} and FtsH^{-} containing *drrAB* (pDx108) and *drrB* (pDx203) cloned in pUC18 over-expressing plasmid. Different results were observed in this case (compare figures 3A and 3B). While cells expressing DrrAB together (Figure 3B) grew normally, only the cells expressing

DrrB protein alone (Figure 3B) showed significant inhibitory effect on growth. Since strains containing both pSU2718 and pUC18 clones were upshifted at 42^{o}C, this rules out the temperature shift as being the reason for growth inhibitory phenotype seen in pSU*drrAB* (pDX101). If FtsH is also required for assembly of DrrAB complex, then why DrrAB protein expression from pUC18 plasmid did not cause growth inhibition? It is possible that the over-expression of DrrAB from pUC18 (a very high copy number plasmid) results in a different conformation, e.g. Inclusion body formation of the proteins, which may not cause growth in hibition.

A

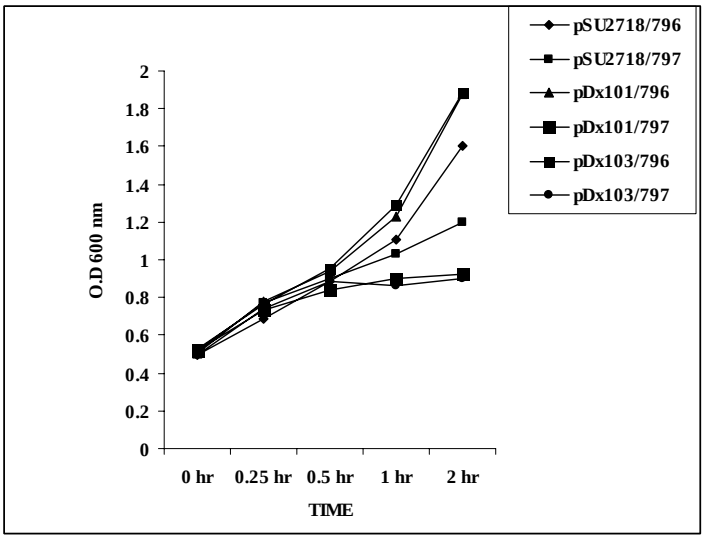

B

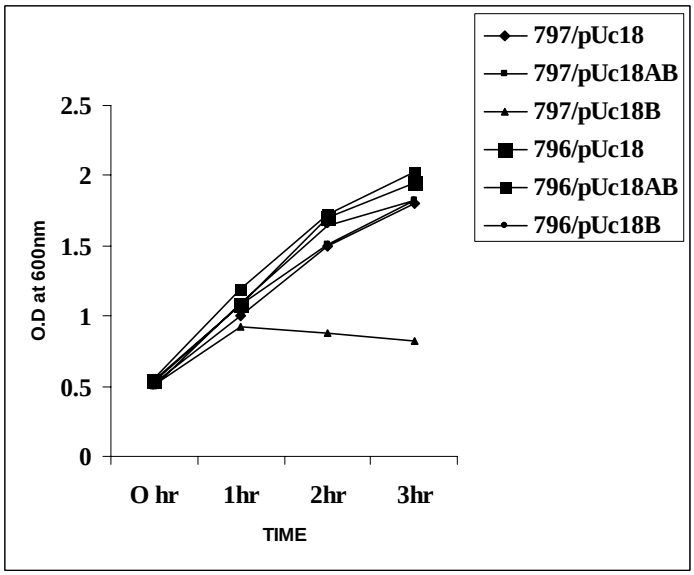

FIGURE 3: Growth analysis of FtsH-deficient strain expressing the drrAB or *drrB* genes. Growth curve analysis was conducted as mentioned under "Experimental procedures". Cells were grown at 30^{o}C to a mid-log phase followed by induction at mid-log phase with 0.25mM IPTG. Following induction, the samples were immediately shifted to 42^{o}C. A600 of the cells containing various were recorded after induction at 1 hour intervals for 3 hours.

Fig 3A: Growth analysis in *ftsH*$^{-}$ strains expressing drrAB or drrB from a low-copy number plasmid (pSU2718). Fig 3B: Growth analysis in *ftsH*$^{-}$ strains expressing drrAB or drrB from a high-copy number plasmid (pUC18).

To further establish the role of FtsH in DrrAB expression, we examined whether overproduction of FtsH could alleviate the growth defect in FtsH depleted cells caused by DrrAB or DrrB. *FtsH* gene from *E.coli* was cloned into pUC18 and pSU2718 plamids. FtsH was co-expressed with DrrAB or DrrB in the FtsH depleted strains. Results observed in Figure 4A or 4B indicate, that overproduction of FtsH can alleviate the growth defect in FtsH depleted cells containing DrrAB and/or DrrB.

A **B**

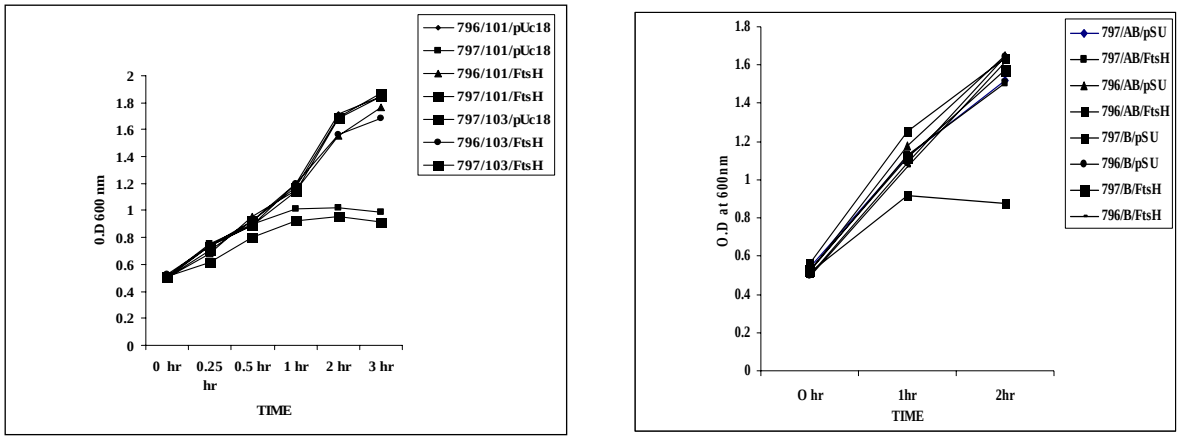

FIGURE 4: Growth analysis of AR796 (ftsH$^{+)}$ and deficient AR797 (*ftsH* $^{-}$) strains expressing *drrAB* or *drrB* along with *ftsH*.

Growth analysis was conducted as mentioned under "Experimental procedures". Cells were grown at 30^{o}C to a mid-log phase followed by induction at mid-log phase with 0.25mM IPTG. Following induction, the samples were immediately shifted to 42^{o}C. A600 of the cells containing various were recorded after induction at 1 hour intervals for 3 hours.

A pSU*drrAB* (pDX101) or pSU*drrB* (pDX103) in combination with pUC*ftsH*.

B pUC*drrAB* (pDX108) or pUC*drrB* (pDX203) in combination with pSU*ftsH*.

Effect of FtsH expression on levels of DrrAB: To further characterize the effect of FtsH on the levels of DrrAB, 50 ml of cells from the above growth curve experiments were harvested at 2 hr post induction and membrane proteins were prepared. Western blot analysis of 50 µg membrane protein was carried out with either anti-DrrA or anti-DrrB antibodies. The expression of DrrA and DrrB from pSU*drrAB* (pDX101) in ARK796 (*ftsH*$^+$) was less (Figure 5A, lane 1) as compared to levels of DrrA and DrrB from pSU*drrAB* in AR797 (*ftsH*$^-$) (Figure 5A, lane 3). Similar results were obtained when pUC*drrAB* (pDX108) were expressed in ARK796 (*ftsH*$^+$) (Figure 5B, lane 1) and AR797 (*ftsH*$^-$) (Figure 5B, lane 3). The data suggest that the DrrAB proteins accumulate in the absence of FtsH, thus resulting in toxic effect to the cells. When FtsH was over-expressed from a plasmid along with DrrAB in the FtsH depleted strains, the levels of DrrA and DrrB in either plasmid combination (Figure 5A, lanes 2 and 4 and 5B, lanes 2 and 4) were significantly decreased in either strain (ARK796 (*ftsH*$^+$) or AR797 (*ftsH*$^-$)). These data further indicates that FtsH is involved in degradation of DrrA and DrrB.

A

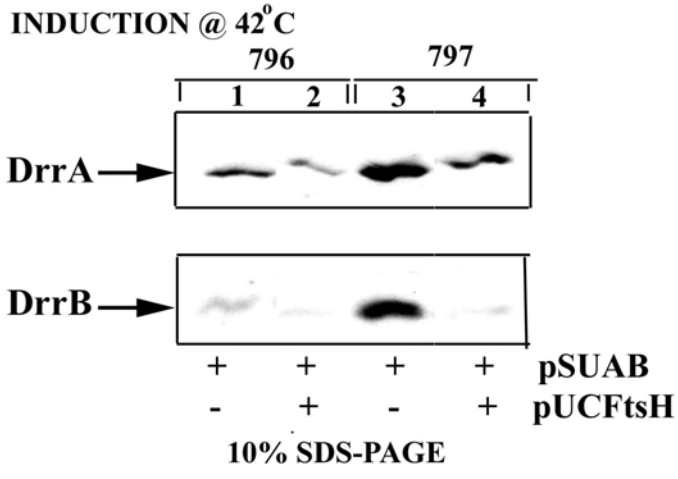

B

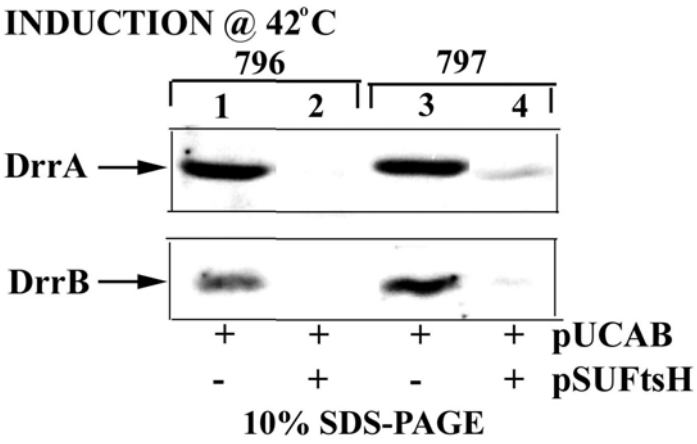

FIGURE 5*: Effect of FtsH on expression levels of DrrAB*

AR796 and AR797 cells containing the appropriate plasmid/s were grown at 30°C to mid-log phase followed by induction with 0.25mM IPTG. Following induction, the samples were immediately shifted to 42°C. Membrane fraction was prepared as described in "Experimental Procedures". 50 μg membrane protein was analyzed by 10% SDS-PAGE, followed by Western blot using anti-DrrA and anti-DrrB antibodies.

Fig 5A: Lanes 1, AR796/pSUAB; Lane 2, AR796/pSUAB/pUCFtsH; Lane 3, AR797/pSUAB; Lane 4, AR797/pSUAB/pUCFtsH.

Fig 5B: Lanes 1, AR796/pUCAB; Lane 2, AR796/pUCAB/pSUFtsH; Lane 3, AR797/pUCAB; Lane 4, AR797/pUCAB/pSUFtsH

Effect of FtsH expression on expression levels of DrrB: When DrrB was expressed in the absence of DrrA, the level of DrrB from pUC*drrB* (pDX203) in ARK796 (*ftsH*$^{+}$) was much less (Figure 6A, lane 1) as compared to pUC*drrB* in AR797 (*ftsH*$^{-}$). Accumulation of high levels of DrrB in FtsH^{-} strain confirms that FtsH is involved in the degradation of DrrB.The above data confirms that FtsH is involved in the degradation of DrrB. In addition, it suggests that DrrA may regulate the synthesis of DrrB so that in the absence of DrrA, high levels of DrrB accumulated due to unregulated expression

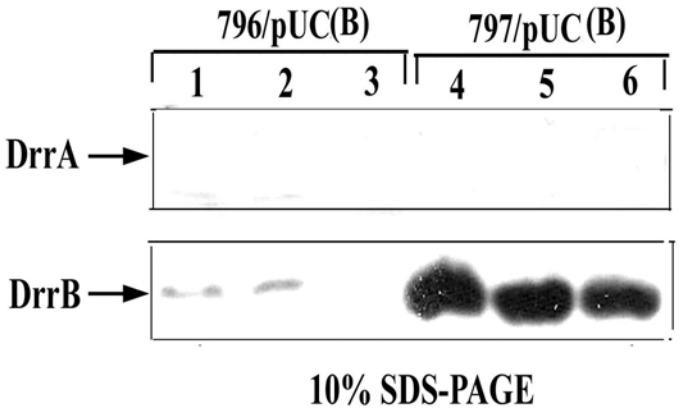

FIGURE 6*:* Effect of FtsH on expression levels of DrrB in the absence of DrrA

AR796 and AR797 cells containing the appropriate plasmid were grown at 30^{o}C to a mid-log phase followed by induction at mid-log phase with 0.25mM IPTG. Following induction, the samples were immediately shifted to 42^{o}C. Membrane fraction was prepared as described in "Experimental Procedures". 50 µg membrane protein was analyzed by 10% SDS-PAGE followed by Western blot using anti-DrrB antibodies. Lanes 1, AR796/pUCB- 1 hr induction; Lane 2, AR796/pUCB- 2 hr induction; Lane 3, AR796/pUCB- 3 hr induction; Lane 4, AR797/pUCB- 1 hr induction; Lane 5, AR797/pUCB- 2 hr induction; Lane 6, AR797/pUCB- 3 hr induction.

Suppression of growth defect by the over expression-of GroEL: We further tested whether over expression of GroEL was able to restore the growth defect caused by DrrAB or DrrB in FtsH-depleted strains. *GroEL* gene from *E.coli* was cloned into pSU2718 plamid. GroEL was co-expressed with DrrAB or DrrB in the FtsH-depleted strains. Results in Figure 7A (pSU*drrAB* or pSU*drrB* in combination with pUCGroEL) indicate that overproduction of FtsH can alleviate the growth defect in FtsH-depleted cells expressing DrrB. Studies with alkaline phosphatase that was fused to the SecY membrane protein have shown that the growth defect and the abnormal translocation of alkaline phosphatase in *ftsH* mutant strains can be suppressed by the overproduction of the molecular chaperone Hsp90 (*22*). Thus, FtsH may have an additional chaperone-like activity that has been proposed for other AAA ATPases (*23-26*).

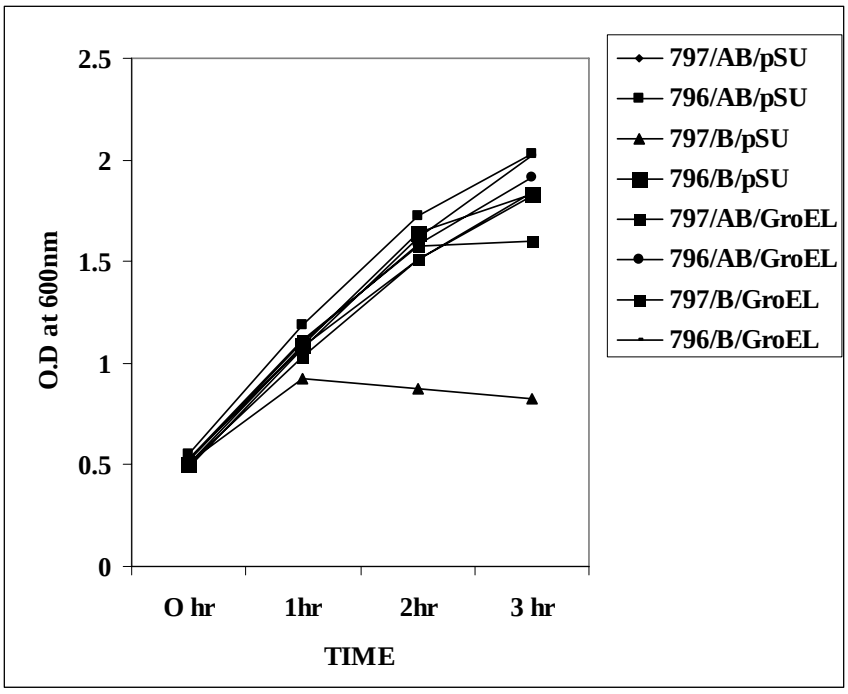

FIGURE 7: Growth analysis of wild-type FtsH (AR796, *ftsH*$^{+)}$ and deficient FtsH (AR797, *ftsH* $^{-}$) strains simultaneously expressing two genes, *drrAB* or *drrB* along with wild type *groEL*.

Growth curve analysis was conducted as mentioned under "Experimental procedures". Cells were grown at 30^{o}C to a mid-log phase followed by induction at mid-log phase with 0.25mM IPTG. Following induction, the samples were immediately shifted to 42^{o}C. A600 of the cells containing various were recorded after induction at 1 hour intervals for 3 hours.

Role of FtsH as a chaperone for DrrAB: Construction of FtsH mutants in the AAA domain and the HExxH domain: To study the role of FtsH as a potential chaperone for DrrAB assembly, mutants in the ATPase domain (K198R) and the protease domain (E415Q) of *ftsH* were constructed within the plasmid containing the *ftsH* gene. In ATP-dependent proteases, Lon (*26*) and YmeI (*24*), a mutation in the conserved lysine residue of the ATPase domain was found to prevent chaperone function while retaining the protease function, and a mutation in the glutamine residue of the protease domain abolished proteolytic activity while maintaining the chaperone activity of the protease. Similar mutants constructed in FtsH by two groups show contradictory results. Ito's group (*10*) has shown that the glutamine mutation in the proteolytic domain retained the proteolytic function of the protein while Holler's group (*11*) have shown that the mutation completely lacks protease activity. In this study, the FtsH mutants (K198R and E415Q) were co-expressed with DrrAB or DrrB in the $FtsH^-$ strains. Our results show that the mutation in the proteolytic domain (E415Q) of FtsH was able to restore the growth defect caused by DrrAB or DrrB in FtsH depleted strains, while a mutation in the ATPase domain (K198R) was unable to restore the growth defect in these strains.

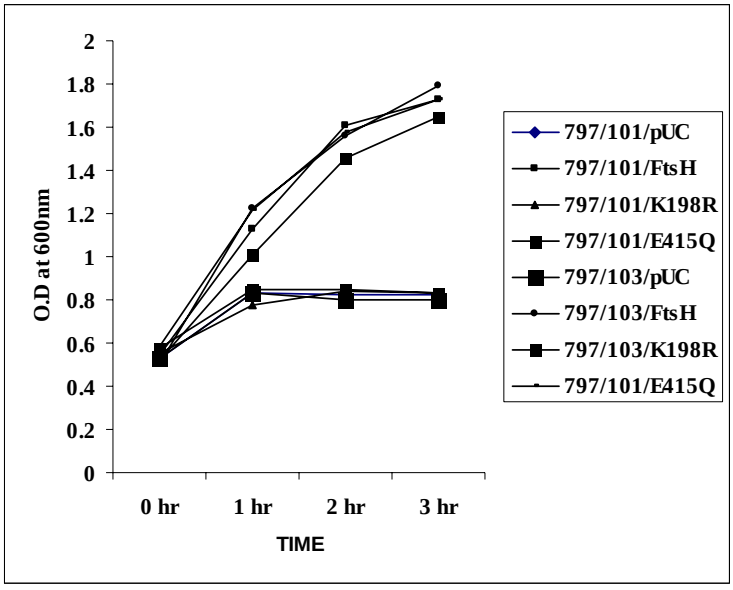

FIGURE 8: Growth analysis of AR796 (*ftsH*$^{+}$) and AR797 (*ftsH* $^{-}$) strains expressing *drrAB* or *drrB* along with wild type *ftsH* or its mutants *FtsHK198R* and *FtsHE415Q*.

Growth analysis was conducted as mentioned under "Experimental procedures". Cells were grown at 30^{o}C to a mid-log phase followed by induction at mid-log phase with 0.25mM IPTG. Following induction, the samples were immediately shifted to 42^{o}C.A600 of the cells containing various were recorded after induction at 1 hour intervals for 3 hours.

Effect of FtsH mutants on levels of DrrA and DrrB: The levels of DrrA and DrrB in the above mutants were analyzed. Differences in the levels of DrrA and DrrB accumulation indicate that the K198R, a mutation in the ATPase domain of FtsH, also abolished the proteolytic function (Figure 9, lane 5 and 6), thereby causing the accumulation of DrrA and DrrB, and growth inhibition seen in Figure 8. The E415Q mutant lost about 75% of its proteolytic function (Figure 9, lane 7 and 8) resulting in accumulation of 1/4th the amount of DrrA and DrrB proteins. From the above data, no conclusions could be made on the chaperone effect of FtsH, since the E165Q mutant still retains potential protease activity. Thus restoration of growth seen in Figure 8 would result from either chaperone effect of the functional AAA domain or due to proteolysis of DrrAB proteins.

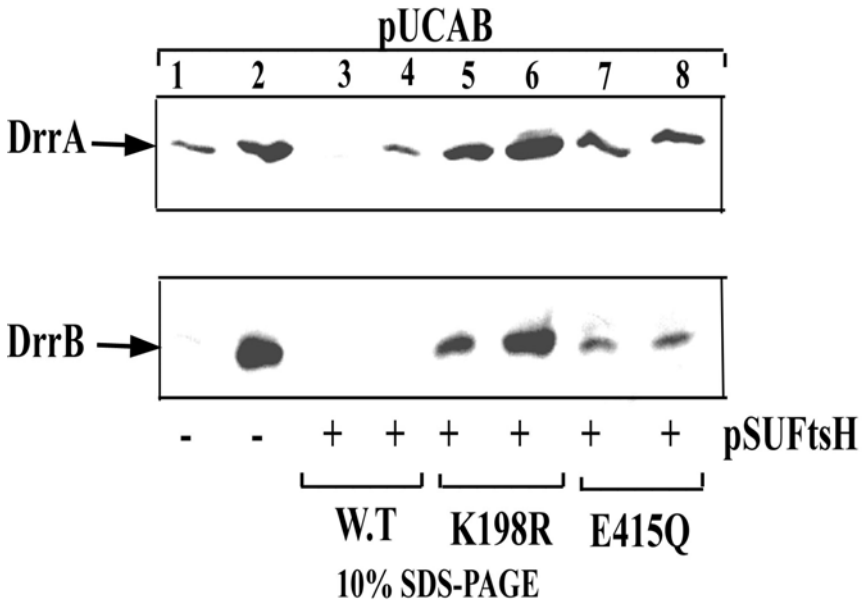

FIGURE 9: **Effect of FtsH mutants on expression levels of DrrAB in wild type *E.coli* TGI cells.**

TG1 cells containing the indicated plasmids were grown at 37^{o}C to a mid-log phase followed by induction at mid-log phase with 0.25mM IPTG. Following induction, the samples were incubated for 3 hrs at 37^{o}C. Membrane fraction was prepared as described in "Experimental Procedures". 50 µg membrane protein was analyzed by 10% SDS-PAGE followed by Western blot using anti-DrrA and anti-DrrB antibodies. Lanes 1-2, pUCAB/ pSU2718; Lanes 3-4, pUCAB/ pSUFtsH; Lanes 5-6, pUCAB/ pSUFtsHK198R; Lanes 7-8, pUCAB/ pSUFtsHE415Q.

Effect of FtsH on misassembled or over expressed DrrAB proteins: To further examine the degradative effect of FtsH on the DrrAB complex, wild-type *E.coli* cells were co-transformed with plasmids carrying *drrAB* and *ftsH* genes. Following induction, cells were grown for an additional 3 hours at 37°C and not at 42°C as with the previous experiments performed with ARK796 (*ftsH*$^+$) or AR797 (*ftsH*$^-$) strains. Results in Figure 10A, (where DrrAB was expressed on a low copy number plasmid, pSU2718), show that FtsH has no degradative effect on DrrAB when expressed in low copy numbers at 37°C. However, when the temperature was shifted to 42°C soon after induction (Figure 10B), FtsH degraded DrrB as indicated by the complete loss of protein in this situation. When DrrAB was expressed on a high copy number plasmid, pUC18, FtsH degraded the over-expressed proteins even at 37°C induction (Figure 10C, lanes 3 and 4). Thus FtsH may play a crucial role in quality control and biogenesis of the DrrAB complex by removing improperly assembled DrrB or DrrAB protein. These results show that expression of DrrAB from a low copy number plasmid results in proper assembly of the complex, which is not susceptible to cleavage by FtsH (Figure 10A). However, expression from a high-copy number plasmid (pUC18) results in improper assembly and these proteins are targeted by FtsH (Figure 10C).

A

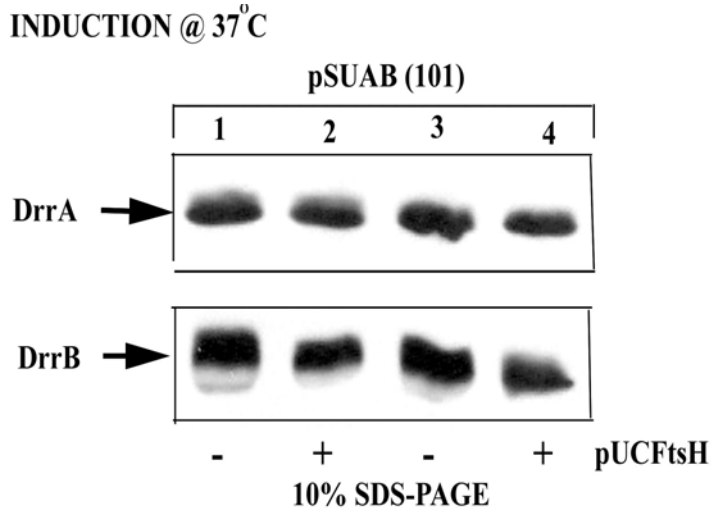

B

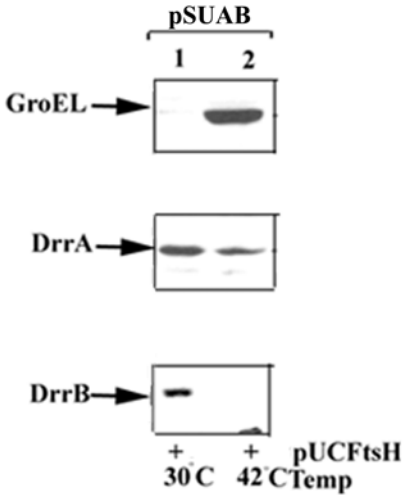

C

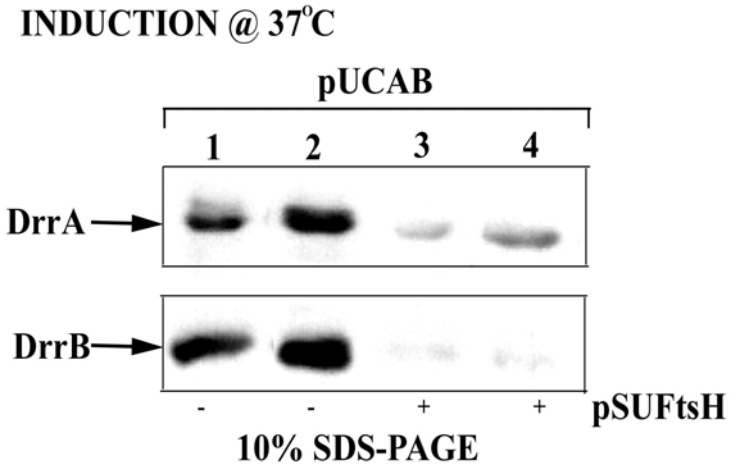

FIGURE 10: Effect of FtsH on misassembled proteins

TG1 cells containing the appropriate plasmid/s were grown at 37°C to a mid-log phase followed by induction at mid-log phase with 0.25mM IPTG. Following induction, the samples were incubated for 3 hrs at 37°C. Membrane fraction was prepared as described in "Experimental Procedures". 50 μg membrane protein was analyzed by 10% SDS-PAGE followed by Western blot using anti-DrrA and anti-DrrB antibodies.

Fig 10A: Lanes 1 and 3, pSUAB/ pUCFtsH; Lanes 2 and 4, pSUAB/ pUC18.

Fig 10B: Lane 1, pSUAB/ pUCFtsH induced for 2 hrs at 30°C; Lane 2, pSUAB/ pUCFtsH induced for 2 hrs at 42°C.

Fig 10C: Lanes 1 and 3, pUCAB/ pSUFtsH; Lane 2 and 4, pUCAB/ pSU2718.

Co-purification of DrrA and GroEL: During the purification of soluble DrrA containing an his-tag at the N terminus, a 68 kDa protein co-purified along with DrrA. N-terminal amino acid sequencing followed by immunoblotting with anti-GroEL identified the 68 kDa protein to be GroEL. GroEL does not co-purify with the complex of DrrAB (data not shown). These indicate that GroEL might have a role in the assembly of DrrAB.

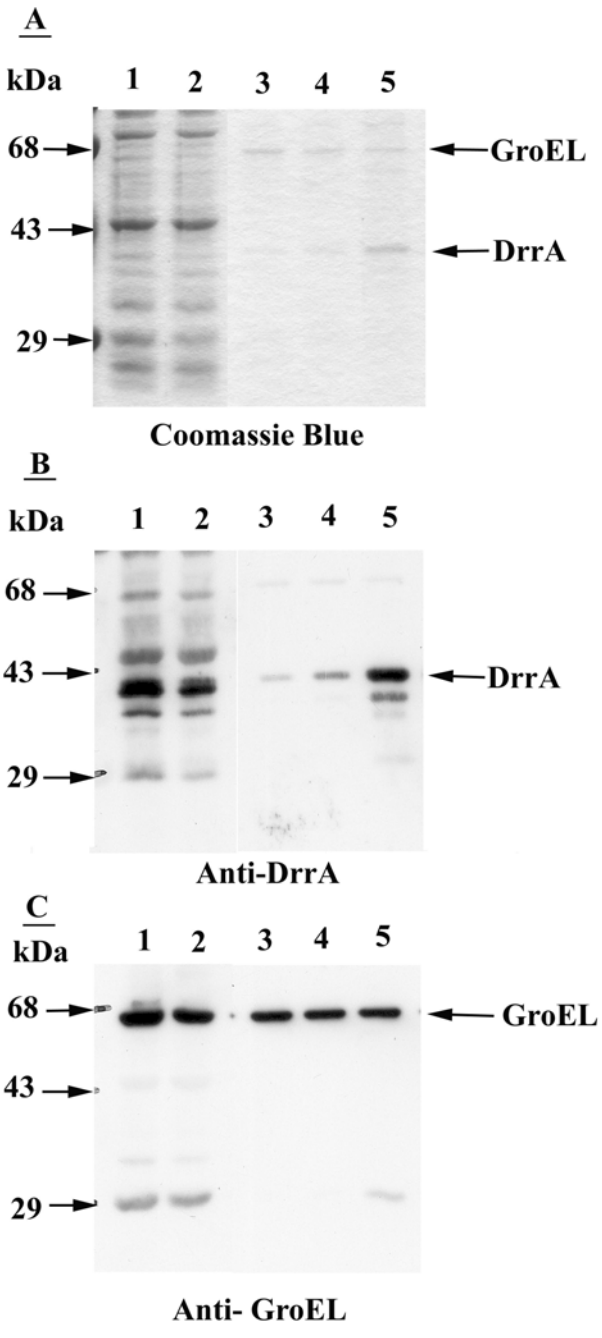

FIGURE 11: Purification of DrrA

His-tagged DrrA protein was purified from HMS174 cells containing only drrA gene on the plasmid pDX132. The total cell lysate was loaded onto a Ni-column and eluted with different concentrations of imidazole. 50ug protein was loaded on a 12% SDS-PAGE gel for electrophoresis. Lane 1, total lysate; lane 2, unbound; lane 3 100mM imidazole elution; lane 4, 20mM imidazole elution; lane 5, 500mM imidazole elution. The western blot analysis was carried out buy using anti-DrrA or anti-GroEL antibodies.

Effect of a GroEL ts mutation on expression of DrrAB: To characterize the role of GroEL, we used a strain with a ts mutation in GroEL. The effect of this mutation on levels of DrrA and DrrB in vivo was determined. Data in Figure 12A show that the levels of DrrA and DrrB were severely affected in this mutant background. Over production of GroEL in the ts strain restored normal levels of DrrA and DrrB. The above data indicate that GroEL is essential for their expression or assembly, and that unassembled protein in the absence of GroEL might be degraded by FtsH.

A

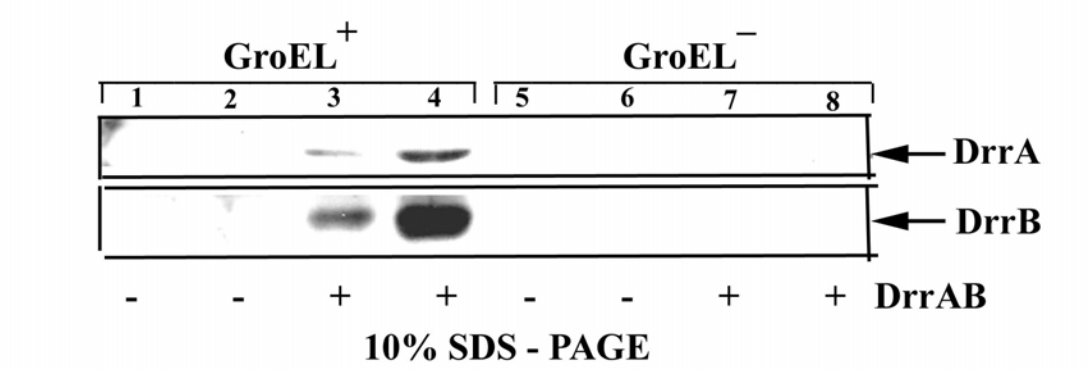

B

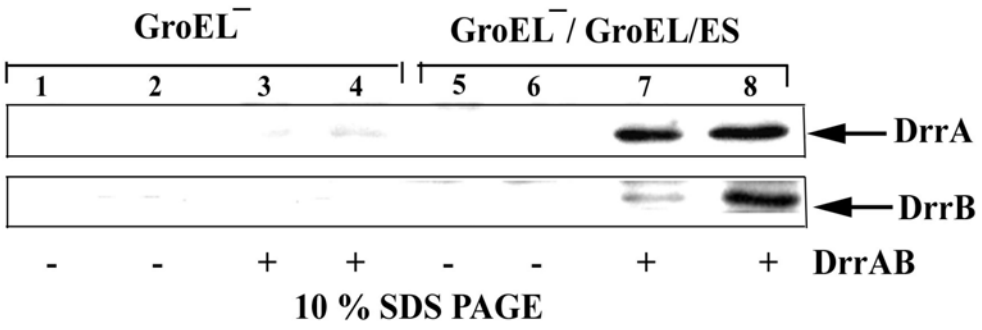

FIGURE 12: Effect of GroEL ts mutations on expression of DrrAB:

TG1 cells containing the indicated plasmids were grown at 37^{o}C to a mid-log phase followed by induction with 0.25mM IPTG. Following induction, the samples were incubated for 1.5 hrs and 3 hrs at 37^{o}C. Membrane fraction was prepared as described in "Experimental Procedures". 50 µg membrane protein was analyzed by 10% SDS-PAGE followed by Western blot using anti-DrrA and anti-DrrB antibodies.

Fig 12A: Lanes 1-2, GroEL^{+}/pUC18 ; Lanes 3-4, GroEL^{+}/pUCAB; Lanes 5-6, GroEL^{-}/pUC18; Lanes 7-8, GroEL^{-}/pUCAB. Samples were induced for 1.5 hrs and 3 hrs respectively.

Fig 12B: Lanes 1-2, GroEL^{-}/pUC18; Lanes 3-4, GroEL^{-}/pUCAB; Lanes 5-6, GroEL^{-}/GroEL/ES/pUC18; Lanes 7-8, GroEL^{-}/GroEL/ES/pUCAB. Samples were induced for 1.5 hrs and 3 hrs respectively.

GroEL (pSU*groEL*) was co-expressed with DrrAB (pDX108) or DrrB only (pDX203) in ARK796 (*ftsH*$^{+}$) or AR797 (*ftsH*$^{-}$) and the levels of DrrA and DrrB proteins were analyzed. Interestingly, we see that the levels of DrrA and DrrB were reduced in ARK796 (*ftsH*$^{+}$) strains while the levels of DrrA and DrrB seemed to be stable in ARK797 (*ftsH*$^{-}$) cells (Figure 13B). when GroEL was over-expressed in these strains. On the other hand, levels of DrrB when expressed alone were reduced in both ARK796 and ARK797 strains (Figure 13A). These results imply that GroEL and FtsH may function together in proteolysis and biogenesis of DrrAB. The effect of GroEL seems to promote proteolysis of DrrB by FtsH (Figure 13 A and B), or by another unknown protease as seen in Figure 13A, lane 3-4).

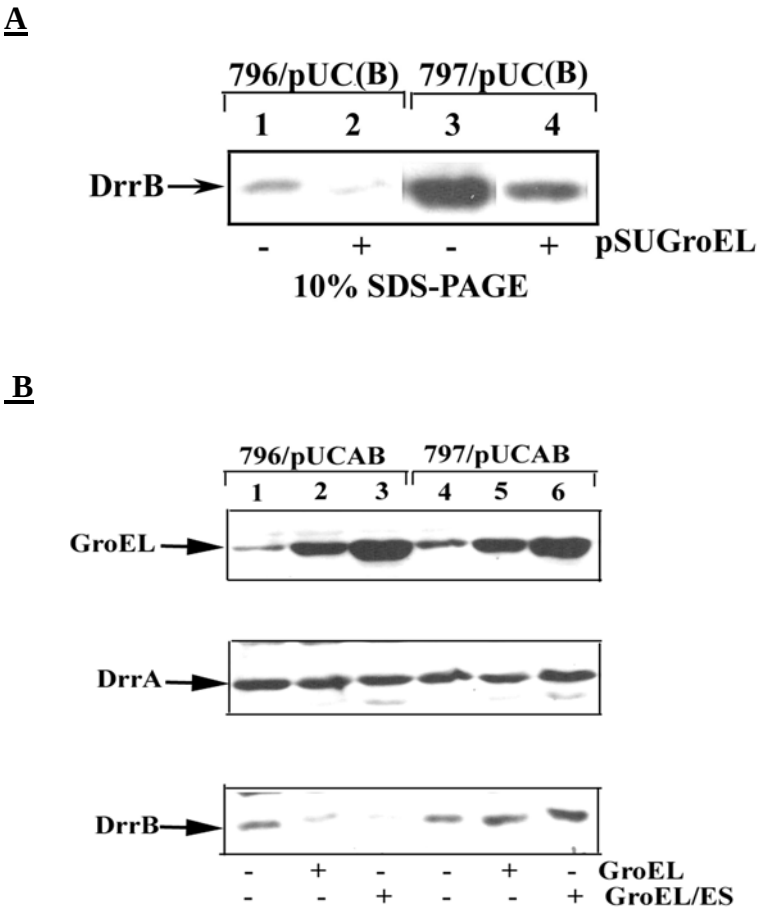

FIGURE 13: Effect of GroEL on DrrAB and DrrB protein levels in wild-type or FtsH deficient strains:

AR796 and AR797 cells containing the appropriate plasmid/s were grown at 30^{o}C to a mid-log phase followed by induction at mid-log phase with 0.25mM IPTG. Following induction, the samples were immediately shifted to 42^{o}C. Membrane fraction was prepared as described in "Experimental Procedures". 50 μg membrane protein was analyzed by 10% SDS-PAGE followed by Western blot using anti-DrrA and anti-DrrB antibodies.

Fig 13A: Lane 1, AR796/pUCB/pSU2718; Lane 2, AR796/pUCB/pSUGroEL; Lane 3, AR797/pUCB/pSU2718; Lane 4, AR797/pUCB/pSUGroEL.

Fig 13B: Lane 1, AR796/pUCAB/pSU2718; Lane 2, AR796/pUCAB/pSUGroEL; Lane 3, AR796/pUCAB/pKYGroEL/ES; Lane 4, AR797/pUCAB/pSU2718; Lane 5, AR797/pUCAB/pSUGroEL; Lane 6, AR797/pUCAB/pKYGroEL/ES.

DISCUSSION

With the goal of finding out which protease in particular cleaves DrrB, when DrrA is not simultaneously present, we procured *ftsH* (*14*), *lon* (*15*) , *clpA* (*16*) and *clpP* (*17*) deficient strains from Dr. Ito in Japan. We have seen before that stabilization of DrrB in the absence of DrrA could become inhibitory to the growth of the cells (*2*). Expression of DrrB in a protease-deficient strain might have a similar effect. Initial growth analysis of the protease-deficient strains expressing DrrAB or DrrB indicated that FtsH may be the protease involved in the degradation of DrrB. Wild-type FtsH co-expressed in FtsH-depleted strains containing DrrB was found to suppress the growth defect. Wild-type GroEL co-expressed in FtsH-depleted strains containing DrrB was also found to suppress the growth defect. An analysis of levels of proteins in these strains showed that in the absence of FtsH, DrrB alone was found to accumulate in very large quantities indicating that FtsH is involved in degradation of DrrB. In FtsH-depleted cells expressing both DrrA and DrrB together, an accumulation of both proteins was seen, however, DrrB did not accumulate as much as when it was expressed alone in the absence of DrrA. There may be a possibility that DrrA regulates the synthesis of DrrB so that in the absence of DrrA, high levels of DrrB accumulated due to unregulated expression. FtsH functions as a quality control protein, which degrades over-expressed proteins as well as misassembled or unfolded proteins as experimentally verified in Figure 10. FtsH is a Zn-dependent metalloprotease that belongs to a subfamily of the AAA family of ATPases (*14*). It is an inner membrane protein that is generally involved in membrane functions, especially proteolysis of improperly assembled proteins. Degradation of unassembled SecY (when SecE is absent), a subunit of the protein translocase (*6*), as well as the subunit 'a' of the F_o subunit of the H^+- ATPase (*7*) has been shown to be brought about by FtsH. This is similar to the

situation with DrrB when DrrA is not available or when proteins are over-expressed or misassembled.

Proteases from the AAA ATPases family, for example, (Clp (*25*), Yta10 and Yta12 (*23*) homologs of FtsH, Lon (*26*) and YmeI (*24*))have been demonstrated to have a chaperone-like role independent of proteolysis. While our preliminary data tended towards a possible role of FtsH on the DrrAB complex, our initial experiments with FtsH mutants were inconclusive. We will continue to explore the possibility of FtsH having a chaperone-like role by constructing mutants that totally lack protease activity but retain the ATPase domain. If this mutant is able to suppress the growth defect of FtsH-depleted strains expressing DrrAB, it would imply that FtsH may have an additional chaperone-like role independent of proteolysis.

Our understanding that GroEL may seem to play a role in the assembly of DrrAB came from the purification of His-tagged DrrA protein. The 60 kDa GroEL protein co-purified with DrrA when it was expressed by itself but did not co-purify with the complex of DrrAB. Data is Figure 12A further showed that the levels of DrrA and DrrB are severely affected when expressed in a ts mutant GroEL strain, thus indicating that GroEL is essential for the expression or assembly of DrrA and DrrB. When wild-type *groEL* was expressed in FtsH-depleted strains containing DrrB, it was found to suppress the growth defect caused by overexpressed DrrB (Figure 12B). An analysis of the effect of GroEL on DrrA and DrrB protein levels in wild-type or FtsH-deficient strains suggested that GroEL may have different roles to play in the biogenesis of the DrrAB complex as also shown in the model illustrated in the model below.

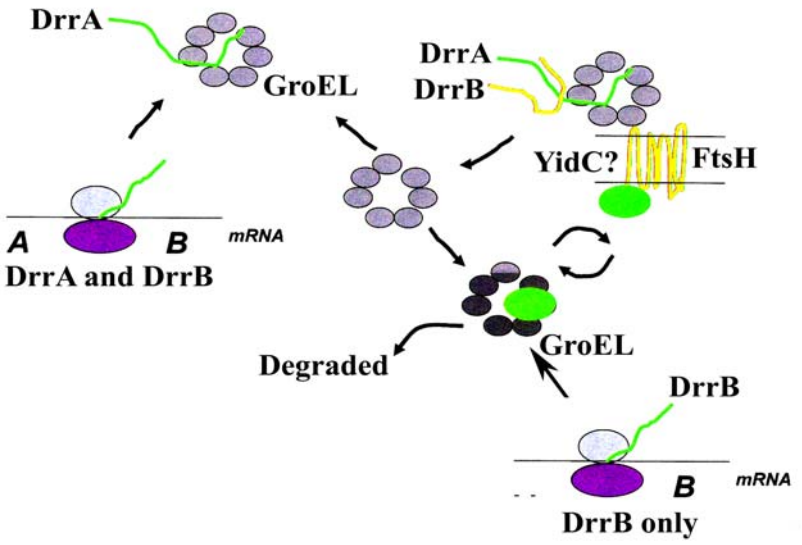

FIGURE 14: Model illustrating the role of GroEL and FtsH in the biogenesis of DrrA and DrrB protein.

When DrrB protein was expressed in the absence of DrrA, GroEL enhances its degradation in the presence or absence of FtsH. Since we know that FtsH is the major protease that acts on DrrB, therefore in its absence, GroEL may be recruiting another protease for degradation of DrrB. When DrrA and DrrB are expressed together, GroEL may play a dual role depending on the presence or absence of FtsH. In the presence of FtsH, it may enhance the degradation of DrrB while in its absence, it may be involved in proper folding and stability of the complex. Levels of DrrA are stabilized in either strain indicating that GroEL might help maintain DrrA in a partially unfolded state before it is presented to DrrB.

It has previously been shown that GroEL plays an important role in the biogenesis of lactose permease (LacY) and in secretion of beta-lactamase by keeping it in an unfolded, translocation-competent state. The LacY-GroEL complex can then be post-translationally

transferred to the membrane vesicles (*8*). Thus, GroEL is believed to play a variety of roles, which include promoting folding, assembly, secretion, or membrane insertion of proteins. The data shown here also suggest that GroEL has a role to play in promoting folding of DrrA, enhancing degradation of DrrB in the absence of DrrA and perhaps in the assembly of the proteins when they are expressed together.

REFERENCES

1. Guilfoile, P. G., and Hutchinson, C. R. (1991). A bacterial analog of the mdr gene of mammalian tumor cells is present in Streptomyces peucetius, the producer of daunorubicin and doxorubicin. *Proc Natl Acad Sci U S A* 88, 8553-7.
2. Kaur, P. (1997). Expression and characterization of DrrA and DrrB proteins of Streptomyces peucetius in Escherichia coli: DrrA is an ATP binding protein. *J Bacteriol* 179, 569-75.
3. Kaur, P., and Russell, J. (1998). Biochemical coupling between the DrrA and DrrB proteins of the doxorubicin efflux pump of Streptomyces peucetius. *J Biol Chem* 273, 17933-9.
4. Kaur, P., Rao, D. K., and Gandlur, S. M. (2005). Biochemical characterization of domains in the membrane subunit DrrB that interact with the ABC subunit DrrA: identification of a conserved motif. *Biochemistry* 44, 2661-70.
5. Gandlur, S. M., Wei, L., Levine, J., Russell, J., and Kaur, P. (2004). Membrane topology of the DrrB protein of the doxorubicin transporter of Streptomyces peucetius. *J Biol Chem* 279, 27799-806.
6. Akiyama, Y., Kihara, A., Tokuda, H., and Ito, K. (1996). FtsH (HflB) is an ATP-dependent protease selectively acting on SecY and some other membrane proteins. *J Biol Chem* 271, 31196-201.
7. Akiyama, Y., Kihara, A., and Ito, K. (1996). Subunit a of proton ATPase F0 sector is a substrate of the FtsH protease in Escherichia coli. *FEBS Lett* 399, 26-8.

8. Bochkareva, E., Seluanov, A., Bibi, E., and Girshovich, A. (1996). Chaperonin-promoted post-translational membrane insertion of a multispanning membrane protein lactose permease. *J Biol Chem* 271, 22256-61.

9. Miller, J. (1992). "Experiments in Molecular Genetics," Cold Spring Harbor, NY.

10. Karata, K., Inagawa, T., Wilkinson, A. J., Tatsuta, T., and Ogura, T. (1999). Dissecting the role of a conserved motif (the second region of homology) in the AAA family of ATPases. Site-directed mutagenesis of the ATP-dependent protease FtsH. *J Biol Chem* 274, 26225-32.

11. Jayasekera, M. M., Foltin, S. K., Olson, E. R., and Holler, T. P. (2000). Escherichia coli requires the protease activity of FtsH for growth. *Arch Biochem Biophys* 380, 103-7.

12. Vale, R. D. (2000). AAA proteins. Lords of the ring. *J Cell Biol* 150, F13-9.

13. Langer, T. (2000). AAA proteases: cellular machines for degrading membrane proteins. *Trends Biochem Sci* 25, 247-51.

14. Ito, K., and Akiyama, Y. (2005). Cellular functions, mechanism of action, and regulation of FtsH protease. *Annu Rev Microbiol* 59, 211-31.

15. Charette, M. F., Henderson, G. W., and Markovitz, A. (1981). ATP hydrolysis-dependent protease activity of the lon (capR) protein of Escherichia coli K-12. *Proc Natl Acad Sci U S A* 78, 4728-32.

16. Gottesman, S., Clark, W. P., and Maurizi, M. R. (1990). The ATP-dependent Clp protease of Escherichia coli. Sequence of clpA and identification of a Clp-specific substrate. *J Biol Chem* 265, 7886-93.

17. Maurizi, M. R., Singh, S. K., Thompson, M. W., Kessel, M., and Ginsburg, A. (1998). Molecular properties of ClpAP protease of Escherichia coli: ATP-dependent association of ClpA and clpP. *Biochemistry* 37, 7778-86.

18. Miroux, B., and Walker, J. E. (1996). Over-production of proteins in Escherichia coli: mutant hosts that allow synthesis of some membrane proteins and globular proteins at high levels. *J Mol Biol* 260, 289-98.

19. Dong, H., Nilsson, L., and Kurland, C. G. (1995). Gratuitous overexpression of genes in Escherichia coli leads to growth inhibition and ribosome destruction. *J Bacteriol* 177, 1497-504.

20. Suzuki, C. K., Rep, M., van Dijl, J. M., Suda, K., Grivell, L. A., and Schatz, G. (1997). ATP-dependent proteases that also chaperone protein biogenesis. *Trends Biochem Sci* 22, 118-23.

21. Akiyama, Y., Ogura, T., and Ito, K. (1994). Involvement of FtsH in protein assembly into and through the membrane. I. Mutations that reduce retention efficiency of a cytoplasmic reporter. *J Biol Chem* 269, 5218-24.

22. Shirai, Y., Akiyama, Y., and Ito, K. (1996). Suppression of ftsH mutant phenotypes by overproduction of molecular chaperones. *J Bacteriol* 178, 1141-5.

23. Arlt, H., Tauer, R., Feldmann, H., Neupert, W., and Langer, T. (1996). The YTA10-12 complex, an AAA protease with chaperone-like activity in the inner membrane of mitochondria. *Cell* 85, 875-85.

24. Leonhard, K., Stiegler, A., Neupert, W., and Langer, T. (1999). Chaperone-like activity of the AAA domain of the yeast Yme1 AAA protease. *Nature* 398, 348-51.

25. Pak, M., Hoskins, J. R., Singh, S. K., Maurizi, M. R., and Wickner, S. (1999). Concurrent chaperone and protease activities of ClpAP and the requirement for the N-terminal ClpA ATP binding site for chaperone activity. *J Biol Chem* 274, 19316-22.

26. Rep, M., van Dijl, J. M., Suda, K., Schatz, G., Grivell, L. A., and Suzuki, C. K. (1996). Promotion of mitochondrial membrane complex assembly by a proteolytically inactive yeast Lon. *Science* 274, 103-6.

DISCUSSION

DrrA and DrrB proteins of *Streptomyces peucetius* belong to the ABC family of transporters that have been implicated in a number of diseases, such as cystic fibrosis, Tangiers disease and Dubin Johnson syndrome, among others (*1*). The study of these drug pumps has also become of utmost importance with the occurrence of multidrug resistance in human cancer cells and its direct correlation with the overexpression of several ABC transporters, namely, P-glycoprotein (Pgp, ABC1), multidrug resistance associated protein (MRP1, ABCC2) and breast cancer resistance protein (BCRP, ABCG2) (*1*). The DrrAB system bears sequence, structural, and functional similarities to Pgp (*2-4*). An understanding of the DrrAB transporter is thus expected to help in obtaining a better understanding of the origin and mechanism of action of drug restistant proteins such as Pgp. A major question that researchers are posed with is how the nucleotide binding domains and the membrane domains interact with one another during the catalytic cycle of the transporter. While most ABC transporters, such as Pgp (*5*), CFTR (*6*), LmrA (*7*) and MsbA (*8*), have the nucleotide binding domain and the membrane domain on the same molecule, they are present on separate subunits in DrrAB. This unique feature of DrrAB makes it a prototype for the study of NBD:TMD and NBD:NBD interactions.

Previous cross-linking studies in this laboratory employed membrane-permeable and impermeable amine to amine cross-linkers, DSP and DTSSP, and identified a complex of DrrA and DrrB (*9*). However, using DSP and DTSSP, it was not possible to easily determine the regions involved in cross-linking. In the present study, we have utilized a more direct and specific approach to identify the regions in DrrA and DrrB that interact with one another. DrrB protein contains a single cysteine at position 260, whereas DrrA protein contains none. The presence of only one cysteine in our system enabled us to use heterobifunctional and homobifunctional thiol cross-linkers to probe the interacting sites within each protein. To

identify regions in DrrB that were involved in interaction with DrrA, a cysteine-less DrrB was first created by substituting a serine at position C260 by site-directed mutagenesis. Twenty single-cysteine substitutions were thus introduced at various positions in the cysteine-less DrrB. The location of the cysteine substitutions in DrrB was based on a recently developed topological model for DrrB, which suggests that DrrB consists of eight transmembrane domains with both the N-terminal and the C-terminal ends of the protein directed in the cytoplasm. To directly identify the regions of DrrB that interact with DrrA, a heterobifunctional cysteine to amine chemical cross-linking agent, GMBS (N-[-maleimidobutyryloxy]succinimide ester), was employed. Our Studies show that DrrA cross-links with both the N-terminal and the C-terminal ends of DrrB, suggesting that these two regions may participate in interaction with DrrA. An in-depth sequence analysis with exporters, including DrrB, LmrA, MDR1, CFTR, and MsbA, as well as the importer BtuC allowed us to identify a conserved motif bearing the amino acid sequence $GE_{-1}..A_3R/K..G_7$ within the N-terminal cytoplasmic tail of DrrB. This analysis led us to conclude that this conserved sequence is a modified version of the EAA motif $E_1AA_3RALG_7$ previously identified in the interaction interfaces of importers of the ABC family. The present study is the first analysis where interacting domains in the membrane component of a drug efflux system have been biochemically analyzed by using a cross-linking approach.

To identify the domains in DrrA involved in interaction with DrrB, several cysteine substitutions in and around the conserved domains of DrrA were made in constructs already containing a S23C substitution (cysteine in the interacting domain at N-terminal tail of DrrB) in DrrB. By using the disulphide cross-linking strategy, we conclude that the Q-loop region (cysteines in position Y89 and S91) of DrrA is involved in interaction with DrrB. We also found that by placing a cysteine in the Q-loop, DrrA was trapped in the dimeric state, indicating that

this region is present at the dimeric interface. Fourier Resonance Energy Transfer (FRET) was then carried out to identify the conformation of the dimers. It was found that these dimers were arranged in an "head-to-tail" conformation, as seen with other ABC proteins. In the closed conformation of NBD's of MalK (*10*) and MJO796 (*11*), the dimers have nucleotides bound at their interface. In our study we found that with the addition of a non-hydrolysable ATP analog, ATPγS, a stable Y89C DrrA dimer was produced even in the absence of the cross-linker, suggesting that in this situation the ATP analog serves to hold the Y89C dimer together. If E165Q, a mutation in the Walker B domain that prevents hydrolysis of ATP, is simultaneously present along with Y89C, then either ATP or ATPγS could substitute for the disulfide cross-linker. Based on these observations, we can conclude that the Y89C-Y89C contact is sensitive to binding of ATP/ATPγS so that the Y89C dimer can be stabilized either by the disulfide cross-linker acting directly on the Q-loop or by binding of ATPγS to the interface of the dimer. These data imply that the Y89C dimeric conformation indeed resembles the closed state.

With the use of different arm-length cross-linkers, it was seen that substituting S23 residue with S23C in DrrB produced a significant effect on the behavior of Y89C in DrrA. DrrA (Y89C) can be cross-linked with linkers varying in length from 0 (CuPhe) to 24 Å (MTS). However, when S23C is simultaneously present in DrrB, the results were strikingly different: copper and DTME (13.3 Å) can still cross-link DrrA and produce DrrA homodimers very well, but MTS was not able to do so. These data indicate that placing a cysteine in this region of DrrB produces a conformational change in the helical domain of DrrA. We propose that the two Y89C residues (or the Q-loops) from opposing monomers are in flexible contact until a conformational change in DrrB (produced by S23C substitution here) produces a change in DrrA which fixes it in one position. Instead of resulting in opening of the NBD dimer, the result of this interaction

between Y89C and S23C seems to be to fix the distance between DrrA monomers at less than 13 Å. It seems that the overall effect of this conformation of DrrB is to facilitate the closed conformation of DrrA. This is the first biochemical analysis that shows the long-range effects of conformational changes in TMD (DrrA) on the NBD (DrrA).

To further our understanding of the mechanism of the DrrAB complex, we analysed the accessory factors involved in the biogenesis of the DrrAB complex, mainly the proteins involved in degradation of unstable DrrB (when DrrA is not simultaneously present) and in folding/assembly of the protein. Several known AAA metalloproteases have been known to degrade misassembled membrane proteins (*12, 13*). Using various protease deficient-strains, we could directly conclude that FtsH, a member of the AAA family of proteases, was involved in the proteolysis of DrrB. Initial data also suggest that FtsH may have an additional chaperone-like role in assembly of the DrrAB complex. Studies are currently underway to demonstrate the possible chaperone function of FtsH.

Finally, we found that GroEL is also essential for the expression or assembly of DrrA and DrrB. In a GroEL-defecient strain, stable assembly of the DrrAB complex was not seen. A further analysis of effect of GroEL suggests that it may enhance the degradation of DrrB (when it is expressed by itself in the absence of DrrA) and may stabilize/maintain the DrrA and DrrB proteins when they are expressed together. Studies are underway to characterize a more defined role that GroEL may play in the biogenesis of the DrrAB complex.

REFERENCES

1. Borst, P. & Elferink, R. O. (2002) Mammalian ABC transporters in health and disease, *Annu Rev Biochem. 71*, 537-92.

2. Higgins, C. F. (1992) ABC transporters: from microorganisms to man, *Annu Rev Cell Biol. 8*, 67-113.

3. Litman, T., Druley, T. E., Stein, W. D. & Bates, S. E. (2001) From MDR to MXR: new understanding of multidrug resistance systems, their properties and clinical significance, *Cell Mol Life Sci. 58*, 931-59.

4. McKeegan, K. S., Borges-Walmsley, M. I. & Walmsley, A. R. (2003) The structure and function of drug pumps: an update, *Trends Microbiol. 11*, 21-9.

5. Gottesman, M. M. & Pastan, I. (1993) Biochemistry of multidrug resistance mediated by the multidrug transporter, *Annu Rev Biochem. 62*, 385-427.

6. Ostedgaard, L. S., Rich, D. P., DeBerg, L. G. & Welsh, M. J. (1997) Association of domains within the cystic fibrosis transmembrane conductance regulator, *Biochemistry. 36*, 1287-94.

7. van Veen, H. W., Venema, K., Bolhuis, H., Oussenko, I., Kok, J., Poolman, B., Driessen, A. J. & Konings, W. N. (1996) Multidrug resistance mediated by a bacterial homolog of the human multidrug transporter MDR1, *Proc Natl Acad Sci U S A. 93*, 10668-72.

8. Chang, G. & Roth, C. B. (2001) Structure of MsbA from E. coli: a homolog of the multidrug resistance ATP binding cassette (ABC) transporters, *Science. 293*, 1793-800.

9. Kaur, P. & Russell, J. (1998) Biochemical coupling between the DrrA and DrrB proteins of the doxorubicin efflux pump of Streptomyces peucetius, *J Biol Chem. 273*, 17933-9.

10. Chen, J., Lu, G., Lin, J., Davidson, A. L. & Quiocho, F. A. (2003) A tweezers-like motion of the ATP-binding cassette dimer in an ABC transport cycle, *Mol Cell. 12*, 651-61.

11. Yuan, Y. R., Blecker, S., Martsinkevich, O., Millen, L., Thomas, P. J. & Hunt, J. F. (2001) The crystal structure of the MJ0796 ATP-binding cassette. Implications for the structural consequences of ATP hydrolysis in the active site of an ABC transporter, *J Biol Chem. 276*, 32313-21.

12. Langer, T. (2000) AAA proteases: cellular machines for degrading membrane proteins, *Trends Biochem Sci. 25*, 247-51.

13. Vale, R. D. (2000) AAA proteins. Lords of the ring, *J Cell Biol. 150*, F13-9.